NASA CONTRACTOR REPORT

NASA CR-190

BIOLOGICAL CONTROL SYSTEMS — A CRITICAL REVIEW AND EVALUATION

DEVELOPMENTS IN MANUAL CONTROL

by Laurence R. Young and Lawrence Stark

Prepared under Contract No. NAS 2-1372 *by*
BIOSYSTEMS, INC.
Cambridge, Mass.
for

NATIONAL AERONAUTICS AND SPACE ADMINISTRATION • WASHINGTON, D. C. • MARCH 1965

BIOLOGICAL CONTROL SYSTEMS – A CRITICAL REVIEW AND EVALUATION

DEVELOPMENTS IN MANUAL CONTROL

By Laurence R. Young and Lawrence Stark

Prepared under Contract No. NAS 2-1372 by
BIOSYSTEMS, INC.
Cambridge, Mass.

for

NATIONAL AERONAUTICS AND SPACE ADMINISTRATION

For sale by the Office of Technical Services, Department of Commerce,
Washington, D.C. 20230 -- Price $6.00

ABSTRACT

Recent developments in mathematical models for the human manual control system are reviewed and evaluated as part of a study of the field of biological control systems. Application of control models for investigation of the "fine structure" is stressed, rather than human engineering aspects. Evidence for and against discrete models of the human operator is presented and a number of such models are compared. The adaptive characteristics of the operator and two basic modelling approaches are presented and several models reviewed. Detailed discussion is included on correlation of manual response characteristics and physiological data for muscle, leading to models for the postural control and voluntary control system interactions.

TABLE OF CONTENTS

SUMMARY

As part of a critical review of the entire field of biological control systems, this report deals with recent developments in the area of manual control. It is concerned with systems analysis models for manual control, and the attempts to more fully explain the biological operation through servoanalysis and computer simulation.

The report does not deal with the "human engineering" aspects of manual control, such as display-control compatability or system equalization. The emphasis is on recent (post 1957) development of more sophisticated mathematical models to describe and perhaps explain some of the "fine structure" in control of manual responses. These models fall primarily into the basic research catagory rather than as guidelines for man-machine integration.

A number of models dealing with discrete aspects of human response are reviewed and evaluated. The research of Bekey, Lemay and Westcott, Young, Navas, Elkind, Raoult and Naslin, and Pew is examined in detail, and several cautionary comments are included concerning the limitations of sampled data models.

The adaptive characteristics of manual tracking are also explored in some detail, and the current state of hypotheses about the adaptive mechanism is investigated. Recent experiments pertaining to adaptation to input, controlled element and tasks are considered, as well as the question of limits of controllability and measures of adaptation. "Model reference" and "error pattern recognition" classes of adaptive models are introduced, and the relevant work of Knoop and Fu, Raoult and Elkind is discussed.

The third major area treated in the report is the development of mathematical models correlating physiological evidence on muscle and muscle spindles with manual response to a variety of visual and force inputs and eye-hand coordination. The work of Stark and his coworkers is reviewed in detail, leading to models of the motor control system showing the interaction of the postural and voluntary control systems.

DEVELOPMENTS IN MANUAL CONTROL

I. INTRODUCTION

The aspects of manual control discussed in this report are concerned with a description of the characteristics of the human operator in a control task. In general the human is involved in visual-manual tracking, in which his task is to manipulate a manual control stick in accordance with input information presented to him through a visual display.

Of all the biological control systems considered in this review, the manual control system has been the subject of the most intensive study by investigators from the fields of psychology and engineering. The reason for this attention stems from the practical importance of understanding the role of the human operator in a closed loop control task. Thus, driving an automobile, controlling the position of a milling machine, aiming an anti-aircraft gun, or landing an

airplane on the deck of an aircraft carrier, are all important practical situations in which the visual-manual control characteristics of the human operator are of crucial importance to the successful performance of the man-machine system.

The interests of psychologists in the manual tracking problem dates back many years to the early studies of reaction times and simple tracking. The contribution of engineers, and in particular control engineers, dates to World War II, in connection with studies of the abilities of a gunner to operate as part of a fast fire-control system. The first genuine use of servomechanism theory to describe the human operator was by Tustin in 1944 (77), when he described the input-output relationship of a man in terms of linear operators and an additive "remnant" of noise at the operator's output. Using the developing notions of servomechanism synthesis, and in particular "proportional plus derivative" compensation, Sobczyk and Philips (65) determined the optimum "aiding constant" for lead compensation for use by the human operator in controlling the position and velocity of a gun.

Following the war a number of independent thorough investigations were carried out to determine the "quasi-linear" models of the human operator in a tracking loop. The block diagram of Fig. 1 is representative of the form assumed for all these investigations. The quasi-linear descriptions may be defined as the "best fit" linear model of the human operator for a given control task, in which the form of the input signal and the nature of the controlled process are specified. For different input spectra or controlled process or task specifications, the model takes on a different though still linear representation, thereby accounting for the name quasi-linear. Since these models do not account for all the manual output motion of the human operator, usually a remnant term is added to account for the output "noise" not correlated with the input signal. Most of the quasi-linear models may be cast in the form

$$H(S) = \frac{Ke^{-t_d s}(T_L s + 1)}{(T_N s + 1)(T_I s + 1)}$$

This expression represents the quasi-linear describing function of the human operator from observed error as an input to displacement of the control stick as the

output. The gain K and the lead and lag time constants T_L and T_I, are generally considered to be varied according to the control task to yield satisfactory closed loop response. t_d represents a pure delay time and T_N the short neuromuscular delay.

The work of Russell (57), Hall (20), Krendel (36), and Elkind (12), using linear identification techniques, led to quasi-linear models valid for a variety of input spectra and control system dynamics. These models and their implications were reviewed in detail by McRuer and Krendel in 1957 (40). More recently Sheridan (62) and Adams (2) have added to the literature on quasi-linear models.

As the quasi-linear approaches to human operator modeling reached satisfactory results in the late 1950's, research attention shifted to several other phases of manual control. The emphasis in this report will be on those aspects which have been most intensively studied in the period 1959-1964, and which seem most relevant to the central control problem.

The first of these newer areas is the physiological approach to modeling the neurological and neuromuscular systems underlying manual control. In sections II

through IV a mathematical model is presented to account for observed behavioral tracking characteristics and mechanical impedance properties of the arm. This model, based on the research of Stark and his coworkers, includes relevant biophysical relations pertaining to the nerves and muscles.

A second area of great interest has been the "fine structure" of the operator's response. Whereas the quasi-linear models matched the average gain and phase lag sufficiently well, they were unable to describe the detailed transient responses or deterministic inputs or the discrete nature of human tracking movements. Some of the older ideas concerning the psychological refractory period have been revived to stimulate several different sampled-data and discrete nonlinear models for visual-manual tracking. These models are reviewed and compared in Section V.

The ability of human beings to change their characteristics depending upon the task input and the dynamics of the controlled element has long been noted with interest. With the recent activity in adaptive systems by automatic control specialists a parellel effort has been observed in descriptions of the

adaptive characteristics of the human operator. These descriptions and the attempts at adaptive models are reviewed in Section VI.

II. PHYSIOLOGICAL BACKGROUND OF THE PERIPHERAL ADAPTIVE MECHANISM

Mechanism of Motor Control

Two mechanisms which play an important role in manual control and in providing the manual control system with its adaptive capability are the postural control system and the voluntary control system.

The postural system is a feedback system which functions to maintain the posture or position of the body and its limbs. It is essentially a position servoloop with position sensors, motor elements, and some data processing. The postural servosystem is controlled by higher centers which provide reference inputs and which control the parameters of some of the elements of this system as shown in Figure 2.

The voluntary control system provides the mechanism for executing skilled precise movements. It too is composed of sensory, motor and computational components. It is quite different from the postural control system, however, in that its controller is thought to be open-loop and sampled-data, executing pre-programmed control movements. These movements are proprioceptively

open-loop in the sense that the postural control system appears to be at least partially disabled when voluntary control movements are being executed. Feedback is obtained from a variety of sensors, including joint position receptors and the visual system, but the information obtained from these feedback elements must be processed by higher centers before effecting movement. An important part of the control of the voluntary movements is the predictive system which is able to extract information to predict the future course of events from signals and responses. It is this predictive ability which is responsible for some of the input adaptive properties of manual control systems.

Variable Topology of the Neurological Control System

In this section some experimental responses which may correspond to three states of the neurological control mechanism are discussed (66). A general model for certain aspects of movement and postural coordination is introduced.

A subject instructed to rotate a handle back and forth as rapidly as possible, produced a record of handle angle as a function of time, similar to the top

line of Fig. 3. During the high velocity portion of the movement, the antagonists (opposing muscles) were quite relaxed and limp. Because of this inactivity, in spite of marked stretching of the antagonists by the agonists (contracting muscles), it is concluded that the stretch reflex was inoperative. Either the afferent feedback from the muscle spindle was markedly reduced, or more likely it was functionally ineffective in exciting the alpha motor neurons (final common path). Figure 4a shows a simplified block diagram of the situation. It is important to note: (a) the back-to-back pair of control systems (agonist-antagonist) that are always present in movement and represent the inability of muscle to push; (b) the open-loop mode that permits the high frequency oscillation; and (c) the pre-programmed set of alternating contractions sent down from the brain.

Subsequently in the experiment, the subject performed successive movements again, this time under instruction to prevent deflection of his hand by random input disturbances. Only secondarily was he to oscillate his hand at as high a frequency as possible. (As a result of these factors the frequency of oscillation is slowed as shown in the middle recording of Fig. 3.) Figure 4b shows the nature of the neurological

organization of this mode of operation. The essential features are: (a) the muscle spindle system acting as a high-gain length regulator; (b) the resultant increased stiffness or spring constant of both agonists and antagonists; (c) the sharing of the alpha-motor neuron (final common pathway) by this length regulator and the cortico-spinal input.

It might be well to mention that the diffuse anatomical organization of the gamma input makes it a highly inappropriate follow-up servo system. In fact, it is not used for this function but for postural tone and end-of-movement damping and clamping.

Finally the subject was asked to imagine a pointer moving back and forth and to track this imaginary pointer, and attempt to oscillate his hand as fast as possible. The arrangement of the neurological apparatus is shown in Fig. 4c. The position of afferent information feeds back to a visual-motor orientation complex that is postulated to exist in the brain. The oscillation is markedly slowed, perhaps, because of the necessity to transmit and process all control signals through the imagery of the mental tracking process. This is shown in the bottom recording of Fig. 3.

That the gamma-spindle system may be utilized in this mode of operation at the end of each high velocity portion of the oscillation is indicated by an experiment performed by Stark and Rushworth (73). The gamma gain controls to the spindles were blocked with procaine producing the so-called cerebellar syndrome of hypotonia, astenia, taxia, overshooting, rebound, dysmetria and postural drift. Skilled voluntary movements were still possible with attention. However, when sinusoidal tracing was being performed, similar in principle to mental tracking, errors were made in a particular fashion. Occasionally at the end of the high velocity portion of the sinusoid, the pencil hand would continue in the tangential direction. This indicates that the damping and clamping functions of the length regulator (spindle) would normally be active in the precise termination of a high velocity movement.

In summary, experimental definition has been attempted for a facet of the complex neurological control system for movement: the ability to change the topology of the multiloop neural system. This introductory material points up the interaction and indeed competition between the postural servo-loop (stretch reflex) and the proprioceptively open-loop voluntary control of the musculature.

A Quantitative Model

While the general model may be useful in conceptualizing the physiology of the spinal and peripheral mechanism, it should clearly be supplemented by a quantitative model (33). The BIOSIM program, providing for the simulation of a general class of dynamical systems from specifications of their block diagram representation, has been used for this application. It is run on a 7090 digital computer and contains its own Fortran-like compiler for ease of communication between user and program.

The expanded and modified form of the block diagrams of Fig. 4 for closed-loop operation of the postural musculature system and open-loop operation of the voluntary control system is shown in Fig. 5 (3). In one experiment the subject is instructed to hold his arms fairly tense and to maintain this position despite possible deflecting forces. A force of 5 kg lasting 0.2 sec is applied. The subject's arm is deflected and then returns to its desired position after a slight overshoot. The BIOSIM analog behaves as shown in Fig. 6. Tensing of the muscles is modeled by inserting a bias signal using SPE 6 and SPE 7 (See Table 1.).

Table 1. Definitions of Special Functions

SPECIAL FUNCTION(SPE)	DEFINITION
SPE 6 and SPE 7	Muscle Tone = 0.001 u - 1(t)
SPE 8	(-Y(11)+100 Y(11)*Y(13) if Y(13) < 0 (-Y(11)+600 Y(11)*Y(13) if Y(13) ≥ 0
SPE 9	(Y(12)-600 Y(12)*Y(05) if Y(13) ≥ 0 (Y(12)-100 Y(12)*Y(05) if Y(13) < 0
SPE 10	Disturbing Force = 5[u-1(t-0.2)]
SPE 2 and SPE 3	Not used for this experiment

The disturbing force whose time function is shown, is applied by means of SPE 10. As the hand is deflected from its zero position the error signal of the stretched muscle increases and the error signal of the slackened muscle decreases. When the disturbing force ceases, these signals, by operating on their respective muscles, drive the hand back to its zero position with a slight overshoot. The initial biasing, hand position, disturbing force, and error signals are shown as time functions in Fig. 6, and indicate a qualitative and rough quantitative agreement with the experiment. In Fig. 6, α_2 represents input to muscle which restrains initial motion; α_3 represents input to muscle slackened by initial motion; θ represents deflection of the arm in degrees; and the dashed line indicates the bias level.

BIOSIM analog results are encouraging and indicate that further development in the directions of (a) better definition of the physical elements of the control system, (b) more accurate descriptions of system topology, and (c) further comparison with experiment, might increase our understanding of this complex system.

Muscle Physiology: BIOSIM Model

Muscle is unique in converting chemical energy directly into mechanical work. Limitation in the rate of this conversion acts as an apparent viscosity which plays a role in the over-all dynamics of movement. This section summarizes the physiological evidence relating to this conversion and the simplified mathematical model used in BIOSIM (69).

The dynamic characteristics of a maximally stimulated shortening muscle can be summarized by an exponential relationship between the load on a muscle and the maximum velocity of shortening, as shown by the dashed curve in Fig. 7 from Fenn and Marsh (15). In 1938, Hill (23) showed in a thermodynamic study of muscle that the force-velocity relationship could be approximated very closely by the equation

$$(v + b)(P + a) = (P_o + a)b = \text{constant} \qquad (1)$$

where a and b are constants that are dependent on the particular muscle, P is load force, v is shortening velocity, and P_o is isometric tension. When experiments were extended to lengthening, as well as shortening muscle,

Hill's equation failed. Katz (31) found a steep linear relationship between muscle opposition force and lengthening velocity, as seen in the dashed line of Fig. 8a. Ten years later, Wilkie (81) repeated Hill's experiments for the shortening muscle in the human arm by using subjects directed to exert maximal voluntary effort. His results fit Hill's equation after correction for the inertia of the arm. These data were most useful in our approximation of a muscle model for digital computer simulation with BIOSIM.

Using BIOSIM an investigation of the behavior of a complete agonist-antagonist muscle system was undertaken (69). Simple straight line approximations to the physiological model were adequate for this work. With the use of the parameters in Wilkie's paper and measurements on human subjects, estimates of P_o (maximum isometric force) and v_o (maximum velocity with no load) were made. The slope of the straight line representing lengthening, B_L, is made six times greater than that for shortening, B_s as shown in Fig. 8b. The following parameters were selected:

$$P_o = 100\text{kg}$$
$$v_o = 0.01\ \text{m/sec}$$
$$B_L = -6\text{x}10^4\ \text{kg-sec}^2/\text{m}$$
$$B_s = -10^4\ \underline{\text{kg-sec}^2}/\text{m}$$

Force velocity relationships beyond the initial velocities pose a problem. If a muscle is shortened at a velocity greater than that at which it is capable of shortening itself, it exerts no force. Thus P is zero for velocities greater than v_o. When a muscle is stretched more rapidly than its critical stretching velocity, several things may happen. A phenomenon called "slipping" or "yielding" occurs first. Hill (22) wrote: "Under a load rather greater than it can bear an active muscle lengthens slowly, under a considerably greater load it 'gives' or 'slips.' We can regard the first process as 'reversible' in the thermodynamic sense, the second as largely 'irreversible '".

Katz found (31) that contractile structures of a muscle may be damaged if its velocity of lengthening is increased rapidly while the muscle is active. Normally the Golgi tendon organ (a tension-sensing device) reflexly causes the muscle to relax before this damage occurs.

It is expected that simulation will seldom operate in the critical region. Thus a compromise between complete relaxation and increased resistance caused by slipping is used. For velocities of lengthening which are

greater than critical, the BIOSIM model saturates at 2P as shown in Fig. 8b. When a muscle is stimulated at half maximum, we assume that the active muscle has the same length, but only one-half the cross-section area, as the fully activated muscle. Therefore the force output, proportional to cross-section area, is halved while the maximum velocity of shortening, proportional to muscle length, remains constant. These relationships between force and velocity in a half-activated muscle may be obtained by applying the P_o and v_o values for $\alpha = 0.5$ to our original approximations, that is, straight-line relationship and $B_L = 6B_s$. The resultant relationships are shown in Fig.8b and expressed in Eqs. (2) and (3)

$$F_{muscle} = \alpha(P_o + B_s v) \qquad 0<v<v_o \tag{2}$$

$$F_{muscle} = \alpha(P_o + B_L v) \qquad -\frac{v_o}{6} < v < o \tag{3}$$

$$F_{muscle} = 0 \qquad v>v_o$$

$$F_{muscle} = \alpha P_o \qquad v< -\frac{v_o}{6}$$

Figure 9 illustrates a model experiment conducted on the 709 computer (69). The model response in displacement

has a shape similar to that of a plot of the same variables for frog muscle in the Fenn and Marsh experiments. The dead time in the physiological studies is the time taken for the muscle isometric force to build up to the static friction in the load force. A comparison of velocity versus time in the model with Wilkie's data was also obtained.

The asymmetrical characteristics become very important in smoothly terminating a rapid voluntary movement. The asymmetry increases the effective damping over that of a possible symmetrical relationship. Addition of the postural system (muscle spindle and afferent feedback) as shown by the middle recording of Fig. 3 further increases man's power of rapidly damping his motion. Therefore, an examination of the muscle spindle is in order.

Muscle Spindle Physiology: BIOSIM Model

The muscle spindle receptor is a differential length receptor found in parallel with contractile fibers of muscles of many species as first demonstrated by Fulton and Pi-Suner (17). Its importance in human motor coordination is great, since its positional feedback characteristics are basic to the stretch reflex. It may

also send kinesthetic information to higher centers to help control complex motor coordination tasks. A model of this mechanism has been formulated as one component in the more complete model of human motor coordination.

The spindle is connected in parallel with the muscle contractile fibres as shown in Fig.10a and its direct mechanical effect on the muscle is negligible. The inertial forces resulting from accelerating the mass of muscle may be neglected in comparison with elastic forces for the low accelerations involved. Thus, we can consider the length of the muscle, X_m, to be an input produced either through the alpha efferent nerve or through stretch by external forces. The afferent nerve carries information concerning the length of the nuclear bag to the central nervous system. Continuous signals representing short term average pulse frequency are used in our model. The gamma efferent nerve excites the contractile element, or intrafusal fiber, of the spindle. It is another input that may bias the output of the nuclear bag or may, perhaps, act indirectly as an input that might control movement; this follow-up servo configuration has been suggested by Merton (44) and Roberts. This input is simplified in our model to a change in length of the intrafusal fiber, X_γ , and added to X_m (Fig.10b). The

dynamics of this input may have to be considered more explicitly upon investigation of coordinated movements through this input.

The response of the spindle receptor to a step input of stretch, as found by Lippold, Nicholls and Redfearn (38) (Fig. 11a) shows approximately 400 percent overshoot; this differential effect is called the "phasic response". After approximately 200 msec the output settles down to its steady-state value; the steady-state response is called the "tonic response". They also found good evidence to suggest that the phasic response is caused entirely by mechanical factors and that the mechanical-to-electrical transducer is a no-memory device. This information has been incorporated into our model.

The transfer function for the mechanical model of Fig. 10b is of the form

$$\frac{X_{SB}}{X_m} = H(S) = G_m \frac{(T_1 S + 1)}{(T_2 S + 1)(T_3 S + 1)}$$

Table 2 summarizes the rough estimates of the spring constants and damping tonus of the spindle receptor model, based on physiological evidence and analysis of transient and steady state responses.

TABLE 2

	HUMAN	FROG
K_F	0.1 newton/m	0.1 newton/m
K_B	0.4 newton/m	0.5 newton/m
K_T	1.5 newton/m	1.3 newton/m
B_F	0.015 newton sec/m	0.5 newton sec/m
B_B	0.015 newton sec/m	2.9 newton sec/m

Inspection of Granit's data (19) shown in Fig. 11b reveals that the tonic input-output characteristic of the spindle receptor is somewhat parabolic. Furthermore, other curves show that the tonic gain increases with increased gamma bias (X_γ). A squaring operator fits these data quite well (Fig. 12a). The increased slope at $X_\gamma 2$, as compared with $X_\gamma 1$ shows the increased small-signal gain for an increase of gamma bias. This reconciles the opposing views of Granit who claimed the gamma input is an input bias level, and Hunt and Kuffler (27)(28) who felt it had a role in maintaining sensitivity of the spindle to stretch. Both functions are subsumed in our model. Negative signals cannot be generated by the transducer; thus, a saturation at zero is inserted before the squarer (Fig. 12a). Also, there is an upper limit to the number of impulses that can be carried by the spindle efferent nerve; an upper limit saturation provides this limit.

An asymptotic Bode plot of H(s) in Fig. 12b illustrates the approximate frequency response of the model to small signals in normal operating ranges of bias. Note that between 7-18 radians per second the response is to muscle velocity. In this range the spindle receptor should cause viscous damping effects on the over-all

system rather than spring effects. A sinusoidal analysis of the stretch receptors in the frog's extensor longitus digitus, IV muscle was undertaken by Houk, Sanchez, and Wells (25). A sample record of their work is shown in Fig. 13a. Figure 13b illustrates the amplitude vs. frequency plot and the phase vs. frequency plot. Although their data are crude first runs, the break frequencies of rough asymptotes drawn on the gain plot of Fig. 13b were used to form a tentative transfer function

$$H(s) = \frac{K(30s + 1)}{(5s + 1)(0.35s + 1)} \qquad (5)$$

with K = 27 pulses per second/mm. By assumption and calculation similar to those above, the values in Table 2 for the frog were obtained. These findings, although crude, lend support to the model and provide some feeling for the functional significance of the anatomical structure of spindle receptors.

Gamma Ratio

The spindle system has a differentiating action over an important part of the frequency range; 1/2 - 3 cps. Since it is in the feedback path of the proprioceptive

stretch reflex, or postural servomechanism loop, this obviously acts as a damping element in movement. It can be shown that in ordinary movements the muscle apparent viscosity is of importance only in a region of lesser interest; below 0.25 cps. The muscle damping is the result of asymmetrical energy conversion saturation and thus has, strictly speaking, no restricted frequency range.

However, the spindle is an ideal damping element and the gamma bias which sets its activity level and gain is well suited to modify the system damping on command in an adaptive fashion.

Boyd (7) and Matthews have found another type of spindle receptor lacking the nuclear bag. Thus, the dashpot is missing and a quite different dynamical situation results. The intrafusal muscle fiber without a nuclear bag, but with an afferent receptor is innervated by a different gamma efferent motor fiber type; the gamma-two fiber. While this has not been worked out quantitatively, it is clear that the gamma-two is more like a pure gain element as opposed to the gamma-one which operates as a differentiator. Thus, by altering the gamma ratio, gamma-one activity divided by gamma-two

activity, the damping can be altered independently of the loop gain. This permits even more powerful control of overall dynamics and damping, and similarly is even more suited for the adaptive role.

Summary

The postural and the voluntary control systems which are important to the manual control system are reviewed utilizing various anatomico-physiological data and current servoanalytical investigation in order to present a relatively simple analytical model of the system.

III. DYNAMIC CHARACTERISTICS OF THE MOTOR COORDINATION SYSTEM IN MAN

Introduction

The behavioral characteristics of the human motor coordination system should be quantitatively defined before testing our model. The methods discussed in this section represent attempts to accomplish this quantitative definition for steady-state behavior.

Linearity is a reasonable approximation in many aspects of this system, as certain control experiments show, and thus frequency response data may be used for analysis.

Experiments in this section indicate the presence of a sampling system similar to the one present in the eye tracking system. In the eye movement system the muscles are so powerful with respect to the mechanical characteristics of the eyeball that the limiting dynamics are the neurological control dynamics. With the hand, however, inertia of the forearm, the requirement for fuller activation of the muscles and the resultant apparant viscosity of the muscles all limit system bandwidth. Thus, the sampled-data phenomena that are clearly seen in eye movements are partly obscured in manual control behavior.

Experiments

In an effort to develop a system model which fits the well-known input-output data and clarifies anatomical, phsyiological and neurological facts, Stark et al. (71) studied rotation of the wrist in an awake, cooperative human subject. In the first series of experiments wrist movement is limited to pronation and supination by means of the apparatus illustrated in Fig. 14. The pointer serves as input signal. The subject is instructed to keep the indicator on the handle in coincidence with movement of the pointer. The instantaneous positions of both pointer and handle indicator are recorded.

Predictable input experiment. Figure 15 illustrates the sinusoidal pattern of the input pointer in this experiment. The dynamic characteristics of the hand during a steady state predictable experiment is obtained by measuring gain and phase lag from the recordings. These analyses of gain and phase lag are based on average response. The variability of phase lag does not become large except at frequencies which are on the limit of the ability of the human motor coordination system.

Complex input experiment. The input shown in Fig. 15 is completely predictable, and provides little useful information about the basic neurological control system. It is therefore important to use an unpredictable input. A stochastic signal may be approximated by adding a number of non-low-harmonically related sinusoids to form a fairly complex input signal. This signal is not an analytic function to the prediction apparatus of the human operating instantaneously on the pointer movement. Only the sum of a small number of these sinusoids, three, if they are relatively prime to each other, are required to make the prediction apparatus of the subject inadequate. This was demonstrated in early experiments which showed no reduction in phase lag or amplitude error with considerable practice, and indeed knowledge of the structure of the input signal by the subject. Verification for this interesting physiological result is contained in the analysis section under the discussion of Fig. 23.

Both the single input frequency of interest, and its component of the output were recorded, as shown in Fig. 16. The phase lag between channels three and four has two components: one due to the subject, another, to the pointer servo and filter. The phase lag due to the pointer servo and filter were eliminated by calibration.

The pointer and handle servomechanisms contain a summing network, an electronic amplifier, a servomotor, and a controlled rotational element attached to the servomotor shaft. This rotational element is a pointer on one servo, and a handle on the other. Each servo has position and velocity feedback, and these two parameters as well as the gain are individually adjustable. The "stick dynamics" were controllable through these adjustments.

The dynamics of the handle servomechanism were adjusted so that the subject rotated the handle against a spring force of 1 inch-ounce-second per radian. The stiffness was an important factor limiting the subjects' response. It was not frequency-dependent, however, and therefore did not change the form of the Bode plot. The viscous friction was a much smaller factor, even though frequency-dependent. It did not contribute as much torque as the stiffness until the frequency reached 15 cps. The frequency responses of both servos were obtained in the usual manner, and neither limited the experiment or experimental accuracy.

Predictable input and transient experiment. The response of a subject to a suddenly applied sinusoidal input

signal from the pointer goes through three successive phases. In the upper recording of Fig. 17 the movement of the pointer is displayed, and on the lower recording, the movement by the subject. The first of the three phases is a reaction time delay, and is the period between numbers 1 and 2 along the time axis in Fig. 17. When the subject finally makes a movement and enters into the second, or "neurological response" phase, shown between numbers 2 and 3 along the time axis in Fig. 17, he generally starts in the proper direction to catch up with the pointer. Sometimes the initial movement of the subject is in the opposite direction, but the subject soon corrects himself and attempts to follow the pointer movement. For a variable period of time lasting approximately 0.5 to 1.0 seconds during this neurological response phase, there is a phase lag in the subject's following movement as well as an amplitude difference, generally resulting in a fairly sizeable error. The subject, however, soon predicts the future course of a simple sinusoidal motion and is able to phase-advance and correct his following movement so that he eventually synchronizes his response with the input signal, as shown to the right of number 3 along the time axis in Fig. 17. It is this third or "predicted response" phase of operation

which is the steady-state response of a subject to a simple predictable input. Rarely does it take a subject longer than a second or two to get into phase three and remain there.

Unpredictable input experiment. In order to prolong the "neurological phase" and eliminate prediction, experiments of the unpredictable signal input type were performed. The top recording of Fig. 18 shows the sum voltage of the three input sinusoids, as they appeared at the position feedback potentiometer of the signal input pointer. The waveform as seen by the human eye across the stretch of graph paper, comprising 20 seconds of time, shows certain regularities. However, to the subject who is concentrating on the motion of the pointer, attempting to remain in coincidence by moving the handle --loaded with moderate viscosity and stiffness--, and having only instantaneous knowledge of pointer position, the signal in the top recording appears quite unpredictable.

The second recording of Fig. 18 shows the total output of the subject in following this complex input signal and it is seen to resemble the form of the input with some degree of precision.

The components of the input and output signals which were analyzed are shown in the remainder of this figure. The third recording represents one frequency component of input. The bottom recording is obtained from the total output by passing it through a narrow bandpass filter set to the single frequency of the input signal to be studied. With the data obtained from the simplified input and output, gain and phase lag parameters between input and output were determined exactly as in the steady-state response to a predictable input. Thus the prediction apparatus of the human subject is prevented from dominating the physiology of the neurological response.

Linearity. An essential portion of the main experimental design is a study of the variation in subject performance over the range of input amplitudes. To utilize linear system analysis a check on the linearity of the subject over the ranges of amplitudes of the experiment is required. The experiment of Fig. 19 shows the effect of different input amplitudes. Again, the four recordings are labeled as they were in the previous figure. The central frequency component of the unpredictable input was mixed at three pointer amplitude levels, $\pm 10^{\circ}$, $\pm 5^{\circ}$, and 0°; the central frequency component of the output obtained in each of these conditions is demonstrated

in Fig. 19. Notice the presence of the remnant response, due to subject motion which transiently shocks the filter. This is most apparent in the 0^{o} recording, and its amplitude is considerably smaller than the signal obtained under normal experimental conditions.

Experimental data justifying the linear approach are displayed in Fig. 20, linearity control experiment. This is a plot of the output amplitude in degrees versus the input amplitude in degrees, for three frequencies commonly used in the experiments. These frequencies were the central frequencies of a complex unpredictable input for three different sets of input triads of frequencies. Notice that the subject's response at any one frequency is linear over a very wide range of input amplitude. The differences in slopes for the three frequencies indicate some of the information obtained in the Bode plot of the subject; it is easier for the subject to follow 0.6 cps than 1 cps, and easier to follow 1 cps than 2.5 cps. Hence, his gain is higher at 0.6 cps than at one of these higher frequencies. The data used in the experiment of Fig. 20 were obtained from experiments designed to eliminate trend effects. A rough estimate of the variance of this type of experiment is indicated by the scatter of the points in this figure.

Freewheeling experiment. One further type of experimental mode remains to be described. In this situation the pointer is not used as an input signal, but the subject is asked to oscillate the handle back and forth as rapidly as possible with varying amplitudes of oscillation being requested.

Figure 21 shows a set of freewheeling mode experiments of the type mentioned in the introduction to this section. These illustrate an interesting fact concerning the human motor coordination system. The upper recording shows a set of oscillations with a mean frequency which is quite high. This was obtained by asking the subject to rotate the handle as fast as possible, picking a comfortable amplitude of swing. It was noted that the subject always let his muscles go quite lax when doing this experiment. This means that the system might well be operating as an open loop bang-bang control system.

In the second recording, the subject was requested to oscillate as rapidly as he could, provided always that his hand was stiff enough to be able to receive a blow without being deflected very much from its course. In this condition, the subject kept his agonist and antagonist contracted against each other to a considerable degree.

The lowest recording of this figure indicates still another and very interesting operating mode. The subject is told to keep the frequency as high as possible, in the mode of the first part of the figure. However, he is instructed to imagine the pointer oscillating back and forth as fast as he can possibly track it and is then instructed to track this imaginary pointer. The oscillation is markedly slowed. Perhaps because of the necessity to transmit and process all control signals through the imagery of the mental tracking process.

Frequency Response Analysis

Experiment. A large number of frequencies were arranged in random order and the tracking responses of fairly well trained subjects were studied. At each frequency the responses to both predictable and unpredictable inputs were obtained.

The ratio of the amplitude of the central frequency component of the unpredictable input to the amplitudes of the outer frequency components was either 1.0, 0.5, or 0.0; corresponding to $\pm$ 10°, $\pm$5°, and 0° respectively. Gain and phase lag analysis of the experiments was done immediately following each run. In addition a set of

freewheeling experiments was performed; these represent limits of the physical capacity of the hand in any type of oscillation, whether coherent with an input signal or not.

Analysis. The basic relationships which will be displayed are those of gain and phase lag as functions of frequency. A composite Bode plot is shown in Fig. 22. The response to the predictable input has a gain of one for almost the entire range of frequencies studied. At approximately three cycles per second the gain decreases somewhat until the end of the range. However, the data are somewhat scattered in this high frequency end of the behavioral range of the subject.

To delineate further the actual frequency range of the mechanical behavior of the human hand in this experiment, condition one of the freewheeling experiment is also plotted on Fig. 22. There is, of course, no "gain" value possible for this freewheeling, because there is no physical input signal to the system; therefore, the amplitude is plotted on Fig. 22 in magnitude figures relative to the driven responses. It can be seen that an almost vertical line becomes less steep at low freewheeling oscillation amplitudes, and this line apparently represents

the maximum performance of the hand in amplitude and frequency.

The curve showing the response to an unpredicted signal over this range of frequencies is markedly different from the other two. This unpredicted response shows a gain of one up to 1 cps and then a gradual reduction at a minus 1 slope with increasing frequency except for two suggestive peaks at approximately 1 cps and 3 cps. There is a large area beyond 1 cps between the gain curves of predicted and unpredicted responses. This region represents increased performance of the system due to the prediction operation which enables the subject to correct phase and gain error in his response, and so reduce the total error.

In Fig. 23 are shown the phase data as a function of frequency corresponding to the gain data of Fig. 22. The upper curve shows the phase response to the predicted signal input. The phase changes from 0° to a slight phase advance. Above 1 cps, while the mean phase relationship continues to be one of slight phase advance, the scatter of the phase increases markedly. The cone-shaped limits at the high frequency end of the upper curve are crude variance limits of this phase behavior in the predicted experiments.

The lower curve in Fig. 20 represents the phase relationship obtained with an unpredictable signal input. Several interesting points are seen in this phase plot; for one, the phase lag is steadily increasing with frequency, an increase more rapid than is possible for a minimum phase lag system having the gain characteristics of Fig. 19. This means the human servo has a non-minimum phase lag element or elements, when investigated as a linear servo. Another aspect of the phase curve is its several peaks and notches, showing irregularities corresponding to peaks of the gain curve and confirming the presence of these features in the gain curve.

Figures 24 and 25 show the gain and phase plots of the unpredictable experiment for two amplitudes of the central frequency components of the input triad. The two gain and the two phase lag curves are very similar, not only in their general patterns but also in much detail. There are small but significant differences between the responses to the two amplitudes; however, these differences in the gain and in the phase curves are similar in direction. For example, the high frequency peak in the gain curve of the $\pm 5^{\circ}$ amplitude is at a lower frequency than the high frequency peak of the $\pm 10^{\circ}$ amplitude gain curve. It can be seen that the phase

crossover frequency is at a lower frequency in the $\pm 5^{o}$ phase curve than in the $\pm 10^{o}$ phase curve. These correlations show the data to be consistent within themselves and suggest that the detailed features are reliable observations. The effect of amplitude change demonstrates the presence of some nonlinearities in the system. This is similar to the experiment reported by Stark and Baker (68) wherein the transfer function characteristics of the pupil servo control system were changed and the frequency of the high gain oscillation which represented its resonant peak was shifted in a parallel manner.

Figure 26 is a polar plot of gain and phase data from the unpredictable experiment. This Nyquist plot of gain as a function of phase lag has frequency as a monotonically increasing function clockwise around the curve.

Summary

The dynamic characteristics of the human motor coordination system differ depending upon the physiological state. By using complex inputs the predictive apparatus is eliminated and steady-state experiments can be used to study the neurological response. A series of linearity

and other control experiments elucidate the limitations and adequacies of the methods. Some of the features shown are resonant peaks near 1 and 3 cps and both minimum and non-minimum phase elements.

IV. TRANSIENT RESPONSE DYNAMICS OF THE MOTOR COORDINATION SYSTEM IN MAN

Introduction

The methods discussed in this section represent attempts to quantitatively define the transient dynamics of the motor coordination system in man. A new hypothesis is suggested which separates adaptation into two components: (1) a peripheral adaptation involving gain settings and dynamic control of the peripheral postural control system, and (2) a central prediction of input characteristics and a pre-fitting of ballistic command signals for compensation.

A study of the time domain behavior in this section exposes the intermittent characteristics of manual control behavior. Further, it permits demonstration of the time-varying and adaptive nature of the movement control system. First, the importance of the prediction operator is shown. Next, interactions between the eye and hand control mechanism are seen to be intricate. Mechanical disturbance impulse responses defining the postural control system are demonstrated to be fitted by quasi-linear second-order system models, while responses to visual inputs, involving an interaction between the voluntary control system and the postural servo, are more complex.

Most quantitative descriptions of human motor coordination rely extensively upon frequency response data both because it is possible in those steady-state experiments to maintain the control system in a quasi-stationary and quasi-linear state, and because of the power of analytic mathematical methods in the frequency domain. The aim, however, is not only to approximate accurately behavioral characteristics of the system by some analytical expression but also to determine the underlying neurological and physiological mechanisms which compose human movement control. For this purpose the time domain shows more clearly and rapidly the changing characteristics of the movement control system under different experimental operating conditions. Also, certain interesting discontinuous or sampled-data properties become apparent when viewed in the time domain. The experimental results referred to in this section are all based on the results of Stark, Houk, Okabe and Willis at M.I.T.

Experimental Apparatus

The experimental apparatus was designed to handle transient visual and mechanical inputs, to quantitate the steady tension level and to record both responses in the form of wrist rotation and angle of horizontal gaze of the eyes. Predictability of the target position was controlled and eye and wrist movements were

compared in order to ascertain their respective roles in visual-motor tracking. With the use of visual and mechanical impulses it was possible to compare the voluntarily controlled movement to the subsequent damping. This following phase was shown similar to the position regulation response to mechanical impulse disturbances.

Experimental Method

The method of studying the rotation of the wrist of an awake cooperative subject has been described in the previous section. Certain modifications were made in the apparatus as shown in Fig. 27. Accordingly a mirror galvanometer was employed for visual target generation, having a frequency response flat to 80 cps when set for critical damping and being linear over a range of $\pm$ 25°. A wide range of stimuli could thus be employed.

A further addition to the apparatus was a mechanical pendulum whose position was monitored by another potentiometer, in addition to the one measuring the response of the subject and the rotation of the wrist. It delivered impulses of torque to the handle shaft and thus to the subject's wrist.

Travel and rebound angles, length and weight of the pendulum, and elasticity of impact determine the input energy injected into the system.

For measuring voluntary tension, the height of the mercury column controlled by a sphygnomanometer cuff attached to the forearm was used.

A number of experiments comparing eye and hand movement were performed. Direction of gaze of the subject was monitored by a pair of lamps and photocells connected in a bridge so as to produce an output voltage proportional to differential area of the sclerae on either side of the iris. The method has been described in a recent paper on eye tracking movements (74).

Experimental Results

Square wave experiments. The importance of sufficiently controlling those characteristics of the input signal which make it either predictable or unpredictable has been experimentally demonstrated for both the hand and the eye tracking control system (71)(74). The following experiments were designed to study these input characteristics and some of the interactions between hand and eye movement.

The experimental records such as those of Fig. 28 show a subject responding to an unpredictable step change in target position. In addition to time functions as shown in Fig. 28, several other displays of system behavior were obtained. These include sequential patterns of response times as in Fig. 29, histograms of response times in Fig. 30 and median response times as a function of frequency of input square wave in Fig. 31.

When the steps are unpredictable or when the period between steps is apparently too long for predictions to be attempted, response times show an average value of approximately 0.25 seconds (Figs. 28a, 28b, 30a, 30b). If the time interval between target jumps is reduced and if dynamical characteristics of the mechanical system --(muscles, loads, apparatus)-- permit rapid following movements, then the responses often show effects of prediction. Prediction can be observed most simply as a diminution of individual response times as in Figs. 28b, 28c and 28f, as well as in the median response times shown in Fig. 30c.

A negative response time sometimes occurs if the subject anticipates the target jump. Furthermore the negative response time may be large enough to permit the subject to arrive at the new target location before

the target does, even after allowing for time of actual movements; this is termed "over prediction". The sequential pattern of response times in Fig. 29 shows that there is no consistent trend effect (after initial transient) in these changing response times but rather an irregular series of delays (positive response times), reduced delays and slight anticipations (predictions), and larger anticipations (over predictions). The dependence of median response time on frequency of repetitive square wave pattern is shown in Fig. 31. Prediction is the rule at the higher frequencies. Eventually at a certain point, the dynamics of the wrist and unloaded apparatus prevent accurate determination of response time even with the use of derivative of input and output as demonstrated in Fig. 28d.

Observation of the subject's eyes during hand tracking indicated that eye movements occurred when the hand is tracking a square wave target motion with a frequency of 1.3 cps and an amplitude of $\pm 10^{\circ}$ or $\pm 20^{\circ}$. However, the hand is still able to track at 2.5 cps, while the eye appears stationary. It appeared that the hand system could operate in a higher frequency range than the eye movement system, suggesting that eye tracking is not a pre-requisite for hand tracking.

Eye-hand comparisons. The eye muscles have considerable power with respect to their constant load, the eyeball, and show faster rise times than the hand when tracking rapidly alternating signals as shown in Fig. 32. Examples of eye and hand responses both recorded simultaneously to irregular steps and slower regular steps are also illustrated in Fig. 32. For these inputs the eye has shorter response times than the hand. At moderate frequencies (0.7 to 1.0 cps) the hand develops prediction faster and to a greater extent than the eye. At higher frquencies (1.2 cps) the hand shows considerable prediction, while the median eye response time begins to lag (see Fig. 30c, 31 and 32c).

At low frequencies there is some correlation evident between eye and hand response times as is shown in Fig. 32. However, at high frequencies, the eye may spontaneously stop moving without noticeably interfering with hand tracking, as clearly demonstrated in Fig. 33. The target swing was $\pm$ 20^{o} in this experiment. The triangular points in Fig. 31 are data from wrist tracking movements while the eye was held stationary, again showing hand movement independent of eye tracking movement under these experimental conditions. On the other hand, hand movement clearly and consistently seems to aid the eye tracking

movement control system. Figure 33b shows a typical example of improved eye movement performance when hand tracking occurs. Similarly, deterioration of performance is noted when hand tracking is stopped as the result of an instruction to the subject.

Impulse response experiments. Experiments were performed in order to attempt to quantitate the mechanical state of the position control system of the wrist and the ability of the voluntary tracking system to reproduce impulses of visual target motion.

The mechanical system of the pendulum, apparatus and forearm for these impulse response experiments are represented in the mobility analog of Fig. 34. With the use of equivalent second order systems for the apparatus and the wrist with all elements in parallel, subtraction of the equivalent admittance values of the machine from the respective values of the total response is permitted.

The mechanical impulse response ($h_m(t)$) of the wrist seems to be well fitted by a simple underdamped second order equation as shown by the examples in Fig. 35. Approximate values found for the equivalent mechanical parameters of wrist rotation are: inertia: $J = -0.5 \times 10^{-4}$ newton-meters-second^2-radians^{-1}; viscosity, $B = 1.5 \times 10^{-3}$ newton-meters-

second-radian^{-1}; and elasticity, K = 2.0 x 10^{-2} newton-meters-radian^{-1}. The negative value for inertia is the result of subtracting two larger values and is not believed to be significant.

The characteristics of the response ($h_v(t)$) of the wrist to an impulse of visual target movements are more complex, as shown in Fig. 35b. It is postulated that $h_v(t)$ has two phases: the first, consisting of the time delay and the first overshoot, is considered a visually driven response. After a transition period, the second or "follow-up" movement, $h_f(t)$, is considered to be controlled by the postural reflex loop attempting to bring the hand to rest. Thus it is only this second portion, $h_f(t)$, that is comparable to the mechanical response. However, only 30% of the $h_v(t)$ records yielded $h_f(t)$ portions that could be reasonably described by a second order fit, and even these data show considerable scatter.

Effects of tension on impulse responses. Striking effects were obtained in freewheeling experiments as shown in Fig. 36 with change in subject set, especially with change in tension set to control expected impulse disturbances that occurred randomly. In order to further

quantify the behavior of the control mechanism for movement and posture, the impulse experiments were conducted at a variety of levels of tension. Five different levels of tension produced smoothly graded response characteristics from most relaxed to most tense states.

The most striking effects were the decrease in amplitude of $h_m(t)$, the mechanical impulse response with tension; this was accompanied by an increase in ringing frequency as can be seen by comparing Figs. 35a and 35c. Similar effects were shown in several hundred experiments on about six subjects. Figure 37 shows a plot of the variation of the equivalent mechanical parameters J, B and K as a function of tension. K is a strong function of voluntary tension, while B increases only slightly with increase in tension; as before, values of J are small, the results of subtracting two large values, and are not believed to be significant.

The poles of the equivalent second order system are at $S = -\gamma \pm j\omega_d$ where γ and ω_d are the real and imaginary components of the complex poles. The effect of tension on the system is shown in Fig. 38 by the locus of upper half plane poles. The principal effects of an

increase in voluntary tension on the $h_m(t)$ equivalent second order system are an increase in absolute bandwidth and a slight decrease in damping constant. When J, B and K parameters are determined for $h_f(t)$ portions of $h_v(t)$ and the pole configuration computed it is seen that the pole path as a function of tension is rather similar for $h_f(t)$ and $h_m(t)$ (Fig. 38). Considerable scatter in $h_f(t)$ poles can be noted. The principal correlation of the $h_f(t)$ equivalent second order system with increase in voluntary tension is increase in absolute bandwidth.

As discussed above the response $h_v(t)$ of the eye-forearm rotation system to a visual impulse is considerably more complex than the response $h_m(t)$ to a mechanical impulse, and only the "follow-up" portion $h_f(t)$ was compared to the mechanical response. Nevertheless, for both visual and mechanical response, Figs. 35b and 35d show that the same qualitative changes appear with increase in tension. When the $h_v(t)$ curves are parameterized as to (a) number of ringing cycles; (b) average ringing frequency; (c) amplitude ratio; and (d) time delay, all as a function of tension, it can be noted (see Fig. 39) that similar changes (b), or lack of change (a) and (d), occur with both $h_m(t)$ and $h_v(t)$ responses. Time delay is, of course, zero for $h_m(t)$.

Little change in amplitude or shape of the initial portion of $h_v(t)$ or in the time delay is seen as a function of tension. It was felt that unpredictable changes of target position were not fully accomplished in this experiment, because the target pulse was always of constant width, amplitude and duration. With the removal of these restrictions interesting phenomena appeared relating to earlier studies on psychological refractory period and to sampled data approaches to these neurological control systems.

Sampled data characteristics. Recent studies have suggested that the eye movement tracking system can be treated as a sampled data system (84). For present purposes it is sufficient to realize that the discrete nature of sampled data systems is similar to the notion of a refractory period, a common phenomenon in neurophysiology. Other discontinuous control systems such as quantized systems have properties in common with sampled data systems, and indeed the hand movement system demonstrates characteristics of quantization as well.

When slowly moving ramps are used as input target signals, and the subject tracks this input with a device that offers very small mechanical impedance, a response

similar to that of Fig. 40 occurs. The output response consists of step-like changes in position which occur with irregular intervals and amplitudes. The output signal rotary motion transducer had an effectively infinite resolution, and neither friction nor any other component of the mechanical impedance of the transducer was of sufficient magnitude to play an important role in the dynamics of the system. Early studies utilizing this input suggested that the known sampled-data properties of the eye tracking system were possibly related to these steplike responses but recent experiments have failed to confirm this conjecture (50).

When pulses of varying width are used as input target signals and are presented irregularly in time, a response similar to that shown in Fig. 41a is obtained. Delays of approximately 150-250 msec before the rapid response motions occur for both leading and trailing edges of the input target motion. This delay in response has several components in addition to nerve conduction time and is sometimes called the psychological refractory period. When a pulse of extremely narrow width is supplied unpredictably as an input target motion, a normal delay occurs before the response movement to the leading edge of

the input motion, as shown in Fig. 41b. However, the response motion to the trailing edge of the input motion has a much prolonged delay, 400 msec in the case illustrated in Fig. 41b. This prolonged delay can be accounted for as a normal refractory period that starts after the initial response motion, rather than being triggered by the trailing edge of the input target. This behavior would be characteristic of a type of sampled-data system. Contrast this widened response to a short pulse with the rather narrow responses of Figs. 35b and 35d. Here the pulse is unpredictable only in time of occurrence. The subject knows that any disturbance would be a short pulse and accordingly pre-programmed a double sequence of movements to match the short pulse when triggered by the appearance of a disturbance. Similar evidence has been shown for the eye movement control system.

For a motor coordination sampled-data system with the transient responses shown in Figs. 40 and 41, the frequency response to wide bandwidth inputs demonstrated a peak at one-half the sampling frequency, (or at approximately 2-3 cps for sampling intervals 0.16 to 0.25 secs), as well as an absence of coherent tracking characteristics at frequencies greater than this peaking frequency. There exists very little experimental data that clearly support

the occurrence of this suggested peaking frequency, since most of these experiments have used input bandwidths with either much lower frequencies than 3 cps or else too little power at these higher frequencies to obtain effective responses necessary to demonstrate the peak. Bekey (6) in the most complete study of sampled-data properties of the manual tracking control system, was able to show peaking at sampling frequencies only in spectral curves of error. However, Stark, Iida, and Willis (71) have described steady-state frequency response experiments that were not limited by these undesirable input spectrum characteristics and showed clear peaks in gain in the 2-3 cps region.

This clearly defined peak in the response spectrum supports the transient data and the idea that the human motor coordination system can be treated as a sampled-data control system. The various discrete models based on these observations are reviewed in Section V.

Discussion

Processing retinal information is clearly an early operation in hand tracking a visual target. This same information is necessary for eye movement control. Comparison and contrast of the eye movement control

system with the manual control system shows some surprising results.

First, the manual system can track rapidly alternating target movements of a repetitive predictable nature to an octave or two higher frequency than the eye, in spite of the much lower bandwidth of the output elements. The hand has a natural frequency, ω_n = 40 radians/second while the eyeball has a natural frequency, ω_n = 240 radians/second. Evidently the control and predictive apparatus for manual control is more effective than that for eye movement control.

Second, eye movement is not necessary for hand movement in spite of the rather large amplitude, $\pm$ 10° and $\pm$ 20°, tracking signals in the experiments. Clearly, focal fixation of the target is not required for the order of accuracy obtained in these experiments.

Conversely, the physical movement of the hand appears to reinforce the target signal input to the eye movement system so that adequate eye tracking may occur in borderline regions if the hand is tracking and may not occur if the hand is still. This evidence supports the contention that manual control dynamics are of concern here, and not some limitation secondary to eye movement control. Of course,

visual processing is still an integral part of the experimental conditions; it could, of course, be eliminated by proprioceptive tracking, one hand passively moved and the other tracking this motion, or perhaps by auditory input signals.

The neurological control system for motor coordination has been discussed in terms of two signals competing for control of the output elements. These output motor elements are the "final common path" of Sherrington (63), the alpha motor neurons and the muscles they control. The first of the competing signals is that carried by the feedback path of the position control system, the Ia afferent neurons from the spindle receptor system. The second of the competing signals is that carried by the corticospinal pathways subserving voluntary movement.

The two types of impulse inputs presumably test the state of the shared control of the alpha motor neuron. The mechanical impulse response, $h_m(t)$, has no associated time delay and thus tests the gain and dynamics of the postural or position servoloop. As such it is similar to the classical tendon jerk of the clinical neurological examination. Recently this system has been studied by simulation techniques (26) and the representation here

includes two important non-linear dynamical systems, plus time delays for nerve impulse conduction and a variety of saturation and asymmetrical elements. That this can be adequately represented by an undamped, linear second order system is indeed a tribute to the power of these simple analytic tools. The apparent spring constant of the hand is determined by the gain of the position servo, since restoring force is proportional to displacement error. An important non-linearity of the spindle is an increase in slope of the input-output curve with increased input, either by external stretch or by gamma motor neuron stimulation of the intra fusal fibers (26). As a consequence increased spring constant is predicted in the experiment with increasing tension.

The visual impulse response, $h_v(t)$, appears to be a time-delayed pre-programmed control signal, probably corticospinal in route, which is followed by a return to the postural control system with dynamics predictable by the $h_m(t)$ experiments. $h_f(t)$ and $h_m(t)$ have a similar dependence on tension. Evidence for the ballistic pre-programmed input comes partly from the marked disparity between the second order model of the postural system and the initial portions of the $h_v(t)$. More striking are

the results obtained when the duration of the pulse is made unpredictable as in the sampled-data experiments. Here a clear refractory period of about 200 milliseconds is demonstrated, certainly unrelated to the second order dynamics.

In the freewheeling experiment the competition between the voluntary control and the postural servomechanism is illustrated. With increase in mental tension while the subject is awaiting a random disturbance, the frequency of oscillation in successive movements is markedly diminished; the continual activation of the postural servo means that antagonists are of course active, and degrade performance. However, little evidence for reduction in amplitude of voluntary tracking or for increase in response time is noted in these somewhat predictable impulse experiments.

The sampled-data experiments are rather convincing on the basis of the prolonged pulse response, the peak in frequency response, and the irregular positional corrections for slow ramps. The results are especially relevant to the problem of eye and hand interaction. It has been firmly established that the response to unpredictable inputs by the eye tracking control system

can be well predicted by a sampled-data model (83). However, such phenomena as the irregular multiple step responses to a slow ramp are independent of visual tracking. Further, the sampled-data control system for the eye appears to be both position and velocity control while the manual tracking sampled-data seems to be only a position control system; thus indicating rather different origins of the control signals to these two complex motor outputs.

One point of interest is the distribution of response times for hand tracking of unpredictable targets (Fig. 30a); a narrow quasi-gaussian distribution with a mean of 0.24 msec. This indicates that the sampling times are not clock driven, but rather input synchronized; with some random deviations from mean response time (86). If they were clock driven one would expect a rather square distribution from one sampling time to two sampling times with perhaps some additional random variation around this square distribution. The clock driven distribution predicted by Wescott and Lemay (37) is clearly not found under the experimental conditions reviewed here.

Summary

Since the visual system is part of the tracking situation, the control of eye movements and hand movements were studied by comparing simultaneous measurements. It was seen that while the load dynamics of the eyeball were less restricting than the inertia, viscosity, and elastic resistances of the wrist, the hand was better able to follow repetitive square wave patterns at high frequencies (1.5 to 2.5 cps) because of its wider bandwidth control apparatus. Further, it was apparent that eye movement did not aid hand movement, but rather that hand movement helped eye movement at high frequencies.

Mechanical impulse responses, $h_m(t)$, testing the postural control system, were compared with visual impulse responses, $h_v(t)$, testing the voluntary tracking system. The former is well approximated by an equivalent second order underdamped system. The latter has two components, a visually driven initial response and a follow-up portion, $h_f(t)$; only the $h_f(t)$ is at all able to be approximated by a similar underdamped second order system.

On changing steady background levels to tension both $h_m(t)$ and $h_f(t)$ show dynamical changes in the direction of increased bandwidth with increased tension.

Finally, certain experimental evidence for sampled-data properties of the hand movement system is put forward.

V. DISCRETE MODELS FOR MANUAL TRACKING

Although the presence of intermittent behavior in manual tracking has been noted for many years, it is only recently that a concerted effort has been made to develop discrete models for the human operator. The motivation for this research has been three-fold. First, the research in quasi-linear models has reached the point where the gross characteristics are quite adequately described for a wide variety of tasks, and attention can be focused on the fine structure of tracking. Second, the widespread use of analog and digital computers permits real time simulation of models that might be too complex for analysis. Finally, the development and dissemination of the theory of sampled-data systems and the associated use of the Z-transform, originally developed for digital computer techniques, has enabled engineers to treat many discrete systems on a simple analytical basis.

Although many types of experiments have been brought to bear in forming the case for discrete or sampled-data models for manual tracking, most of them can be reduced to one of two closely related sets of observations. The first of these is the presence of <u>intermittent corrections</u> by the operator in tracking a continuous signal. Most

of these corrections are separated by intervals of 0.2 to 0.6 seconds, indicating that at least a portion of the operator's output results from a discrete process leading to sudden ballistic movements. The result of this intermittency is to provide output energy in the frequency range of 1-2 cps, and peaks in this range are observed in Fourier analysis and power density spectra (6). Notice that quasi-linear models can contain at their output only those frequency components present at their input, and therefore this "sampling energy" is included as part of the remnant.

The second body of evidence concerns the psychological refractory period, which describes the inability of the human operator to make two successive responses to discrete stimuli in an interval less than this refractory period of approximately 1/2 second. This behavior suggests a sampled-data model, which can process sensory information or perform output only at certain periodic intervals. Notice that for any quasi-linear model the response to successive stimuli would be the superposition of responses to each individual stimulus, and could never match the refractory delay.

The assumption of a discrete model does not imply that there are no continuous portions of the response. It

merely requires that some portion of the response or its derivatives be determined by a discontinuous operator. This point is emphasized in the early article by Hick (21):

> It is suggested that the notion of discontinuity in the human operator may usefully refer to changes in the characteristics of his behaviour, not necessarily sudden, but such as to indicate separate points between domains where different continuous functions are reasonably applicable. For instance, a characterisation which shows periods of constancy interspersed with periods of change may be placed in this class.

Historically, the first sampled-data model for manual tracking to be developed and tested was by Ward (79). This model, as redrawn by Bekey (6) is shown in Fig. 42. Although this model contains sampling circuits of 0.5 sec period and a hold circuit, both of which are common to all later models, it does not perform very well quantitatively in matching either time or frequency domain data.

Bekey's Model for Manual Tracking

Bekey, in his sampled data model, recognized that the specification of the type of hold circuit following the sampler is of great importance. (A zero order hold $(1 - e^{-Ts})$ keeps the output signal constant between samples. A first order hold $\left[(1 + \frac{Ts}{s})(\frac{1 - e^{-Ts}}{s})^2\right]$ updates the output at each sample instant and imparts to it a rate equal to the average input rate over the last

interval. See Fig. 43.) His proposed model of the human operator tracking a random input in a compensatory loop is shown in Fig. 44. K_E represents the simple gain of the external controlled element, K is the operator gain and T_N the neuromuscular time constant as used in quasi-linear models. The switch represents the sampler, which takes an instantaneous sample of the error every T seconds and transmits it to the hold circuit.

Using only the frequency domain characteristics as a criterion, Bekey found that the first order hold was more appropriate than a zero order or modified first order. With a first order hold he was able to reproduce the "sampling peak" in the error spectra and still give a low frequency fit which approximates that of the quasi-linear models.

An example of the fit to the experimental data for the spectral density of the operator's response is shown in Fig. 45. The continuous model is a simple quasi-linear one of the form

$$G_c(j\omega) = \frac{K_{HE}\, e^{-j\omega D_c}}{1 + j\,\tau_c\omega}$$

in which the gain K_{HE}, delay D_c and lag time constant τ_c are adjusted for a best fit with the power spectrum. The discrete model sampling period (T) was selected to be twice the frequency of the peak in the experimental spectrum, and the delay (D_s) was chosen so that the sum of D_s and the effective delay of the hold circuit was made equal to the continuous model delay, D_c.

In the example shown in Fig. 45, it is seen clearly that the sampled-data model approaches the continuous model spectra and that both are good fits to the data for frequencies below 5 rad/sec. Between 5 and 10 rad/sec, however, only the sampled model exhibits a "sampling peak" to match the relative increase in actual output power. Notice that this range is at frequencies generally considered too high for true manual tracking, even though hand movement may show frequency components that high.

For the record shown the sampling period was chosen as T = 0.33 seconds to match the peak at 1.5 cps. D_s was required to be -0.06 seconds to keep the total delay equal to D_c.

The existence of negative D_s implies, strictly speaking, a predictive mechanism to overcome the delay inherent in a first order hold. A probable explanation is

that the velocity estimate, in a first order hold, based on the difference between the two last samples, is not a correct description. Since velocity can be sensed directly, it is likely that a more recent sample of velocity is used to compute response rate, thus implying less delay in the hold circuit and eliminating any requirement for a pure predictor.

The chief value in Bekey's model is the demonstration that a sampled-data model naturally accounts for the peak in output spectra and that it yields low frequency fits which are as good as the continuous quasi-linear models. The limitations on the model are that it was used to match only those results for which it was designed. Thus the location of the peak is forced to be matched by selection of T. Quantitative evaluation of the model in the time domain and in response to a variety of deterministic inputs would have been very valuable.

Lemay and Westcott "Velocity Triangle" Model

At about the same time that Bekey was developing a sampled data model based on the intermittency in continuous tracking, workers in England were investigating discrete models starting with the psychological refractory period and the shape of the manual step response as a basis.

Lemay and Westcott (37), following the work of Wilde and Westcott (80), proposed a discrete model based on the step response, and extended it to cover the case of tracking a continuous random input. They observed that the fundamental "ballistic movement" of quick hand movements is in the form of a velocity triangle. Such a dynamic shape could easily result from a programmed force of full positive followed by full negative, acting on the pure inertia of the arm. A straightforward means of simulating such a step response, consisting of a pair of parabolas yielding the correct magnitude of hand movement, is shown in Fig. 46 (37). It is interesting to observe that such a response is the time optimal one for the situation of limited available force.

To incorporate the velocity triangle concept and account for reaction time and refractory time, the discrete model of Fig. 47 (37) was developed. This model uses two asynchronous samplers of the same period to produce the desired reaction time and velocity triangle hand movement. "The muscle mechanism" is merely the positive-negative force program shown previously in Fig. 46. This model produces responses to step inputs which approximate those produced by the human operator. The step response can be made to overshoot slightly and

return to zero, as often observed in human responses, simply by increasing the gain of the samplers above unity.

In comparing this model with other sampled data models, it should be noted that the samplers are "free running" and are in no way synchronized to the occurrence of a step input. As a result, the reaction time shown by the model is uniformly distributed over the range between one and two sampling periods. As the authors point out the actual distribution of human reaction times is not uniform but rather peaks about an average value. Other studies show this average value to be approximately 0.3 seconds. (See Fig. 30, for example.)

As a reasonable test of their model developed for step inputs, Lemay and Westcott proceeded to compare their model with the human response in tracking a continuous random input signal, similar to the type used by Bekey, Elkind and others. As might be expected from previous attempts to match both step responses and continuous responses with the same model, the straightforward attempt failed. The step response model introduced too much phase lag for the continuous tracking. The authors then reasoned that in tracking a continuous signal the human operator is able to make use of the error velocity as well as error position, thereby introducing lead into the

system and reducing the apparent phase lag of the response. They therefore modified their model by the addition of the lead network preceding the sampled data model as shown in Fig. 48 (37). The best correspondence between model and human operator outputs were obtained with the following values of proportional and derivative gains:

$$a = 0.2$$

$$b = 0.52$$

These values of a and b, which indicate that the human operator relies heavily on error rate in programming his "basic hand movement", are not in agreement with the values which would be produced by an optimum controller as Lemay and Westcott point out. It is also worth noting that for this task of controlling a simple gain type of plant the quasilinear studies show that the human adopts very little lead and approaches a pure integrator plus delay (40). It can only be assumed that the necessity for lead, which Lemay and Westcott attribute to the ability of the human to predict the signal in a continuous case, is indeed necessary to overcome the excessive delay resulting from straightforward transfer of a step response type sampled data model.

With the lead network predictor the discrete model for tracking continuous inputs achieves 87% correlation with

the actual output in one case quoted by Lemay and Westcott. Of more interest, however, is the ability of this model incorporating the velocity triangle concept to match the operator's output velocity in such a tracking task. Figure 49 is an example of the good correspondence between operator and model velocity (37).

The Lemay and Westcott model has as its most significant contribution the demonstration of the ability of a sampled data model to reproduce some of the more significant aspects of the human operator's tracking in both response to discrete inputs and continuous tracking; a task which has presented workers in the field with some difficulty for many years. The details of their model, especially the use of two asynchronous samplers to achieve the desired output waveform, and the simple introduction of a predictor network, seemed somewhat artificial.

Young's Model for Eye Movements

Although not directly bearing on the problem of discrete models for manual control, the sampled data model proposed by Young for human eye tracking movements is introduced at this point because of its role as a basis for manual control models to be discussed below (83).

In the visual control system the task of the servomechanism is to point the central axis of the eye at the target of interest and follow the moving target so as to maintain the image on the central portion of the retina. It has long been recognized that there are two different types of eye movements used in this tracking movement. The saccadic movements are the rapid jerks which serve to bring the eye quickly onto target and reduce position errors. There also exists pursuit movements, which are slow smooth movements presumably used to allow the eye to follow slowly moving targets and maintain zero velocity error. The intermittent nature of eye movement tracking is more readily apparent than in the case of manual tracking. Since the moment of inertia and effective friction of the eyeball is very small in comparison to the powerful muscles which turn it in its orbit, all abrupt changes in force level are immediately made apparent by relative discontinuities in eye position or velocity. Furthermore, since the "plant dynamics" and effective mechanical impedance of the load are unchanged in the normal course of events, the underlying control logic in the eye movement servomechanism is more easily explored.

The evidence for discontinuous control in the eye movement system is similar to that which has been discovered and proposed as evidence for discontinuous control of manual tracking. The psychological refractory period is observed in eye movements, wherein the system response to a target pulse of less than 0.2 seconds duration is a pair of equal and opposite saccades separated by at least 0.2 seconds. An equivalent phenomenon apparently occurs in pursuit tracking as well, since experiments with constant target acceleration indicate that the eye velocity changes in rather discrete jumps at 0.2 sec intervals with position. The "sampling peak" referred to by Bekey in manual tracking is also even more noticeable in the eye movement frequency response to a random continuous input. A marked peak in gain of the eye movement system appears in the vicinity of 2.5 cps, which is consistent with a sampled data system operating with a sampling period of 0.2 sec. When the eye movement system is operated in an effective open loop tracking situation the sampling characteristic of the system is made very evident. The open loop response to a step input is a staircase of equal amplitude saccadic jumps separated by approximately 0.2 sec intervals.

The Young model for eye tracking movements is based on a 0.2 sec sampling period and the assumption of two separate systems in the forward loop; the smooth pursuit system acting as a velocity tracker and the rapid saccadic system acting as a position servo. The model is shown in Fig. 50 (86). The limiter and saturation element in the pursuit loop reflect the observation that pursuit movements only operate between 1^{o}/sec and 25^{o}/sec. For greater velocity errors the eye movement system uses a series of rapid saccadic movements. Use of a discrete hold for rate estimation is a mathematical convenience rather than any reflection of the actual calculation of error rate.

This model correctly predicts the principal characteristics of eye movements both in terms of frequency response and transient response to deterministic inputs. In addition the validity of the model is supported by its ability to predict the experimental findings for tracking under conditions in which the effective visual feedback is varied over a wide range. The stability of the eye movement system as this feedback is varied is also correctly predicted by the basic sampled data model.

The principal influence of Young's model as it effects manual control research was to encourage other investigators

to look for the equivalent of a "pursuit loop" for velocity tracking in the hand response.

Navas' "Motor-Sampling" Model for Manual Tracking

Building on the background of the Bekey, Lemay and Westcott, and Young models principally, Navas conducted an investigation of the nature of intermittency in manual tracking (47). One of his major points of investigation centered about the question of whether the discrete nature of the operator's output was the result of a regular or almost regular sampling phenomenon or whether it resulted from a quantization phenomenon in which a discrete event took place each time the error exceeded a quantization level. The other central theme was a search for a velocity sampling path similar to the pursuit path described in Young's eye movement monitor. In his model Navas incorporates much of the Stark-Houk model for the motor coordination system discussed in some detail earlier, and leans heavily on the physiological evidence for sampling in the motor coordination system. The experimental investigation conducted by Navas covered both frequency response for tracking of continuous inputs and investigation of transient responses to deterministic inputs. His most interesting results were in the area of

transient responses. The task he dealt with was essentially a pursuit task, with both input and response displayed, in which the subject was instructed to try to reproduce the input, rather than merely minimize the error or rms error as is generally the situation. He was then able to conduct limited open loop experiments in which the subject's response was displayed but also moved the target by an equal distance so that the displayed error between response and target was unchanged by the response. Figure 51 (47) shows the experimental set up for doing open loop tests ($g = 1$). The set up of Fig. 51a is similar to that used by Young and Stark (86). In Fig. 51b the situation is further broken down into two inputs to the human operator, k_2 representing the pursuit tracking branch and k_1/s representing the compensatory branch, including an assumed integration in the central nervous system. Using this open loop configuration Navas was able to explore the basic step response of the forward loop of the manual control system by putting in low frequency square wave inputs. Some of the results are shown in Fig. 52 (47). The open loop response to a step input, corresponding to a constant error observation, is a rather regular staircase of "basic response motions". These basic motions resemble the velocity triangle, double parabolic movements described by Lemay and Westcott. The period

separating the initiation of successive "saccadic" movements is approximately 0.4 seconds, and, just as in the case of the eye movement system, lends strong backing to the intermittency hypothesis for manual tracking.

The second set of interesting experiments performed by Navas investigate the ability of the human operator to follow a constant velocity target with a simple gain as the plant dynamics. Among Navas' conclusions were the following: 1) Little evidence for sampling is seen when the input is predictable, such as a triangular wave, however, the sampling phenomena is quite apparent for unpredictable constant velocity inputs. The sampling rate of approximately 2.5 cps is fairly independent of ramp velocity, thereby supporting the theory of a sampling intermittency as opposed to a quantization phenomenon. 2) A velocity servo, equivalent to the pursuit loop in the eye movement control system, was not apparent. Navas based this conclusion on a single series of experiments in which no interpolation was noted between samples. Examples of such tracking are shown in Fig. 53 (47). It should be pointed out, however, that in order to bring out this discrete type of tracking without any smooth interpolation between the basic hand movements, Navas had to add considerable friction and inertia to his control stick. With a control stick which was primarily spring restrained, Navas

achieved the results shown in Fig. 54 (47) for tracking in similar type inputs. This tracking shows considerable smooth interpolation and constant velocity segments between the basic double parabola type relative discontinuities, and are similar to the results generally found. Since the presence or absence of a pursuit tracking type of velocity servo seems dependent upon the force-displacement mechanical impedance of the control stick, rather than reflecting any basic logic in the central nervous system, it is difficult to accept Navas' conclusion that no velocity servo exists, and consequently his development of a model on that basis.

The sampled data model proposed by Navas is shown in Fig. 55 (47). Note that this model is hypothesized primarily for pursuit tracking although most of the features follow automatically for the compensatory tracking case. The sampling is not free running, but is triggered by the first error exceeding the dead zone, as in the case of the Young eye movement model, but in opposition to the Lemay and Westcott model. The sampling rate is to be variable and adaptive although the mechanism for this variability is not specified. The sampling takes place in the motor end of the tracking system and is associated with the opening and closing of the proprioceptive loop at the alpha motor neuron. The model acts to clamp the arm in

position to the proprioceptive loop except for brief periodic sampling intervals when the required corrective signal, alpha, is sampled. Following the appropriate corrective movements the spindle feedback is restored and the arm is clamped to a new position. The role of the central nervous system is represented by the delay $e^{-t_{d2}s}$ and the integration k_1/s. The model exhibits increasing gain over a range of frequencies above 0.5 cps, which is in general agreement with results found for pursuit tracking, allowing a certain amount of prediction of the input.

The various latencies involved in the model are tabulated below:

Visual latencies t_{d1} = 40 milliseconds.

Implicit central nervous system and alpha motor neuron delay times - 165 milliseconds.

Conduction time t_{d2} = 15 milliseconds.

Contraction time t_{d3} = 30 milliseconds.

Total delay for basic movement and response total = 250 milliseconds.

The switch at the alpha motor neuron is assumed to be connected to ground, opening the proprioceptive loop for 20 milliseconds every 250 milliseconds. The model does not lend itself to a simple sampled data analysis.

The model proposed by Navas describes in a qualitative manner the pulse and step responses under both closed loop and open loop conditions of pursuit tracking. It also describes the idealized ramp responses, which show no interpolation, and offers a fairly good qualitative approximation to observed frequency responses including the appropriate spectral peak at about 1.5 cps. The average sampling rate of 3 per second is approximately the same as that arrived at by most other investigators. His case for ruling out of quantization in favor of sampling is well documented, however, the evidence for the lack of any velocity servo even in the case of pursuit tracking of unpredictable inputs is questionable. His efforts at correlating some of the more interesting servoanalytic test techniques with advances that have been made in the control descriptions of the basic muscular motor coordination system are quite interesting and represent effort in an area that has been largely overlooked in the bridge between the engineers and psychologists on one side and the physiologists on the other.

Elkind's Two Channel Discrete Model

Elkind et al. (13) have proposed a sampled data model for the human controller based on features of the Young eye movement model and the Lemay-Westcott manual

tracking model. It includes the two channel, pursuit-saccadic control logic proposed by Young for eye movements, as well as the velocity triangle force program for rapid hand movements proposed in the Lemay-Westcott model. The Elkind model, as shown in Fig. 56 (13) should match many of the time and frequency domain characteristics of manual tracking of continuous signals, and includes the mechanism for human adaptation to a variety of controlled element transfer functions. The proposed model is based on the following characteristics:

1) Primary perception of velocity as well as displacement. Velocity sensing is indicated by the differentiation in the upper, pursuit loop of the flow chart. Although this pure differentiation without any low pass filtering may lead to spurious noise, it is presented for simplicity. It replaces the somewhat arbitrary discrete rate estimation used by Young.

2) Intermittency in manual tracking movements. Breaks in otherwise continuous records and peaks in the frequency response, are evidence of sampling and represented by the pair of synchronous samplers, one sampling error and the other sampling error rate. The difference between the average delay time of approximately

0.15 seconds found in continuous tracking, and the sampling interval of approximately 0.3 to 0.4 seconds suggested by the sampling peak in the frequency response, is accounted for by a somewhat arbitrary mechanism in the model. By separating the reaction time (0.15 sec) from the refractory period, which includes the reaction time plus the time taken for a movement to be completed (0.3 sec), the model is capable of describing both the short initial reaction and long intersample period during active tracking. The sampling interval is assumed to be 0.15 seconds prior to the initiation of any movement by the controllor, and 0.30 seconds after he has initiated a response, assuming a movement time of 0.15 seconds. Note that this mechanism still does not account for the discrepancy between step response reaction times (approximately 0.3 - 0.4 seconds) and delays found in continuous tracking (0.15 seconds), the same problem which caused Lemay and Westcott as well as many other investigators considerable concern.

3) Existence of a smooth pursuit as well as a fast saccadic channel in the output of the human controller. Just as had been described in the discussion of Navas' work, Elkind et al. searched for the existence of a pursuit channel giving smooth output motions of approximately constant velocity, similar to the smooth eye

movements system. Unlike Navas, however, they found that such pursuit movements do exist in general and are an essential part of the manual control mechanism. Figures 57 and 58 show the records of hand tracking of ramps and a parabola respectively (13). In both cases the hand response includes constant velocity segments as well as sudden saccadic-like jumps, and the outputs bear considerable resemblance to those cited by Young for the eye movements. Elkind et al. point out that with a pursuit channel the model is given the capability of memory.

4) Force program. The Elkind model includes the basic work of the Lemay-Westcott model including a force program for the fundamental rapid human hand movements. The force program part of the Elkind model achieves the same double parabola wave form as Lemay and Westcott propose for simple gain dynamics, without requiring the feed foward path or the second sampler. Since the basic force program need not always be one resulting in a velocity triangle, but may result in velocity pulses or doublets for cases in which the controlled element is of higher order than pure gain, the Elkind model includes the flexibility of changing the force program by adjustment of the parameters k_{f1} and k_{f2}. The muscle and hand

dynamics are assumed to correspond to pure inertia. The cross branches k_{mp} and k_{rs} are included to allow the human controller logic to provide compensation for different controlled element dynamics, by introducing effective lead or lag. When the samples of error (e^*) drive the pursuit loop to the branch k_{rs}, the effect is of an integration; whereas if samples of error rate ($\dot{e}^*$) are used to drive the saccadic branch through cross coupling k_{mp}, the effect is one of differentiation.

The model discussed above appears to be a promising attempt to describe much of the "fine structure" observed in manual control responses for continuous tracking. It includes the special features of the Young eye movement model and the Lemay-Westcott hand movement model, and overcomes some of the unnecessary artifices used in each. The Elkind model remains to be simulated to verify its ability to correctly predict or describe a wide variety of human responses. There are, however, two major drawbacks in its present form. The specification of a pair of samplers which are presumably free running and which change their sampling period as a function of system activity, appears to be arbitrary and needlessly complex. Although it does produce a range of reaction times distributed between 0.15 and 0.30 seconds, the same result could be achieved by a sampler assumed

synchronized with the input, and additive noise on the sampling period. Secondly the existence of the adjustable direct and cross coupling gains, k_p, k_s, k_{mp} and k_{rs}, as well as the gain adjustments in the force program portion of the model, k_{f1} and k_{f2}, provide such great flexibility in the program as to permit the matching of almost any arbitrary desired response by suitable selection of these six gains. Although all of these branches may very well exist, until some set of rules is suggested for the way in which they should be adjusted, the presence of that many variable gains tends to weaken the model.

Rauolt's Sampled Data Model for Human Tracking

In his doctoral dissertation in France, Rauolt came to the same conclusions as a number of the American investigators over the years concerning the quasi-linear model for continuous tracking (56) (46). His quasi-linear model for the total open loop transfer function, from error to response is

$$D(s) = 5\,\frac{e^{-0.1s}}{s}$$

The human operator is assigned the 0.1 second delay time and the ability to introduce lead or lag as well as

variable gain in order to keep the overall open loop transfer function as given above. This approximation is assumed valid over the range of input frequencies 0 - 1.2 cps; for high input frequencies the only change is an increase in the open loop gain, from 5 to 9.

These approximations, while valid to first order are quite rough in comparison to the experimental results obtained by Elkind for variation in phase and gain lag as a function of input frequency (12). Similarly the study of dependence of operator transfer function on controlled element dynamics does not contribute more than previously found by Russell, Hall and others (57)(20).

Raoult and Naslin are led to the hypothesis of a discontinuous model for manual tracking by observation of the discontinuities in the tracking of continuous input signals and also by the characteristics of the operator remnant, which includes frequencies other than those present in the input. Just as Bekey had done, they required that their sampled data model approach the characteristics of the continuous models for the lower frequencies. In their model, shown in Fig. 59 (56) continuous lead or prediction is given by the lead term $T_1 p$. (p is taken as the Laplace operator and is in all respects equivalent to s in this work.) The sampler is characterized by two parameters, T_e and θ. T_e is the

conventional sampling period, or interval between successive samples and θ is the sampling duration, or period during which the sampler remains closed. Note that this is not the same as the impulse modulator assumed by the other authors, unless θ equals zero. K_h is the variable human operator gain and p in the denominator represents the desired integration taking place in the central nervous system. The block $W(p)$ is the general <u>continuous</u> compensation block which is introduced to compensate for any dynamics in the external plant, K_2. $W(p)$ is cast in the following cannonical form developed by Naslin

$$W(p) = \frac{1}{1 + \alpha^2(hp) + \alpha^3(hp)^2 + \alpha^3(hp)^3 + \alpha^2(hp)^4 + (hp)^5}$$

and represents a general polynomial denominator. The total open loop gain, $K_h K_2$, is designated as K_e.

Raoult recognized the variability of the sampling rate, and commented upon its possible correlation with error magnitude, but did not include this variability in the simulation. Typical parameters taken in their simulation are the following

T_e = 0.4 seconds, corresponding to the average interval between samples

$\theta = \frac{T_e}{5}$ = 0.08 seconds, the supposed duration of each sample, which is greater than the retinal persistence time

$\alpha = 1.9$

$h = \frac{1}{23}$.

The Nyquist diagram corresponding to these choices of parameters is shown in Fig. 60 (56). The heavy line is of little interest, whereas the lighter line almost parallel to the imaginary axis represents the Nyquist diagram of the sampled open loop model. Note that the curve crosses the real axis at $\Omega/2$ or approximately 5 radians per second. Input frequencies above half the sampling rate cannot be resolved unambiguously at the output.

The ability of this model to reproduce the time characteristics of the human operator tracking continuous input signals is shown by the sample record in Fig. 61 (56). The general characteristics of the response are quite convincing, however, Raoult presents no detailed spectral analysis or correlations to quantify the ability of his model to match the experimental outputs.

Pew's Discrete Switching Model

The experimental situation investigated by Pew is shown in Fig. 62 (54) (55). The presence of the two

position controller forces the operator to act in a discrete manner, either commanding full acceleration left or right in the compensatory tracking task. At first glance this situation might appear to be far removed from the case of continuous tracking discussed thus far, but in reality it is found that when the control elements dynamics are $1/s^2$ or higher, the performance of the human operator closely approaches that of a bang-bang control system (32). The control law for a bang-bang controller is entirely determined by the switching lines on the phase plane (for a first or second order system) or the switching planes in state space for higher order systems. These switching planes indicate at what values of error and its derivatives the control direction is reversed. A typical record of operator performance in attempting to reduce the error and error rate to zero from an initial condition is shown in Fig. 63 (54). As seen both in the time record of error and error rate and in the phase plane, the operator brings the error to a low value in two major positive and negative control phases, and then limit cycles about the origin with a period of between 0.4 and 0.6 seconds. An illustration of the phase plane switching locus found for a typical operator is shown in Fig. 64 (54). These switching lines

are not those that an optimum controller would exhibit, the latter passing through the origin and leading to double parabolic responses. The fact that the switching lines run from upper left to lower right indicates that the operator is including lead compensation and switches earlier when the velocity is high. The separation of the two parts of the locus may be attributed to a dead time, and leads inevitably to a stable limit cycle as the operator switches back and forth between the two switching points.

This additional information complements the material described above on sampled data models for the human operator. It is an independent method of exhibiting lead, and its indication of a stable limit cycle lends support to the notion of the psychological refractory period and its associated minimum delay time between discrete output changes.

Summary

A note of caution is introduced at this point concerning the general validity and application of introducing sampling to account for a variety of phenomena. A satisfactory continuous model is not converted into a satisfactory sampled data model by the simple expedient

of adding a sample and hold circuit. The error in such a procedure is illustrated by the slight digression taken by Kohlhaas in his thesis (35). Figure 65 (35) illustrates the insertion of a sample and T_1 second hold circuit in the open loop following the continuous transfer function representation which was found to approximately describe the operator's response with second order control dynamics. The open loop transfer function for this model exhibits considerable excess phase lag, and is not consistent with the stable performance found in practice. The simpliest explanation is that the phase lag implicit in the use of a sample and hold operation causes the difficulty and that the sampler should not merely have been placed as an afterthought to the continuous model.

The conclusion to be drawn from the proliferation of sampled data models described in these sections is that they do succeed in describing some of the fine structure phenomena of human tracking which could not be described by continuous models, and at the same time satisfactorily predict all those characteristics which the quasi-linear models described. The disadvantage of the sampled data models relates primarily to their complexity in comparison to the continuous models. For

many applications, particularly those in which low pass filtering in the controlled element smooths out the high frequency sampling noise, it is quite difficult to tell the difference between the outputs of the continuous and sampled data models, and consequently for all practical purposes one might as well use the continuous model. However, for those situations in which high frequency response is important, or if one is interested in the basic underlying physiological mechanism, the "fine structure" of discreteness should not be ignored. It is undeniable that some manner of discrete processing exists in the human controller. That this discrete process is governed by a sampling clock rather than a quantization phenomenon seems apparent now. It is also apparent that a simple single frequency clock, either free running or synchronized to the input, is not a fully correct description, as witness the wide variability in sampling periods and the relatively wide "sampling peak" in the frequency domain. Whether this variability is merely "biological noise" or represents some manner of adaptive control in which the sampling rate is increased as the difficulty of the task increases, remains to be investigated.

Preliminary reports on an extensive study of the spectral characteristics of the human operator by McRuer, Krendel and Graham (43) fail to reveal any significant, stationary sampling peak. Whether the input conditions and lengths of runs could have caused the variable sampling period to spread out the spectral peak until unrecognizable remains to be seen in examination of the full report of the study. If the sampling peak is shown really not to exist, but is merely an artifact of the various investigators' methods, then one of the major experimental foundations of the sampled data models will have been destroyed.

Another very important question relating to the sampling models concerns the correct position for the sampler. The Bekey, Young and Elkind models place it just after the summing point, the Lemay-Westcott and Raoult models place it in the central processor after some lead, and the Navas model places it at the motor end. Although this question may be of more interest to physiologists than to engineers, it remains a challenging one in any consideration of sampled data models for the human controller.

VI. ADAPTIVE CHARACTERISTICS OF MANUAL TRACKING

Classes of Adaptation

Some of the various classes of adaptation which are of importance in biological servomechanisms are shown in Fig. 66 (75). Of the three classes of adaptation called out in the schematic diagram, input and task adaptation will specifically be considered as important aspects of the human operator in his role as a manual controller. By input adaptation is meant the process whereby the controller adopts a different control "policy" or control loss appropriate to the characteristics of the input. In its most obvious forms this involves the recognition of repeatable patterns in the input, with the resultant change of control from compensatory to precognitive tracking. Adaptation to the statistical characteristics of the input also falls in this class.

The task adaptation processes include adaptation to changes in controlled element gain or controlled element dynamics, as well as instructions and constraints concerning the required level of performance.

Biological adaptation is restricted to primarily sensory phenomena, and is not considered in detail in the

discussion of manual tracking. A fourth class of adaptation, which may be more properly called learning, involves the development of skills, which may be shown as changes in the topology of the model input operator, rather than simple changes in his control law.

Input Adaptation

The simplest form of input adaptation is the ability of the human operator to recognize periodic input signals, or even periodic components in the input signal, and use the predictive nature of these signals to synchronize his response. The human operator response to a single sinusoid hidden in noise, shows gain and phase lag as indicated by the quasi-linear describing functions for closed loop tracking. When the sinusoid is presented by itself however, the human "locks on" and tracks almost perfectly. The two time tracings of Fig. 67(62) indicate the closed loop response expected of compensatory tracking and the synchronous response, also known as precognitive tracking. The ability of the human to detect the presence of a predictable signal in an input consisting of signal plus noise has been treated by detection theory (76). Little quantitative work has been directed to the problem of how tracking behavior is affected by the presence of strong periodic components in a

random input signal. As a practical matter, most input signals encountered in usual tracking tasks have a large predictable portion plus some additive noise.

A second major characteristic of the input to which the human adapts is the bandwidth of the input signal. Using a series of input spectra containing frequencies from zero to a given cut-off frequency, Elkind (12) evaluated the parameters of human operator quasi-linear describing functions. He found that the human operator reacted differently in tracking low frequency inputs than he did in tracking the more difficult high frequency inputs. Specifically, the gain term was notably reduced as the input frequency cut-off increased, and the amount of lag was also reduced. The break-frequency of the proportional plus integral term increased for higher frequency inputs. This parameter adjustment is quite in accord with the adjustments a control engineer would adopt under changes of input frequencies. For low frequency inputs, a "tight" tracking loop can be achieved by using high gain and almost pure integration as the control law. For higher input frequencies however such a control law introduces excessive phase-lag, especially since the high frequency response was necessarily reduced to avoid instability. Therefore, when the input frequency is high (0.4 to 2.4 radians per second)

the operator adjusts his transfer function by accentuating the high frequency response through change in lag break frequency, and reduces his relative gain at low frequencies.

Adaptation to Controlled Element Gain

It is well known that the human operator adjusts his own gain in accordance with the gain of the controlled element to achieve a desired open loop and closed loop level of performance. Thus in a sports car a small deflection of the steering wheel will result in a fairly large rotation of the front wheels and rate of turn, while in a large sedan the same deflection of the steering wheel will typically result in a much smaller front wheel deflection and rate of turn, representing two different levels of controlled element gain. Nevertheless the driver is capable of adjusting his own gain (from error in heading or position to steering wheel displacement) to achieve acceptable levels of control for both automobiles. This is not to imply that an optimum level of control element gain does not exist, for it most certainly does (4). The operator is, however, capable of adjusting his level of gain so that the total open loop gain is close to an optimal level. This adjustment of operator gain does not happen only in such obvious situations but may also be required continuously in

the same task. For example in riding a motorcycle, the gain from handlebar deflection to "roll angle" of the motorcycle varies with the speed, and the rider must make considerably more energetic movements to maintain his balance at low speeds than could be permitted at high speeds. This adaptation to change in control element gain is of course below the level of consciousness and comes quite naturally to the rider.

In the situations described above the operator has a great variety of external cues to indicate the controlled element gain. Recently experiments were conducted in which the controlled element gain was suddenly switched in the course of tracking with no external cues provided to the operator (85). He had only the resultant change in tracking performance to indicate to him that a change in his own gain or polarity was required. A typical example of a step response following such a gain increase is shown in Figure 68. The controlled element gain for this compensatory tracking task was nearly doubled between the first and second steps shown. In the subject's response to the step input following the gain increase he first shows a considerable overshoot, as would be expected, and then returns the error to zero with one or two subsequent rapid movements of

approximately the right magnitude, indicating an adaptation to the new gain level following the first significant hand movement. Responses to subsequent steps at the new level of gain show almost perfect adaptation. Raoult, in his thesis (56) finds step response adaptations very similar to those of Figure 68. To investigate the operator's ability to adapt to sudden changes in gain and/or polarity of the controlled element, Young et. al. experimented with such sudden switches under conditions of compensatory tracking of low frequency continuous random input. Figure 69 shows the process of adaptation to a sudden reversal of the polarity of a simple gain control. Notice that this polarity reversal converts the stable closed loop negative feedback system into an unstable positive feedback system until the human operator adapts by changing his own control polarity. The upper tracing of Figure 69 showing the input signal (the smooth, dark curve) and the subject's response indicates that for a period of approximately 0.5 seconds following the control reversal the subject's response was divergent, moving away from the input and increasing the error. Following 0.5 seconds the adaptation to the new polarity brought the error quickly to zero and tracking continued as accurately as before the transition. The second tracing shows that during this first 0.5 seconds the subject continued to

track as though the controlled element had remained in its original state. The error (third tracing) typically shows a divergence with a fast return to zero and then continued smaller magnitude. To remove the influence of variations in input signal at the time of transition, the average of many error waveforms was calculated for each of these transitions. Average error waveforms for the polarity reversals are shown in Figure 70. Notice that the error has been detected, identified, and is being reduced within 0.5 seconds of the transition on the average, and tracking performance is almost normal within one second following the polarity reversal. Typical time records for sudden gain increase, gain decrease and polarity reversal with gain increase are shown in Figure 71a, b and c respectively. In Figure 71a, the gain increase causes the closed loop system to begin to break into oscillation which is quickly damped after approximately one full cycle. The sudden gain decrease, resulting in a very sluggish system, produces a small amplitude error which is not cancelled out for several seconds, as seen in Figure 71b. The combination of gain increase and polarity reversal, which would be expected to result in an unstable response, shows many of the characteristics of the adaptation to the polarity reversal and to the gain increase separately. In Figure 71c the response

immediately following the transition is the beginning of an exponential divergence. The polarity correction is followed by oscillatory behavior similar to the case of a simple gain increase. Notice that for the example shown in Figure 71c the error is substantially reduced in the first two seconds, but some small oscillatory behavior is seen throughout the remainder of the record.

The conclusion from these studies (in which the subjects were well trained on all tracking conditions and expected some sort of control element change although not knowing exactly what or when) is that the major control adaptation generally occurred 0.4 to 0.8 seconds following a controlled element change. The resulting error is usually reduced to its asymptotic level in the following one to three seconds.

There is some evidence from examination of the time waveforms in the fine structure of the adaptation process to indicate that the operator adjusts first his polarity and second his gain on the basis of sequential samples of the error. It is to be emphasized that the extremely rapid adaptation times shown in these experiments are probably valid only for the ideal laboratory conditions. In a practical situation, in which changes in controlled element gain, polarity or dynamics are most unusual, it is highly unlikely that such rapid adaptation would be observed.

Adaptation to Controlled Element Dynamics

In addition to adjusting his gain, the human operator is capable of introducing a significant amount of dynamic compensation when necessary to equalize the dynamics of the controlled element. Considering the pure time delay as inherent in the human transfer function and unchangeable, the nature of this equalization is to maintain the open loop transfer function, including both human operator and controlled element, in the form of approximately a simple integration plus dead time. Gain is adjusted to yield a gain crossover frequency of the order of one cycle per second with damping constant of 0.3 - 0.6. The operator's equalization and gain adjustment ability is reflected in the following lead-lag term introduced by McRuer and Krendel to summarize many investigations:

$$K \cdot \frac{(T_L S + 1)}{(T_I S + 1)}$$

By increasing T_L the operator can generate lead and compensate for controlled element lags or dead times, or to increase the system bandwidth. By generating increased lag through an increase in T_I, the operator can "tighten" his low frequency response and filter out high frequency

noise. K, the operator gain, may be adjusted to achieve the desired compromise between fast "tight" response and stability. The form of model proposed by McRuer and Krendel showing the human operator's equalization ability is reproduced in Fig. 72 (42). They separate the overall reaction time into components for visual latency, central processing, synaptic and conduction delay, and kinesthetic reaction time. The neuromuscular system including both kinesthetic and proprioceptive feedback accounts for the "neuromuscular lag" $(1/T_N S + 1)$. This model with K adjusted to yield overall system phase margin between 40 and 80 degrees, leads to human operator models more closely approximating well designed servomechanisms, than the criterion of 60 to 110 degrees phase margin previously put forward by the same authors (42).

In their earlier review, based on the work of Russell (57), Hall (20), Tustin (78), Goodyear Aircraft (18), and the Franklin Institute, McRuer and Krendel showed that the operator could detect and compensate for the insertion of a simple lag in the controlled element when the lag time constant was greater than 0.05 seconds. As the lag time constant increased to greater than two seconds, it appeared as a pure integration, and the operator produced sufficient lead to cancel his own internal lag.

An extension of the quasilinear studies to determine the human operator transfer functions for use with controlled element dynamics of second and third order was carried out by Adams and Bergeron (2). Using an analog computer model reference technique to track the parameters of the human operator, they measured operator transfer functions for eight different dynamics, first, second and third order, in a single-axis compensatory tracking task with a continuous random input. They did not include an explicit dead time in their analog model, for the pilot but rather expressed it as

$$Y_p(s) = \frac{K_1 \tau (1 + \frac{K_2}{\tau} s)}{(\tau + s)^2}$$

Their convention is retained here even though it uses the symbol τ for frequency, rather than time. They tracked the parameters K_1, τ and K_2. The results for one of their test subjects is shown in Table 3 (2). In their notation for the single-axis task, D is the disturbance or the input, ϵ is the displayed error, δ is the pilot output, going into the controlled element dynamics, and θ is the system output. In some cases the measurements were open loop measurements "across the pilot" (δ/ϵ) and in other cases they were closed loop

measurements from system input to pilot output (δ/D). In the case of the open loop transfer function calculations, the closed loop (θ/D) damping constant and 180° phase frequency are provided in the table, as well as the location of real roots where they exist for the closed loop. The man-machine closed loop system response amplitude ratio and phase angle for these dynamics are shown in Figs. 73 and 74 (2). It can be seen from the table or the closed loop Bode plots that as the controlled element dynamics go from pure gain to first order lag to pure integration the pilot increases his lead time constant to counter the effect and leaves the closed loop response almost unchanged. Further lag introduced into the controlled element (as in the damped second order system) results in somewhat greater closed loop phase lag and the first indication of a resonance in the closed loop amplitude ratio. For controlled element dynamics of the various second order systems, the third order system and the pure double integration the effect on the closed loop is to decrease the relative damping constant and the natural frequency. The bandwidth of the closed loop system is thus reduced by higher order systems than first order. Furthermore the existence of large peaks in the amplitude ratio with accompanying increase in phase lag, particularly for the pure acceleration ($10/s^2$) indicates

a considerable oscillation in the frequency range 0.5 to 1.0 cps. It should be noted with reference to the section of this report on sampled data models, that these frequency responses were presumably calculated on the basis of the three model reference parameters and the closed loop dynamics, and were not taken from spectral analysis; therefore the lack of the "sampling peak" in the amplitude ratio is not surprising.

A tracking record with pure acceleration control is shown in Fig. 75 (2). Two features are of special interest here. In the second trace showing displayed error notice the existence of the periodic component of the error, at much higher frequency than any component of the input. The average frequency of these oscillations is 0.6 to 0.8 cps, and is presumably a pilot induced closed loop oscillation. Also of interest is the third line, the pilot output (δ). Although engaged in a continuous tracking task the pilot rarely moves his control stick in a smooth continuous fashion, but rather jerks it rapidly from one extreme to another. This discontinuous pilot behavior when confronted with higher order dynamics has been noted by others, and leads to the hypothesis that when a great deal of phase lead is necessary the human operator operates in a bang-bang control fashion rather than as a continuous controller.

A possible explanation for this bang-bang behavior when the controlled element has excessive lag is that for proper system operation the operator must keep in mind the first and second time integrals of his response. To perform these integrations with continuous control requires memory of the length of time and the amplitude of his control responses, whereas with a pure bang-bang controller the operator is required only to remember the length of time in each position, with the amplitude variation removed. On this basis it should be expected that when sufficient operator lead is required he should be able to perform better with a bang-bang controller than with a continuous controller. Kilpatrick performed these experiments and found that this was indeed the case. A schematic of his experimental situation is shown in Fig. 76 (32). When the controlled element dynamics were $10/s^2$ or $\frac{10}{s^2(s/3 + 1)}$, there was no significant difference between the two types of controllers. With a very difficult controlled element requiring more lead $(10/s^2(s + 1))$, the average mean square error for the linear controller was 50% higher than that for the real controller. (Difference in means significant at the 5% level.) Since the input noise was filtered with break frequencies at 0.2 to 0.5 rad/sec, the resulting input was quite challenging and led to large errors for both

controls. The difference in the basic behavior is therefore more clearly seen in the case of zero input, in which the operator is merely tracking his own response and causing self induced oscillations. The subject's response and error is shown for the relay controller in Fig. 77a and for the continuous controller in Fig. 77b (32). Notice that even though the operator uses the continuous controller in a more or less bang-bang fashion, he is able to use the bang-bang controller in a pulse control fashion to achieve considerably lower error and avoid the self oscillation. The frequency of the self oscillation found with the continuous controller is approximately 0.25 cps.

Even more interesting than the steady state equalization introduced by the operator for any given controlled element dynamics, is the adaptation process by which he changes his control law when confronted with a change in controlled element. In an extension of the experiments described above for sudden changes in gain and polarity, Elkind et al. permitted the controlled element dynamics to change as well, among pure gain, single integration and double integration. In the tracking record shown in Fig. 78 (13) the operator was suddenly confronted with the introduction of a double integration at the same time as a controlled element polarity reversal and gain

increase. The polarity reversal was detected and corrected in approximately one second, after which followed a period of damped oscillation lasting for as long as twenty seconds. Although one to two cycles of oscillatory behavior were noted as a result of a simple gain increase, the extended oscillation must be attributed to the operator's delay in achieving the correct lead equalization and proper gain for the new double integration. The oscillation is of frequency 0.5 to 0.7 cps, which is approximately the 180° phase angle frequency for the system with reaction time delay, residual control integration, and external double integration.

A tracking record showing operator adaptation to sudden change in controlled element dynamics taken under situations more closely approximating a realistic emergency is shown in Fig. 79 (58). The result is taken from a test of the pilot's ability to control in the pitch axis of a moving flight simulator when the auxiliary pitch damping system suddenly failed. The effect on the controlled element was to greatly decrease the effective damping constant of the second order dynamics while leaving the undamped natural frequency constant. The damping constant prior to the simulated failure was approximately $\zeta = 0.3$ resulting in an acceptable pilot rating. Following the

damper failure the effective damping was reduced to approximately $\zeta = 0.04$, which was rated unacceptable in the steady state. The tracking record shows several evaluation steps by the pilot to determine the "feel" of the pitch loop, and then approximately 25 seconds of tracking a low frequency random input. At the time the damper failed, the closed loop man-machine system went into unstable oscillation, and continued a wild oscillation of approximately one cycle per second for more than 18 seconds. During the unstable period the pilot was undergoing peak pitching angular accelerations as high as $60^{\circ}/sec^{2}$. When the errors were finally reduced, the steady-state tracking was considerably poorer than that with the pitch damper in the loop, but nevertheless did show pilot adaptation.

Evidence from several aircraft accident reports indicated that control system failures in the form of gain changes, stability augmentation failures or polarity reversals, have caused the aircraft to lose control and crash, even though a pilot might be capable of controlling under these unexpected conditions. Planes are found crashed with the controls "hard over" in the wrong direction, indicating that the pilot did not recognize the nature of the change in the controlled element, and did not assume

the correct adaptive procedure early enough. Since such failures most often happen on take-off, with very little time to test the response, it is not surprising that the human operator adaptive characteristics described above are not immediately called into play in such unexpected circumstances (11).

As shown in the tracking records of Young and Elkind above, the human adaptation process can be very rapid under ideal conditions. To achieve the most rapid adaptation the operator should be thoroughly trained on the controlled elements both prior to and following the switch and should be operating on only one control loop at a time. He should be presented with sufficiently challenging input to call forth a continual series of basic responses and thereby quickly identify any changes in control characteristics by the resultant change in error pattern. Early detection and adaptation is aided by the use of a pursuit display, which allows immediate identification of changes in response characteristics, and also by the use of a secondary signal, such as a tone or warning light, which alerts the operator to the change in conditions.

Limits of Controllability

Although the ability of the human operator to adapt to a wide variety of controlled element dynamics, as discussed above, gives him great versatility, it is nevertheless of considerable interest to determine the limits of controlled element dynamics to which the human operator can adapt for satisfactory closed loop performance. It has long been recognized that some limitation exists in the human's ability to generate sufficient lead to overcome the lag inherent in a control element described by more than two integrations. External filtering of the input or output to the operator, in terms of quickening or aided tracking, has been widely used to assist the operator in generating the lead.

Estimated limits of controlled element dynamics which can be successfully controlled by the human operator may be derived from the general quasilinear model discussed above, in which the operator is permitted the introduction of a single lead term $(T_L S + 1)$. With no lag terms present, as T_L increases the operator describing function approaches that of a reaction time plus pure differentiation. The highest lead time constant published in the literature is $T_L = 5$, (40) although the maximum

single lead time constant selected in a recent report by Jex et al. (30), places the highest value of T_L at about 2.0 seconds. Smith investigated the limit of controllability using an unstable second order control system of the form (64)

$$Y_c(s) = \frac{K_c}{s^2 + 2\zeta_n\omega_n s + \omega_n^2}$$

With ζ negative and less than one, the transient response of the controlled element to an impulse is a divergent oscillation. As ζ becomes more negative the envelope of the response becomes more divergent, and therefore more difficult to control. Similarly larger values of ω_n corresponding to more rapid oscillations, increase the difficulty of control. At several values of negative damping, Smith experimented to find the maximum natural frequency of the controlled element which still permitted the operator to maintain adequate control, which was arbitrarily defined as the ability to maintain the system error within selected bounds for a two minute run. His results are shown in Table 4 (64). Figure 80 (64) shows the expected limits of controllability as predicted on the basis of the quasilinear model by Jex et al. and as revised on the basis of Smith's data. The area

representing controlled elements with dynamics below and to the right of the heavy lines are assumed controllable and above and to the left uncontrollable. The dotted lines represent hypothetical mode switching lines. It is assumed that when the divergent oscillation is clear enough the operator can recognize the sinusoidal form and switch from compensatory tracking to quasi-precognitive tracking, thereby greatly reducing his reaction time and increasing his effective lead. Jex et al. would place this response mode switching line at $\zeta_n = -0.2$ saying that for more negative damping the response becomes quasi-precognitive, whereas Smith's data would place this line at approximately $\zeta_n = -0.5$. It is seen that for both the pure compensatory and quasi-precognitive data, Smith found the operator capable of generating more lead than would be indicated by the simple single lead term of the McRuer and Krendel form of the model. On the basis of the operator's input-output characteristics with the $\zeta_n = -0.7$ controlled element dynamics, Smith found the following describing function:

$$Y_p(s) = \frac{K_p e^{-0.15s}(s+0.2)(s+3)}{\left[s^2+2(0.9)(13)s+(13)^2\right]\left[s^2+2(0.25)(21.5)s+(21.5)^2\right]}$$

This operator model results in a stable closed loop system for the controlled element under investigation, although one with comparatively low phase margin of 14 degrees. For the other data point, at $\zeta_n = -0.35$ and $\omega_n = 7.2$, which results in a great deal of oscillatory response, it is necessary to assume that the operator has recognized this oscillatory behavior and switches to a form of quasi-precognitive tracking which enables him to reduce his reaction time delay from 0.15 seconds to 0.02 seconds, resulting once again in a phase margin of 14 degrees.

It is of importance to note that in the operator transfer function described by Smith it was necessary to assign two lead terms, indicating that the operator is somewhat sensitive to error <u>acceleration</u>, as well as velocity. These findings appear to be substantiated by the investigations of Fujii (16).

<u>Learning and Perception</u>: <u>Compensatory</u>, <u>Pursuit and Precognitive Tracking</u>

The human operator can assume different control characteristics according to the nature of the information display, as well as the controlled element or task. In the compensatory display situation, which has received the greatest attention, the subject observes only the error between input and response. Any

separation of input from response must be accomplished by the operator through observation of the statistical characteristics of the error, knowledge of his own past output, or pattern recognition applied to the error. In the pursuit task, input, response and error are displayed explicitly and give the operator greater opportunity to observe his own response and recognize characteristics of the input. For relatively simple tasks with "easy" controlled element dynamics and random input, there is no important difference in performance between the compensatory and pursuit displays (8). For tasks involving difficult input signals or controlled element dynamics requiring significant operator lead, the superiority of the pursuit display has been established (60). The explicit input information in a pursuit display permits the operator to make predictions about the input and therefore establish the necessary lead required for stable closed loop performance. In precognitive tracking the "display" is assumed to show the entire future course of the input, whether this future course is directly exhibited or is stored in the subject's memory as a result of repeated observation of the same input. Synchronous tracking of a sinusoidal input as described above is a simple example of precognitive tracking.

Since it has been well established that the existence of the finite reaction time of 0.1 to 0.3 seconds is one of the major limitations to the human operator's ability in compensatory tracking, other topological configurations must be assumed to explain his enhanced performance in pursuit or precognitive tracking. Krendel and McRuer indicate three representations for the human operator corresponding to these three different display conditions in Fig. 81 (36). In the compensatory situation the operator observes only the error. In the pursuit situation he has performance blocks acting on error, input and response, although it is established that the response block is probably not used for anything except perhaps controlled element adaptation. The precognitive situation is represented by a "stored program" of response which is triggered by the appropriate input in the synchronous generator. Elkind's describing functions (12) support such a topology by showing the reduced phase lag for pursuit tracking as compared to compensatory tracking and demonstrating that this difference can be described by a lead term (Y_{pi}) acting on the input.

Krendel and McRuer hypothesized a model for skill development based on "successive organizations of perception" (SOP) in which it is assumed that the operator passes

through all three topological phases shown in Fig. 81 in learning any tracking task. First, regardless of the display modality the operator, they claim, begins by concentrating on the error. As he recognizes certain characteristics of his response and becomes aware of the predictability of the input, he uses this information to behave as though he were in a pursuit tracking situation. Note that any input signal other than white noise will have some predictability even if it is not a periodic signal. Any input correlation function other than an impulse at zero indicates that the position of the input or its derivatives may be partially predicted at some future time based on its current position and derivative. Finally, when periodic or otherwise predictable inputs are recognized and learned, the subject begins to respond with well practiced movements and is effectively tracking precognitively. An example of this internal topographical rearrangement was seen in the discussion of Smith's results on the limits of controllability.

It is clear that the simple case of compensatory tracking, although amenable to mathematical modeling, is not representative of most realistic human tracking situations. Consider for example the role of a pilot trying to keep his plane straight and level in the

presence of wind gusts. Under zero visibility conditions, referring only to his artificial horizon, he might be considered in a compensatory loop. However, he is familiar enough with the response of the plane to control inputs to be able to separate the disturbance from the control responses, and therefore is effectively in a pursuit situation. The effects of other inputs to the operator including his tactile and vestibular sensations in response to acceleration give him further cues (sometimes erroneous) to the control corrections required.

Although pursuit tracking and multiple input control involve more difficult mathematical description, it is hoped that they will receive attention in the future, especially as the newer methods of control theory for multi-input control becomes more widely known (45).

Measures of Adaptation

The above discussion has used primarily steady state measurements to demonstrate that the human adapts from one situation to another, but sheds little light on the nature of the adaptation process. The measurements show that he changes from one state to another (adapts) but they do not show how he performs this adaptation, what information he uses, or how rapidly the adaptation is performed.

None of the attempts to measure the dynamic characteristics of this adaptation process have been completely successful, although they have served to place bounds on the process. There is a fundamental problem in any attempt to identify the time varying characteristics of a control system without the use of special test inputs.

To observe the dynamics of the adaptation to changes in forcing function display modality and controlled element dynamics, Sheridan automatically calculated the operator's gain and phase at each of five forcing function frequencies (61). Because the filters for performing the frequency analysis themselves have a rather long response time, the operator's characteristics could only be measured every fifteen seconds, thereby setting a lower limit of time resolution that could be observed in the adaptation process. He found that adaptation to change from pursuit to compensatory display change in controlled element dynamics or input adaptation to a predictable or random input took place within 30 seconds, or within two measurement points. It is felt that because of the time limitation of the analysis method the results merely put an upper bound of 15 to 30 seconds on this adaptation process but did not accurately reflect the adaptation times. For longer adaptation processes, however,

such as in "learning" a totally new response pattern, the operator's characteristics continue to change over a period of several minutes and are so indicated by Sheridan's method.

An example of the type of results found by Sheridan is shown in Fig. 82 (62). In this case the display was changed from compensatory to pursuit at time zero. The operator's characteristics are shown in the complex plane for four test frequencies, at each of six test points. The test point zero was for the compensatory display, and shows a gain of slightly less than one and a phase lag increasing with frequency up to nearly 90^{o} at the highest frequency ($\omega_5 = 0.93$ cps). During the minute following the transition to pursuit display the operator increases his gain and decreases his phase lag, especially at the higher two frequencies. This reflects the increased amount of lead possible with the pursuit display, and shows that this lead is developed gradually over the first 45 to 60 seconds.

Several attempts have been made to construct rapid and stable analog computer techniques for real time parameter adjusting or "parameter tracking" to follow the dynamics of the human operator adaptive process. Ornstein (52) has proposed a technique based on the analog computer

determination of the coefficients of a linear differential equation describing the human. The "model reference" adaptive control system developed by Osburn and Whitaker (53) at M.I.T. has been used to have the "model" track the pilot's behavior, rather than forcing the unknown control system to conform to a desired model. The mechanization of this technique, as used by Adams and Bergeron is shown in Fig. 83 (2), in which the filter characteristics for each parameter should be selected to give a steepest descent correction of the analog pilot, forcing it to approach the characteristics of the actual pilot. In all of these methods a compromise must be struck between stability of the parameter tracking and speed of response. Since the operator's response includes a remnant term, which may be considered as output noise, and since the model chosen may not be the most appropriate, attempts to adjust parameters based on every occurrence of an error between the analog pilot and the actual pilot will naturally cause the system to oscillate or diverge. Although tracking of single parameters may be accomplished quite rapidly, it remains to be seen whether such gains can be made rapid enough to track the complex gain, polarity and equalization changes which occur so rapidly in the human operator under certain conditions.

Returning to the measure of the adaptive characteristics through the frequency response, Elkind et al. (14) have developed a multiple regression analysis technique for rapid identification of time varying linear systems, and applied it to the human pilot adaptation problem. For reasonable confidence levels, and under the types of low frequency inputs used in human tracking, this technique can give a plot of amplitude ratio and phase every five seconds, which is considerably faster than that used by Sheridan. An example of the use of this technique is shown in Fig. 84 (13). The Bode plots are of the human operator input-output characteristics before and following a change in controlled element dynamics from $\frac{-4}{s^2}$ to $\frac{+8}{s^2}$, at time t_0. The required adaptation should consist of a reversal in phase by 180° and a reduction in amplitude ratio of 6db . Prior to the transition low frequency phase is at about -180° and low frequency amplitude ratio at about +9db with some low frequency lead as required for stabilization of the acceleration control (upper diagram). In the middle diagram, taken from three to eight seconds following the transition, it is seen that the polarity reversal by the human has already taken place, with the phase lag changed to zero degrees, but that the gain has been over-compensated. Finally, in the lower portion of the figure, from 8 to 13 seconds following

the transition it is seen that the amplitude ratio is restored to approximately 6db below its pre-transition curve, and the adaptation is nearly complete. This measurement technique shows great promise in understanding the nature of the human operator adaptive mechanism, particularly for complex transitions in which the time domain records do not clearly show the changes in the control law.

The primary limitation on the use of frequency analysis and parameter tracking in some of the very rapid human adaptation processes is clearly one of response time. For this reason a return to time domain analysis is indicated. Individual tracings of operator's response or system error may not give a clear indication of the adaptation process because of the interfering effects of the input, or operator response uncorrelated with the input or the adaptation process. The use of average response computation, which has proven so popular in the field of electrophysiology, may be used satisfactorily for bringing out those features which are consistent in almost all occurrences of a particular type of adaptation. Some of these average wave forms were shown in the discussion of adaptation to gain changes, and another set is shown in Fig. 85a,b,c (85). The average waveforms shown were

each taken from twenty transitions of controlled element gain under pursuit tracking. The upper tracing is for a simple polarity reversal, the middle for a reversal increase and the lower for a reversal decrease. Notice that they all show the beginning of a divergence as a result of the polarity change, and that the reversal point occurs first for the reversal increase, next for the straight reversal and latest of all for the reversal decrease, indicating that it is perhaps the extent of the divergence which alerts the subject to the requirement for polarity reversal. Other characteristics such as the oscillatory behavior associated with a gain increase and the slow adjustment characteristic of a gain decrease are also brought forth quite clearly in the average waveforms, although they are less obvious in the individual time records.

The use of rapid identification techniques, even if not "real time" identification, made possible through inspection of time domain results should not be overlooked when the identification problem presents a serious time restriction.

Models for Human Adaptive Tracking

A "model" is a mathematical description of a process capable of making accurate predictions about

the behavior of the process under situations which had not previously been tested. As of this time there are no published successful models for the adaptive characteristics of the human operator. The descriptions put forth either describe the end states reached by the human operator, without indicating the means by which the adaptive process takes place, or they fall into the catagory of very general "schematic" models. These schematic models all recognize the extreme complexity of the problem of quantitative description of the human adaptive process and offer instead a set of guidelines, hypotheses and constraints to be considered in the actual task of building a detailed model.

The study of adaptive control, currently of great interest among the control engineers is, nevertheless, a relatively recent topic. Electromechanical adaptive control systems, developed primarily for aircraft, aerospace and chemical processing applications, are still relatively primitive in their performance in comparison to the human operator adaptive ability. It is no surprise therefore that we are unable to model the human operator adaptive characteristics using the current techniques of automatic control. This section will therefore be devoted to those schematic models which appear most reasonable, and which cannot be either proved or disproved at this time.

There are two different classes of models which may be used to describe the adaptive process in compensatory tracking; the "model reference" and the "error pattern recognition" models. Figure 86 shows the basic elements of the model reference approach to description of human adaptive tracking. All of the dotted lines correspond to hypothetical paths in the adaptive process, whereas the solid lines correspond to the conventional closed loop control diagram. The heart of this scheme is the box labeled "model of controlled element" which represents the operator's concept of what the output should be doing based on the response he has given it. The difference between this expected output and the expected input (deduced from any knowledge of the error statistics or repeatable input) results in an expected change in the error ($\dot{e}'$). When this expected change is compared with the actual change in error observed on the display ($\dot{e}$), a deviation between the model of the process and the actual process is indicated. The "deviation filter" rejects insignificant deviations but passes "important" deviations between what happened and what was expected on to the "adaptive control operator". This block produces changes in the operator's control law to compensate for assumed changes in the controlled element, and simultaneously updates the operator's hypothetical model for the controlled element.

An error pattern recognition type of model, as illustrated in Fig. 87 is based on the premise that the only information used by the operator in performing his adaptation is the displayed error. In the "error pattern recognition logic" the operator presumably sifts the present and past error searching for predictable components or other significant error characteristics. Discovery of a repetitive pattern, possibly by a process such as autocorrelation of the error, would enable the operator to form a stored program response. Such a stored program could then be triggered in precognitive tracking, thereby bypassing the inherent operator reaction time. Examination of error characteristics might be used to detect changes in the controlled element as reflected in changed closed loop performance. A divergent error, growing increasingly large without changing sign, might be a characteristic of positive feedback and cause the operator to change the sign of his control law. Regular oscillation of the error might indicate the need for the operator to reduce his gain and perhaps introduce some dynamic compensation. Conversely a "sluggish" system in which the error approaches zero very slowly from some initial condition could be interpreted by the parameter adjustment logic to indicate the requirement for increased operator gain. This type of

error pattern recognition model assumes no kinesthetic or proprioceptive feedback about the operator's response.

A recent paper by Knoop and Fu (34) proposes an adaptive model based on the model reference scheme. Their non-adaptive model for the human operator, as shown in Fig. 88 (34), includes a model of the plant to enable the operator to "look ahead" in programming his basic response movements. In this respect it bears a great similarity to the Wilde and Westcott-Lemay models described earlier . The model is based on the use of fixed length control intervals containing "saccadic" type basic response movements. The system performance is presumably evaluated at the end of each of these control intervals, which are "working periods" as opposed to the sampling periods in the sampled data models. Their schematic block diagram for the adaptive control process includes the use of the same plant model mentioned earlier, with differences between the actual plant and model plant results being used to identify and modify the process, as in Fig. 89 (36).

A more detailed schematic model for the human operator including his adaptive capabilities was proposed by Raoult. An adaptation of his block diagram is given in Fig. 90 (56). The lower half of the diagram consists of the model for

compensatory tracking. The error, magnified by an optical display gain (K_a) is detected optically, as represented by the low-pass filter $O_e(s)$ and the visual threshold block. The error and error rate are detected by the eye, and error acceleration is assumed calculated by differentiation of error rate. These three quantities are weighted by the constants a, b, and c in the "command computer". The desired basic response movement is then sampled every T_e seconds for a duration of θ seconds, multiplied by the operator's gain K_{ec} and integrated to yield the desired step command to the muscles. The controllor is assumed to operate with local kinesthetic feedback from the actual arm displacement back to the muscles, and the controlled element output is fed back to the input summing point. A hierarchy of auxiliary organs is hypothesized to describe the operator's adaptive characteristics. At the top of this heirarchy is the "decision center". The decision center chooses between conventional tracking or generation of commands based on programs stored in memory. In the case of the predictable signal, detected and stored in memory, the decision center opens the "switches" A and A_2 to permit the "release of expected response" to trigger the desired output from the memory. The "correlation memory" is used for adjustment of tracking parameters based on minimization of mean absolute

error or mean square error of the overall system. The adjustment of parameters is based on spectral analysis of the input and error. The parameters which may be adjusted are the filter time constants (b/a and c/a), the time between samples (T_e) and duration of each sample (θ), the operator's gain (K_{ec}/K_i) and the gain and time constant of the muscle loop.

This schematic diagram contains elements of both the model reference and error pattern recognition classes, and contains, in common with Elkind's model (13), the possibility of adaptation at the force generating end of the human controller. The concept of adaptive control through varying the sampling rate, with higher sampling frequency called for when the error rates increase, has been proposed by several investigators but still lacks experimental verification.

Summary of Adaptive Characteristics

The experimental studies and control descriptions of the human operator in recent years have extended the knowledge of adaptive behavior in manual tracking from vague generalities to quantitative descriptions. A considerable amount of data has been gathered on the ability of the human to adapt to changes in input spectra, controlled

element gain, polarity and dynamics, display modality, and the limits of controllability under a variety of situations. These results have indicated a greater adaptation versatility than expected from some earlier descriptions, but have also pointed out some of the restricted conditions under which the rapid human adaptation may be expected to be demonstrated.

When it comes to explaining how the human manages his remarkable adaptation abilities, very little real progress has been made. Improvement in the techniques for dynamic measurement of the adaptive process have been helpful in this regard but still fall short of what is required to observe the change in control law. Primarily as a result of the measurement limitation and the lack of sufficient knowledge about adaptive control systems in general, the development of models for human adaptive control has been limited to the very general "schematic models" at this time.

BIBLIOGRAPHY

1. Adams, J.A. Human tracking behavior, Psychol. Bull., 58:55-79, 1961.

2. Adams, J.J. and H.P. Bergeron. Measured variation in the transfer function of a human pilot in single-axis tasks. NASA TN d-1952, 1963.

3. Atwood, J., J. Elkind, J. Houk, M.King, L. Stark and P.A. Willis. Digital computer simulation of a neurological system. QPR 63, Res. Lab. Elec., MIT, Oct. 1961, pp. 215-217.

4. Ashkenas, I.L. and D.T. McRuer. A theory of handling qualities derived from pilot-vehicle system considerations. Aerospace Engineering 21:60 & 83, Feb. 1962.

5. Bekey, G.A. Discrete models of the human operator in a control system. Intl. Fed. of Automatic Control, Basel, Switzerland, 1963.

6. Bekey, G.A. Sampled data models of the human operator in a control system. Ph.D. Thesis, Dept. of Elec. Engineering, UCLA, 1962.

7. Boyd, I.A. The nuclear-bag fibre and nuclear-chain fibre systems in the muscle spindles of the cat. Symposium on Muscle Receptors. Partial Proceedings of Golden Jubilee Congress of the Univ. of Hong Kong. Ed. by David Barker, 1962, pp. 185-191.

8. Chernikoff, R., H.P. Birmingham and H.V. Keller. A comparison of pursuit and compensatory tracking in a simulated aircraft control loop. J. Appl. Psychol., 40:47-52, 1956.

9. Cortes, A. The human servo: arm control. M.S. Thesis, Univ. of California, Engineering Library, Berkeley, 1958.

10. Craik, K.J.W. Theory of the human operator in control systems. Brit. J. Psych. (I) 38:56-61, 1957 & (II) 38:142-148, 1948.

11. Draper, C.S., H.P. Whitaker and L.R. Young. The roles of men and instruments in control and guidance systems for aircraft. 15th International Astronautical Congress, Warsaw, Poland, September, 1964.

12. Elkind, J.I. Characteristics of simple manual control systems. TR 111, MIT, Lincoln Lab., Lexington, Mass., April 1956.

13. Elkind, J.I., J.A. Kelly and R.A. Payne. Adaptive characteristics of the human operator in systems having complex dynamics. Proc. 5th National Symposium on Human Factors in Electronics, San Diego, May, 1964, pp. 143-159.

14. Elkind, J.I., E.A. Starr, D.M. Green and D.L. Darley. Evaluation of a technique for determining time-invarient and time-varient dynamic characteristics of human pilot. NASA TN D-1897, 1963.

15. Fenn, W.O. and B.S. Marsh. Muscular force at different speeds of shortening. J. Physiol., 85:277, 1935.

16. Fujii, T. Human control --its dynamic characteristics. Kagako (Science - pub. by Iwanami Books Inc.) 30, No. 2, Feb. 1960.

17. Fulton J.R. and J.A. Pi-Suner. A note concerning the probable function of various afferent end-organs in skeletal muscle. Amer. J. Physiol., 83:554, 1928.

18. Goodyear Aircraft Corporation. Investigation of control 'feel' effects on the dynamics of a piloted aircraft system. Report GER 5726, April, 1955.

19. Granit, R. Neuromuscular interaction in post-sutural tone of the cat's isometric soleus muscle. J. Physiol., 143:387-402, 1958.

20. Hall, I.A.M. Effect of controlled element on the human pilot. WADC TR 57-509, Wright-Patterson AFB, Dayton, Ohio, October, 1957.

21. Hick, W.E. The discontinuous functioning of the human operator in pursuit tasks. Quart. J. Exp. Psychol., 1-2:36-52, 1948-50.

22. Hill, A.V. A Discussion on muscular contraction and relaxation: their physical and chemical basis. Proc. Roy. Soc. (London) B 137, 40, 1950.

23. Hill, A.V. The heat of shortening and the dynamic constants of muscle. Proc. Roy. Soc. (London), B126, 136, 1938.

24. Houk, J., Y. Okabe, H.E. Rhodes, L. Stark and P.A. Willis. Transient responses of the human motor coordination system. QPR 64. Res. Lab. Elec., MIT, June 1962, pp. 315-326.

25. Houk, J.C., V. Sanchez and P. Wells. Frequency of response of a spindle receptor. QPR 67, Res. Lab. Elec., MIT, Oct. 1962, pp. 223-227.

26. Houk, J.C. and L. Stark. An analytical model of a muscle spindle receptor for simulation of motor coordination. QPR 66, Res. Lab. Elec., MIT, July 1962, pp. 384-389.

27. Hunt, C.C. and S.W. Kuffler. Further study of efferent small nerve fibres to mammalian muscle spindles. Multiple spindle innervation and activity during contraction. J. Physiol., 113:283-297, 1951.

28. Hunt, C.C. and S.W. Kuffler. Stretch receptor discharges during muscle contraction. J. Physiol., 113:298-315, 1951.

29. Iberall, A.S. and S.Z. Cardon. Control in biological systems: a physical review. Ann. N.Y. Acad. Science 117:445-518, 1964.

30. Jex, H.R., C.H. Cromwell III and R.K. Siskind. Correlation of experimental and theoretical limits for pilot control of unstable second order systems. Systems Technology , Inc., Inglewood, Calif., Tech. Memo 56, July, 1960 .

31. Katz, B. The relation between force and speed in muscular contraction. J. Physiol., 96:45, 1939.

32. Kilpatrick, P.S., II. Comparison of relay and manual controllers for systems with high order dynamics. B.S. Thesis, Unpub., MIT, 1964.

33. Kipiniak, V.W. Simulation of biological control systems. QPR 62, Res. Lab. Elec., MIT, July 1961, pp. 284-286.

34. Knoop, D.E. and K.F. Fu. An adaptive model of the human operator in a control system. Proc. 5th National Symposium on Human Factors in Electronics, San Diego, California. May 1964, pp. 252-265.

35. Kohlhaas, R.L. Limits of pilot controllability of a two-axis unstable, second-order system. M.S. Thesis Air Force Institute of Technology, Wright-Patterson Air Force Base, Ohio, 1962.

36. Krendel, E.S. and D.T. McRuer. Servo approach to skill development. J. Franklin Institute 269:24, 1960.

37. Lemay, L.P. and J.H. Westcott. The simulation of human operator tracking using an intermittent model. Presented at Interntl. Congress on Human Factors in Electronics, Long Beach, Calif., May 1962.

38. Lippold, O.C.J., J.S. Nicholls and J.W.T. Redfearn . Electrical and mechanical factors in the adaptation of a mammalian muscle spindle. J. Physiol., 153: 209-217, 1960.

39. McRuer, D.T. and I.L. Ashkenas. Design implications of the human transfer function. Aerospace Engineering 21:76-77, 144-147, September 1962.

40. McRuer, D.T. and E.S. Krendel. Dynamic response of human operators. WADC TR 56-524, Wright-Patterson AFB, Ohio, 1957.

41. McRuer, D.T. and E.S. Krendel. The human operator as a servo system element. J. Franklin Institute 267: 381-403, 511-536, 1959.

42. McRuer, D.T. and E.S. Krendel. The man-machine concept. Proc. IRE, 50:1117-1123, 1962.

43. McRuer, D.T., E.S. Krendel and . . Graham. Adaptive and optimalizing behavior of the human operator in compensatory tracking. 15th International Astronautical Federation Congress, Warsaw, September, 1964.

44. Merton, P.A. Speculations on the servo control of movement. CIBA Foundation Symposium: The Spinal Cord, ed. by G.E.W. Wohrtenholine. J. and A. Churchill, Ltd., London, 1953, pp. 247-260.

45. Mesarovic, M.D. The Control of Multivariable Systems. M.I.T. Press, Cambridge, Mass. and Wiley, New York, N.Y., 1960.

46. Naslin, P. and J.C. Raoult. Modeles continus et échantillonnés de l'operateur humain placé dans une boucle de commande. 2nd Cong. International Federation Automatic Control, Basel, Switzerland, 1963.

47. Navas, F. Sampling or quantization in the human tracking system. M.S. Thesis, M.I.T., 1963.

48. Nelson, G.P., L. Stark and L.R. Young. Phototube glasses for measuring eye movement. QPR 67, Res. Lab. Elec., MIT, October, 1962, pp. 214-216.

49. North, J.D. The human transfer function in servo systems. in Automatic and Manual Control, ed. by A. Tustin, Butterworths, London, 1952, pp. 473-502.

50. Okabe, Y., H.E. Rhodes, L. Stark and P.A. Willis. Simultaneous hand and eye tracking movements. QPR 66, Res. Lab. Elec., MIT, July 1962a, pp. 395-401.

51. Okabe, Y., H.E. Rhodes, L. Stark and P.A. Willis. Transient responses of human motor coordination system. QPR 66, Res. Lab. Elec., MIT, July 1962b, pp. 389-395.

52. Ornstein, G.N. Applications of a technique for the automatic analog determination of human response equation parameters. North American Aviation, Inc., Columbus, Ohio. Report No. NA 61H-1, January, 1961.

53. Osburn, P.V. and H.P. Whitaker and A. Kezer. New developments in the design of model reference adaptive control systems. Institute of Aerospace Sciences, Paper No. 61-39, January 1961.

54. Pew, R.W. A model of human controller performance in a relay control system. Proc. 5th Natnl. Symposium on Human Factors in Electronics, San Diego, California, May, 1964.

55. Pew, R.W. Temporal organization in skilled performance. Doctoral Dissertation, University of Michigan, 1963.

56. Raoult, J.C. Etude de l'operateur humain en tant qu' élément d'un système asservi. Doctoral Dissertation, Université de Toulouse, 1962.

57. Russell, L. Characteristics of the human as a linear servo-element. M.S. Thesis, M.I.T., 1951.

58. Sadoff, M. A study of a pilot's ability to control during simulated stability augmentation system failures. NASA TN D-1552, 1962.

59. Sandberg, A.A. and L. Stark. Analog simulation of the human pupil system. QPR 66, Res. Lab. Elec., MIT, July, 1962, pp. 419-428.

60. Senders, J.W. and M. Cruzen. Tracking performance on combined compensatory and pursuit tasks. WADC TR-52-39, Wright-Patterson AFB, Ohio, 1952.

61. Sheridan, T.B. Experimental analysis of time variation of the human operator's transfer function. Proc. 1st Congress on International Federation of Automatic Control. Moscow, 1960; Butterworth, London, 1961.

62. Sheridan, T.B. The human operator in control instrumentation, in Progress in Control Engineering - 1, Hayward and Co., Ltd, London, 1962.

63. Sherrington, C.S. J. Physiol., 49:331, 1915.

64. Smith, R.H. The limits of manual control. Institute of Electrical and Electronics Engineers, Inc. Trans. on Human Factors in Electronics HFE-4:56-59, 1963.

65. Sobczyk, A. Radiation Lab. Report 430, M.I.T., September, 1943.

66. Stark, L. Neurological organization of the control system for movement. QPR 61, Res. Lab. Elec., MIT, April 1961, pp. 234-238.

67. Stark, L. Stability oscillations and noise in the human pupil servomechanism. Proc. IRE 47:1925-1939, 1959.

68. Stark, L. and F. Baker. Stability and oscillations in a neurological servomechanism. J. Neurophysiol., 22:156, 1959.

69. Stark, L., J. Houk, P.A. Willis, and J. Elkind. The dynamic characteristics of a muscle model used in digital-computer simulation of an agonist-antagonist muscle system in man. QPR 64, Res. Lab. Elec., MIT, January 1962a, pp. 309-315.

70. Stark, L., M. Iida and P.A. Willis. Dynamic characteristics of motor coordination. QPR 60, Res. Lab. Elec., MIT, pp. 231-233.

71. Stark, L., M. Iida and P.A. Willis. Dynamic characteristics of motor coordination system in man. Biophysics J., 1:279-300, 1961.

72. Stark, L., Y. Okabe and P.A. Willis. Sampled data properties of the human motor coordination system. QPR 67, Res. Lab. Elec., MIT, October 1962, pp. 220-223.

73. Stark, L. and G. Rushworth. Voluntary movement without gamma efferent innervation. Tech. Report, Neurology Section, Yale University, May 1958.

74. Stark, L., G. Vossius and L.R. Young. Predictive control of eye movements. QPR 62, Res. Lab. Elec., MIT, July 1961, pp. 271-281.

75. Stark, L. and L.R. Young. Defining biological feedback control systems. N.Y. Acad. Science, Conference on Photo-neuro-endocrine effects in circadian systems with particular reference to the eyes. June 1963.

76. Tanner, W.P. and Swets, J.A. A decision making theory of visual detection. Psych. Rev. 61:401-409, 1954.

77. Tustin, A. An investigation of the operator's response in manual control of a power-driven gun. C.S. Memorandum No. 169. Metropolitan-Vickers Electrical Co., Ltd., Sheffield, England, 1944.

78. Tustin, A. The nature of the operator's response in manual control and its implications for controller design. J. Institute of Electrical Engineers 94 Part IIA:190-202, 1947.

79. Ward, J.R. The dynamics of a human operator in a control system: a study based on the hypothesis of intermittency. Ph.D. Dissertation, Dept. of Aeronautical Engineering, University of Sydney, Australia, May 1958.

80. Wilde, R.W. and J.H. Westcott. The characteristics of the human operator engaged in a tracking task. Automatica 1:1962.

81. Wilkie, D.R. The relation between force and velocity in human muscle. J. Physiol., 110:249-280, 1950.

82. Willis, P.A. Mechanical output impedance of motor coordination transducer. Unpub. data, M.I.T., 1960.

83. Young, L.R. A sampled data model for eye tracking movements. Sc.D. Thesis, Department of Aeronautics & Astronautics, M.I.T., 1962.

84. Young, L.R. A sampled data model for eye tracking movements. Proc. Internl. Conference on Automatic Control. Basel, Switzerland, 1963 (Butterworths, London).

85. Young, L.R., D.M. Green, J.I. Elkind and J.A. Kelly. The adaptive dynamics response characteristics of the human operator in simple manual control. NASA TN D-2255, 1964.

86. Young, L.R. and L. Stark. A discrete model for eye tracking movement. Institute of Electrical and Electronics Engineers Trans. on Military Electronics, MIL 7:113-115, 1963.

87. Young, L.R. and L. Stark. Variable feedback experiments testing a sampled data model for eye tracking movements. Institute of Electrical and Electronics Engineers Trans. on Human Factors in Electronics, HFE-4:38-51, 1963.

TABLE 3

Third test of Pilot E

[Disturbance break frequency, 1 radian/sec]

Test	Dynamics	Measured gains			Transfer function	$\frac{\theta}{D}$ characteristics			Root-mean-square error, volts
						Oscillatory		Real roots	
		K_1	τ, radians/sec	K_2		ω, radians/sec	ζ		
1	1	4	4.5	0.5	$\frac{\delta}{D} = \frac{0.89(1 + 0.11s)}{(1 + 0.22s)^2}$				0.6
2	$\frac{1}{s + 1}$	6	6	5	$\frac{\delta}{D} = \frac{1(1 + 0.83s)}{(1 + 0.16s)^2}$				1.1
3	$\frac{10}{s^2 + 3s + 10}$	4.5	7	1.5	$\frac{\delta}{D} = \frac{0.64(1 + 0.21s)}{(1 + 0.14s)^2}$				1.0
4	$\frac{2}{s}$	4	3	2	$\frac{\delta}{\epsilon} = \frac{1.3(1 + 0.67s)}{(1 + 0.33s)^2}$	4.36	0.54	-1.26	.7
5	$\frac{10}{s(s + 2.5)}$	3	5	2	$\frac{\delta}{\epsilon} = \frac{0.6(1 + 0.4s)}{(1 + 0.2s)^2}$	2.8	.40	-2.5,-7.78	1.2
6	$\frac{10}{s(s + 1)}$	2.5	6.5	5.5	$\frac{\delta}{\epsilon} = \frac{0.38(1 + 0.83s)}{(1 + 0.15s)^2}$	3.45	.37	-1.24,-10.1	1.6
7	$\frac{10}{s^2}$	4	9.5	8	$\frac{\delta}{\epsilon} = \frac{0.42(1 + 0.84s)}{(1 + 0.10s)^2}$	3.9	.40	-1.41,-1.78	2.0
8	$\frac{10}{s(s^2 + 3s + 10)}$	6	7	5	$\frac{\delta}{\epsilon} = \frac{0.86(1 + 0.71s)}{(1 + 0.14s)^2}$	3.2, 7.9	0.18, 0.96	-0.60	1.6

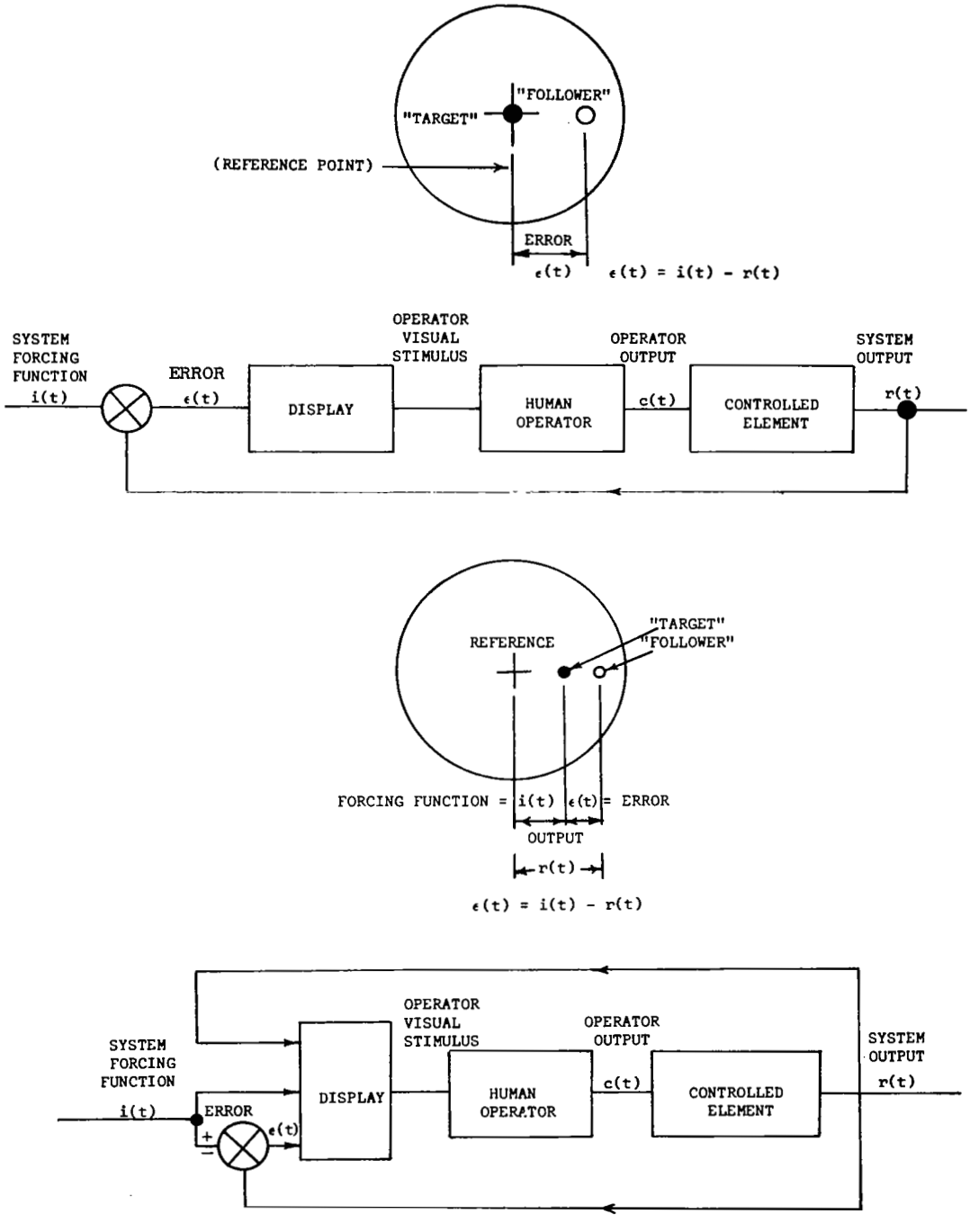

Figure 1. Compensatory (at top) and pursuit closed loop manual tracking systems: schematic displays and functional block diagrams. (Krendel & McRuer, 1960)

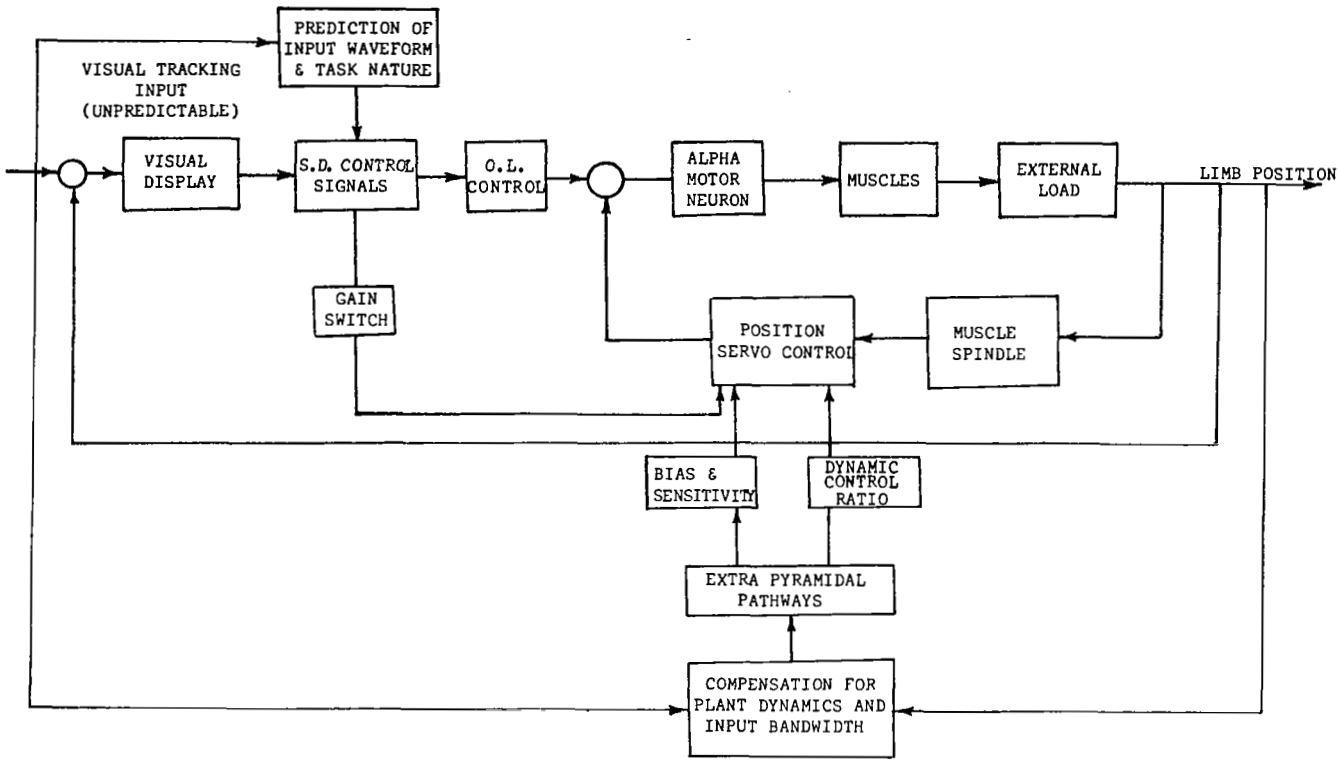

Fig. 2. Simplified Block Diagram for Movement Control

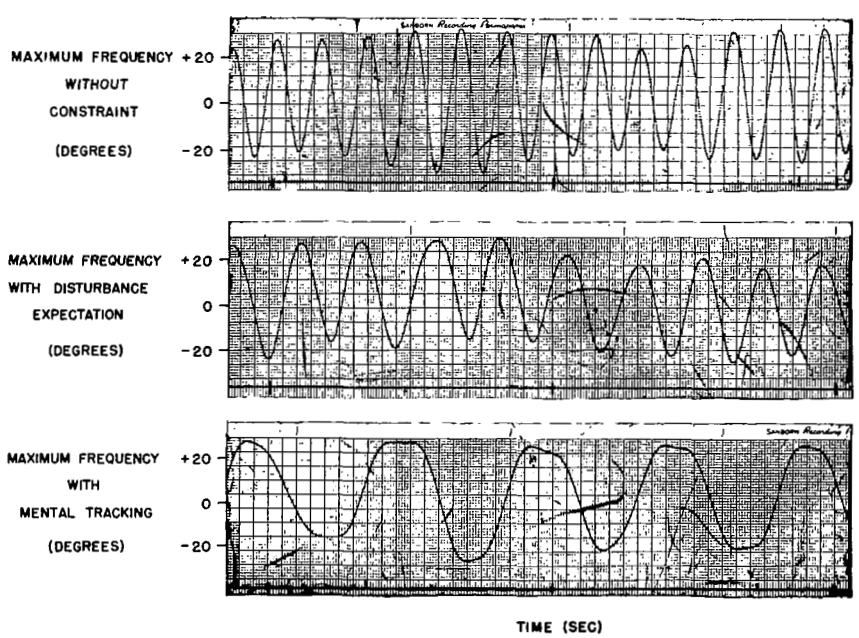

Figure 3. Freewheeling experiment. (Stark, 1961)

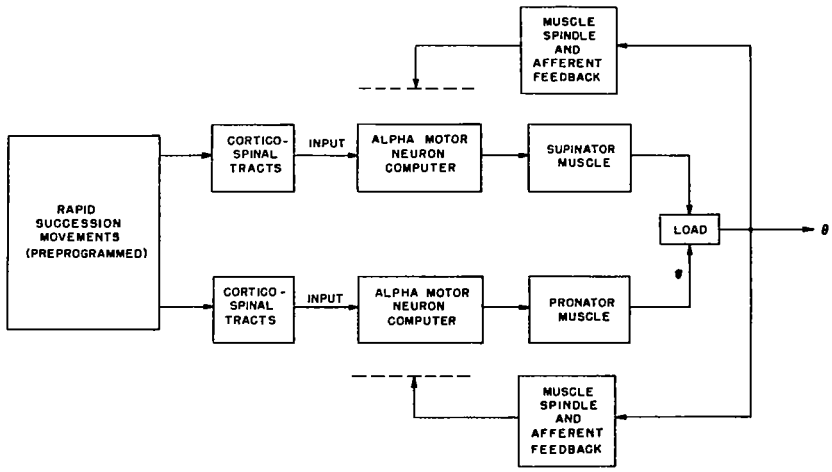

Fig. 4a. Rapid-succession movements: freewheeling. (Stark, 1961)

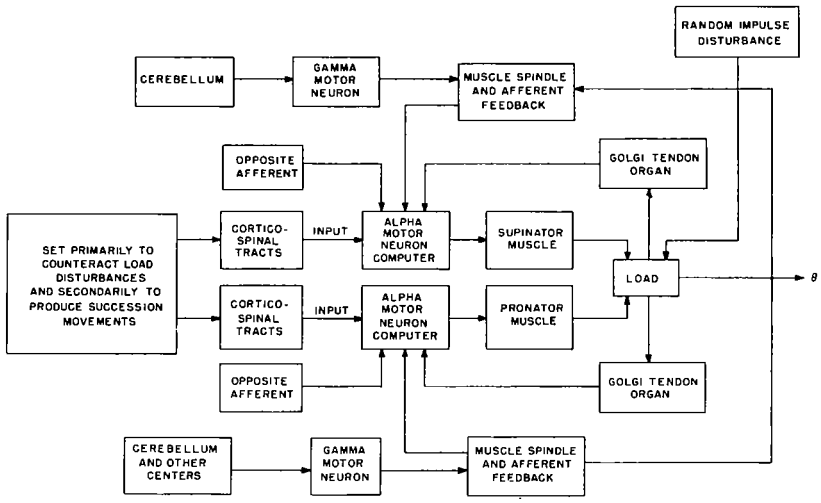

Fig. 4b. Position servocontrol set primarily to counteract load disturbances. (Stark, 1961)

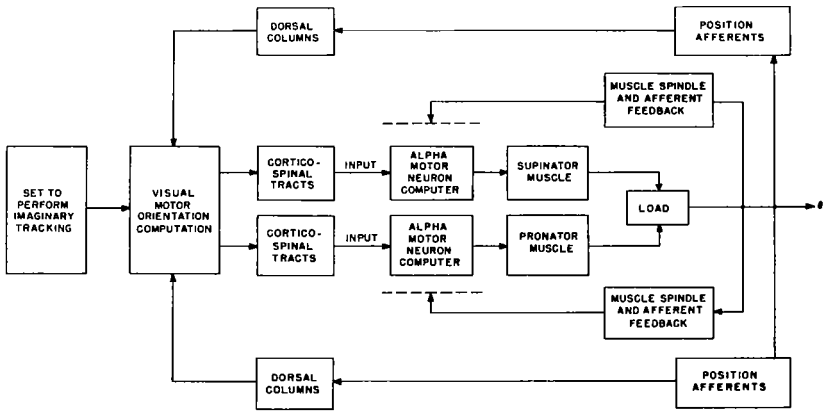

Fig. 4c. Mental tracking mode configuration. (Stark, 1961)

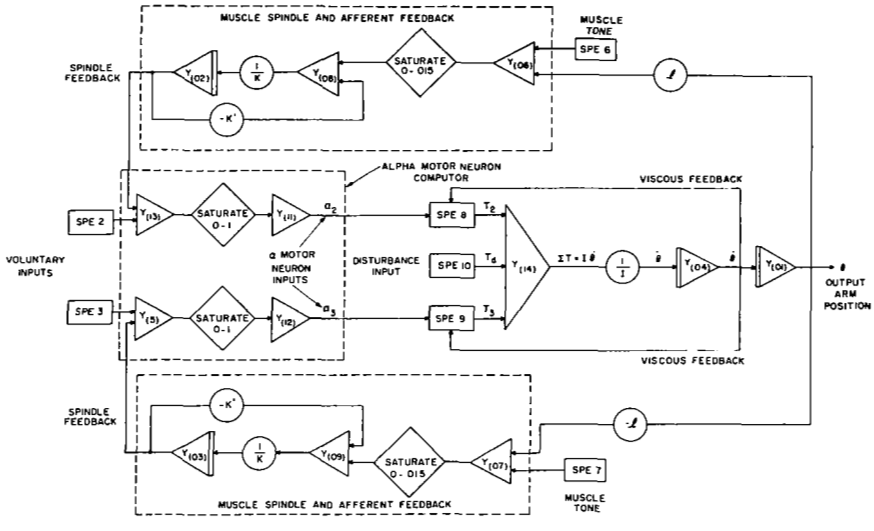

Fig. 5 BIOSIM block diagram of a simple motor coordination system.

Constants: $I = 1/10 \frac{\text{kg-m}^2 \text{ sec}^2}{\text{rad}}$; $k = 0.0014 \frac{\text{m}}{\text{rad}}$; $k' = 0.014$ m;

$\ell = 0.01$ meter; the initial condition on the integraters is zero.

(Atwood et al., 1961)

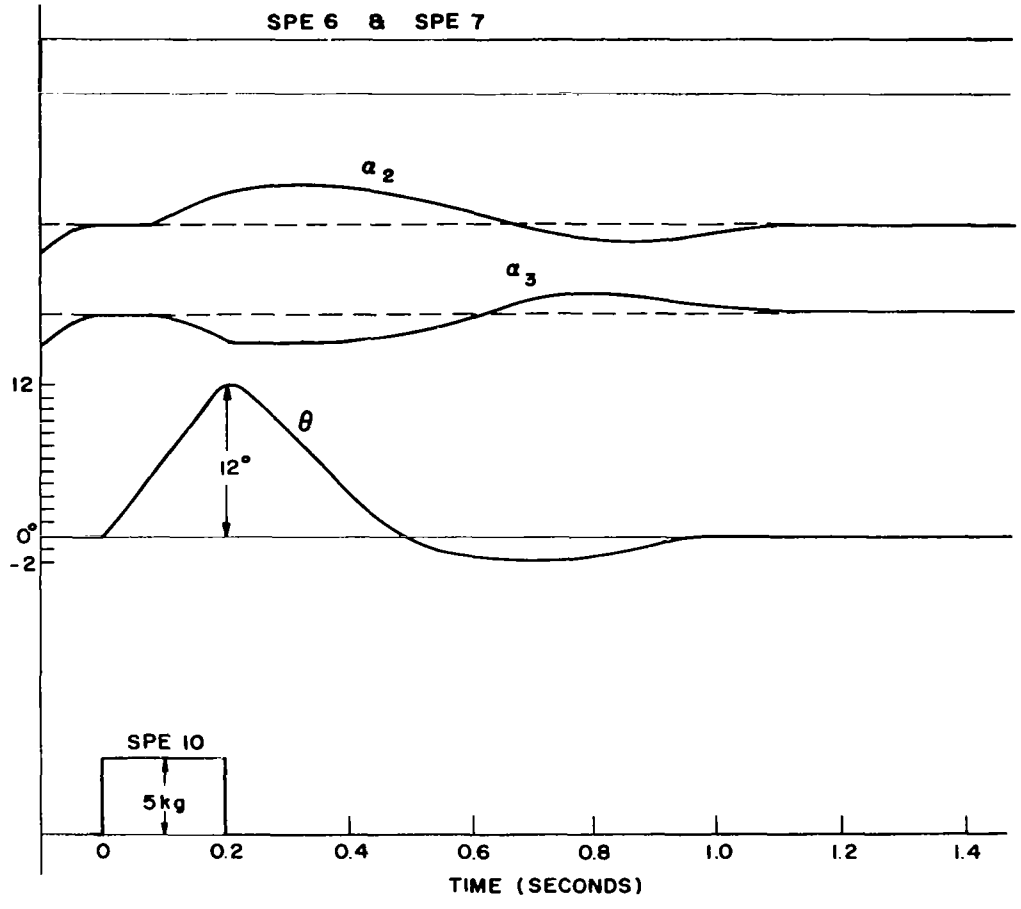

Fig. 6 BIOSIM outputs
(Atwood et al., 1961)

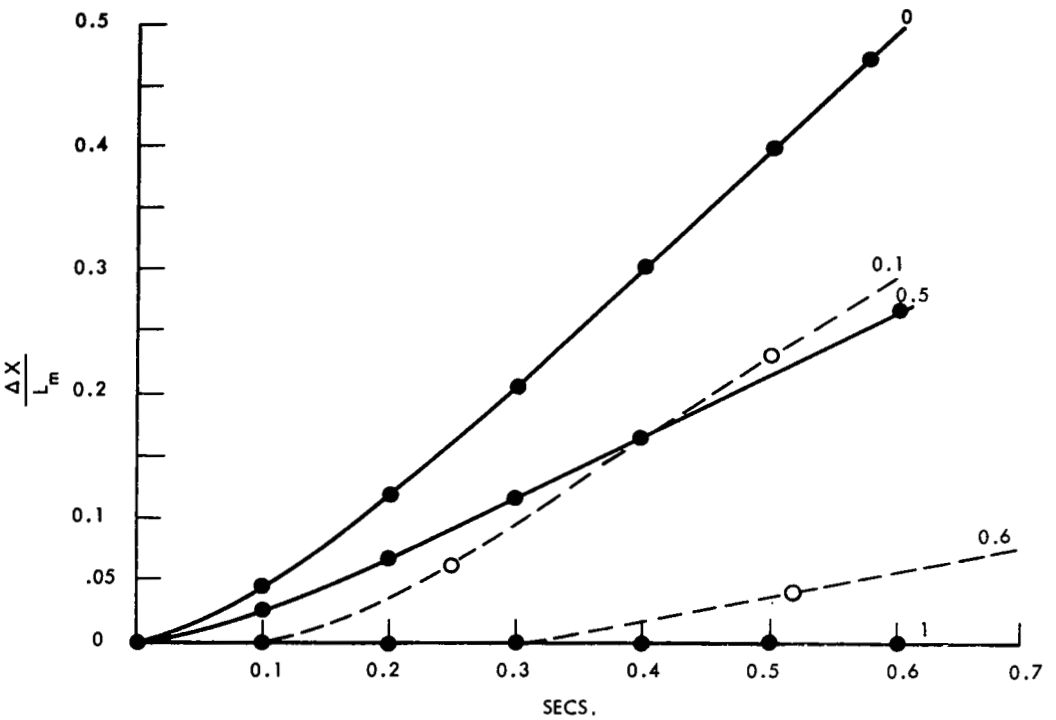

Figure 7. Comparison of BIOSIM model with Fenn and Marsh experiments. The plots show strain in muscle vs time. Solid lines represent data from the BIOSIM model; dashed lines show the similar shape obtained by Fenn and Marsh, when normalized stretch and time are corrected to the physiological scale of man. (The corrections are suggested by Hill.) The parameter noted on the curves is the normalized load, $\frac{F_{load}}{F_{iso}}$.

(Stark, Houk, Willis and Elkind, 1962)

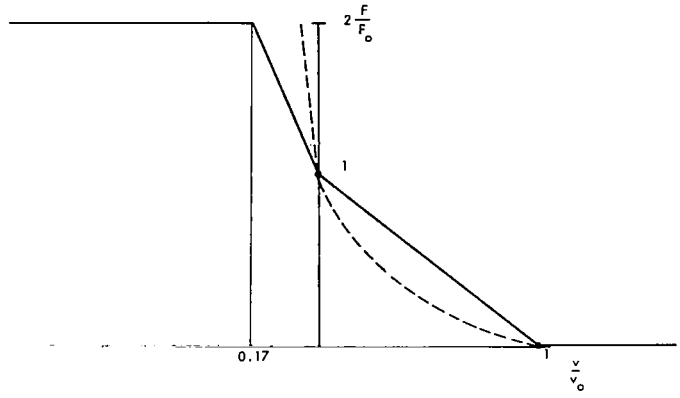

Figure 8a. Comparison of BIOSIM model with experiment. The solid curve shows the force-velocity relationship of the BIOSIM model; the dashed curve, the force-velocity relationship of frog muscle as obtained by Katz. For frog muscle P_0 = 0.1 kg, v_0 = 4 cm/sec.

(Stark, Houk, Willis, and Elkind, 1962)

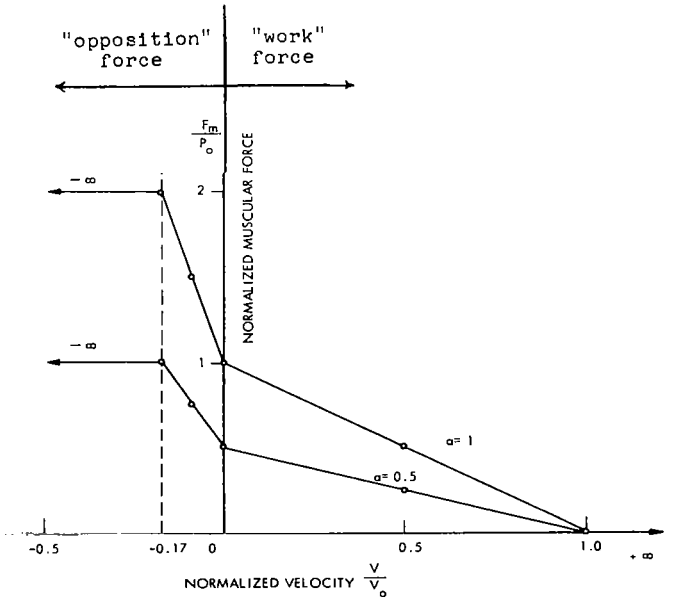

Figure 8b. Force-velocity relationship of BIOSIM model. (α = 1, maximal stimulation; α = 0.5, half-maximal stimulation.)

(Stark, Houk, Willis and Elkind, 1962)

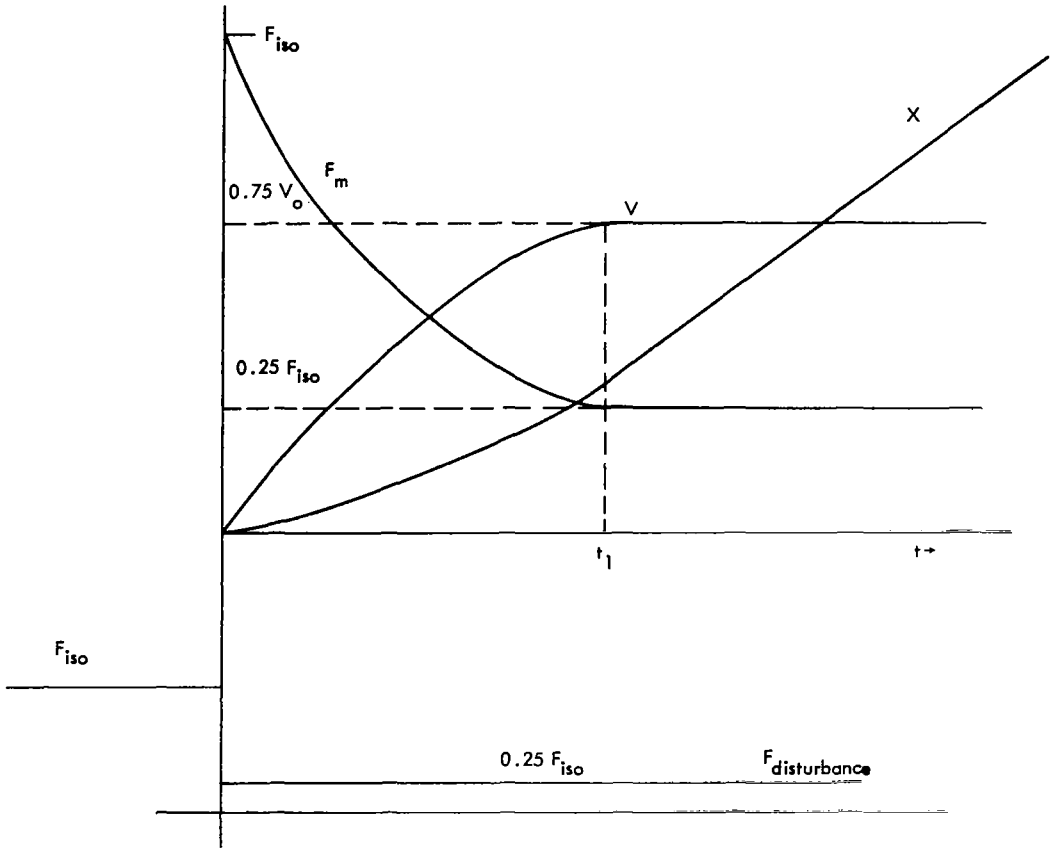

Figure 9. Experiment performed with the BIOSIM model. F_m is the total force exerted by the muscle, x is the muscle displacement, v is muscle velocity, excitation is maximal. The time t_1 was necessary for the model to overcome inertia and reach constant velocity. (Stark, Houk, Willis and Elkind, 1962)

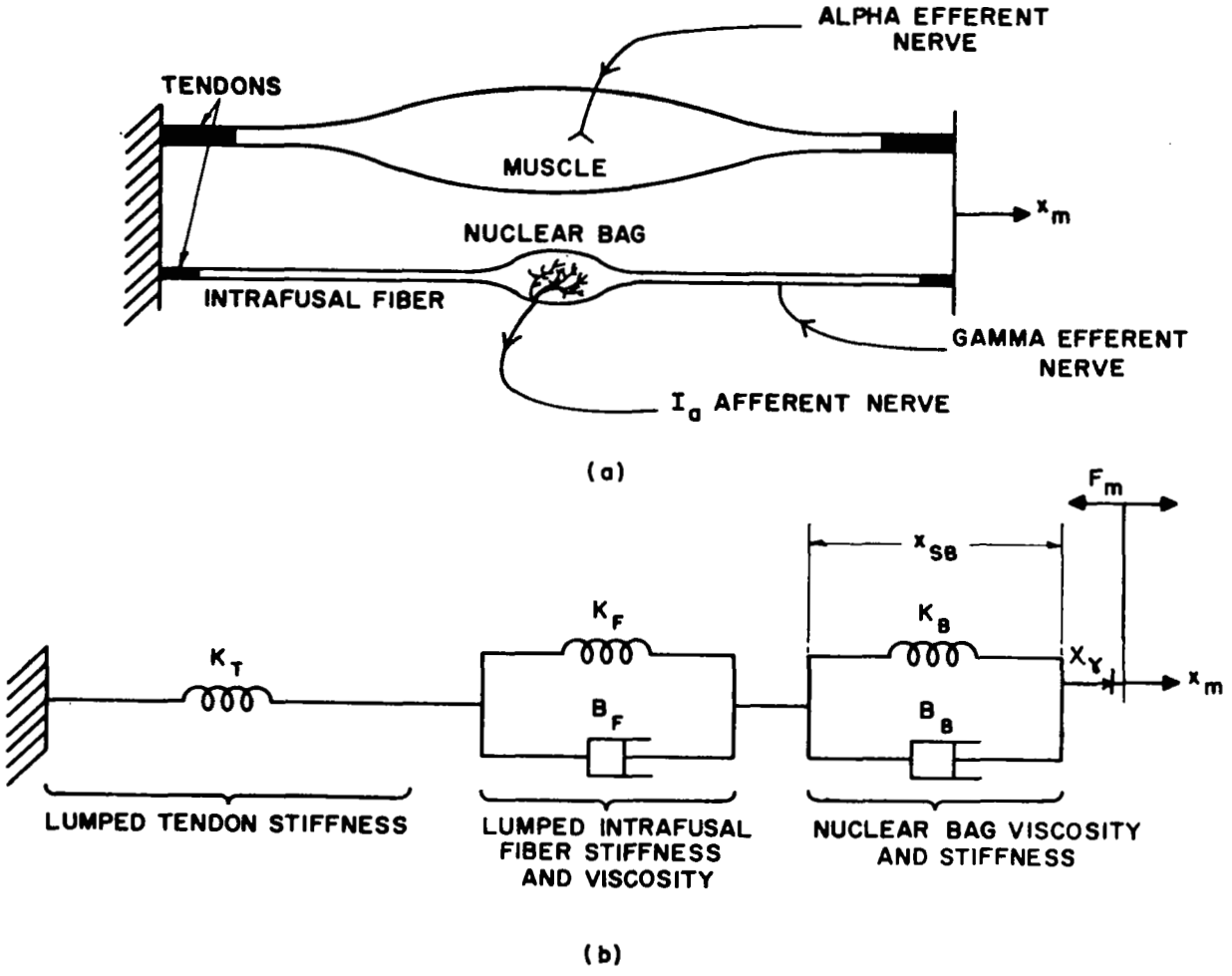

Fig. 10 (a) Diagram showing a simplified muscle with one of its in-parallel spindle receptors removed from the muscle for ease of illustration.
(b) Mechanical model of a spindle receptor. Inputs are X_m (length of the muscle) and X_γ (artificial length caused by an input to the intrafusal fiber); the output is X_{SB} (length of the nuclear bag).
(Houk and Stark, 1962)

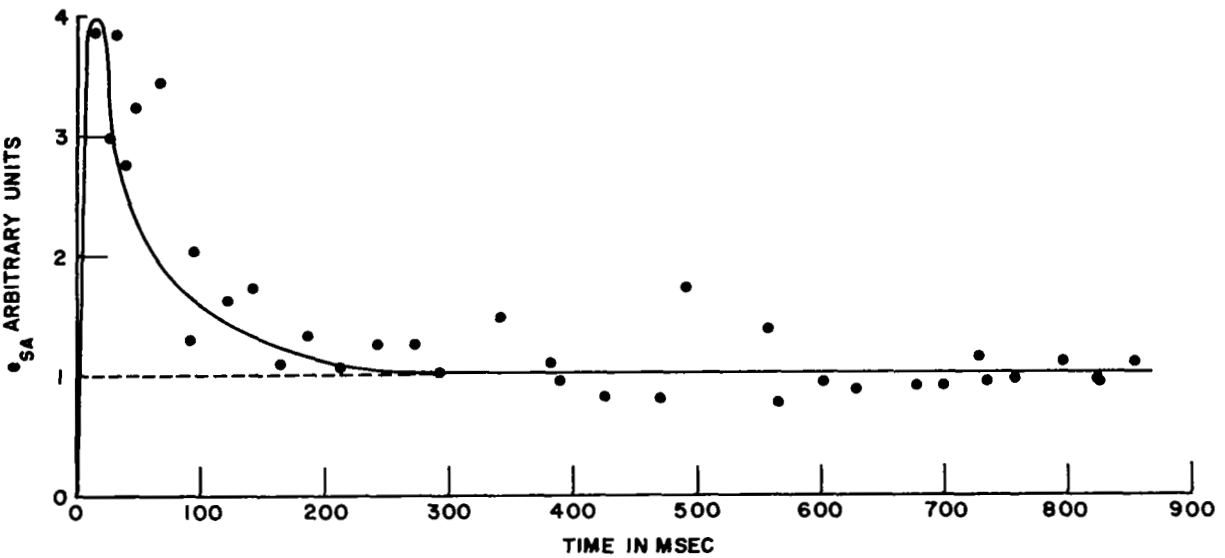

Figure 11a. The response of the spindle receptor to a step input of stretch. (Houk & Stark, 1962)

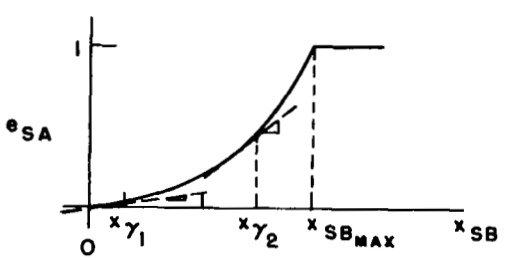

Figure 11b. The tonic input-output characteristic of the spindle receptor. (Granit, 1958)

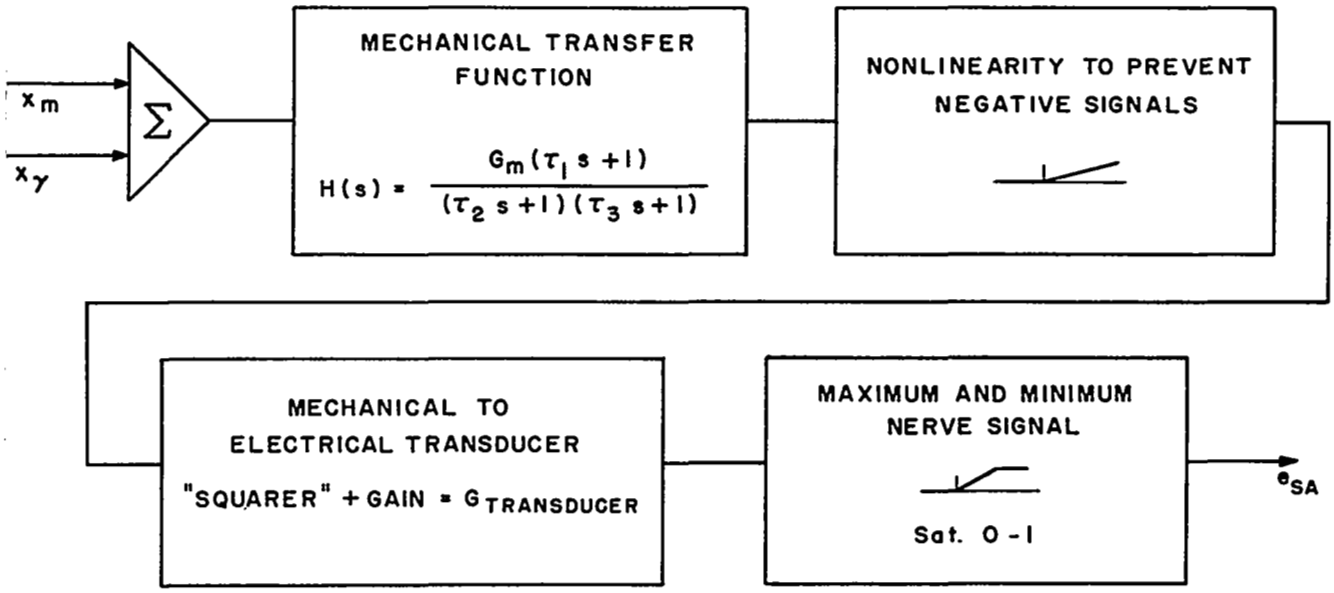

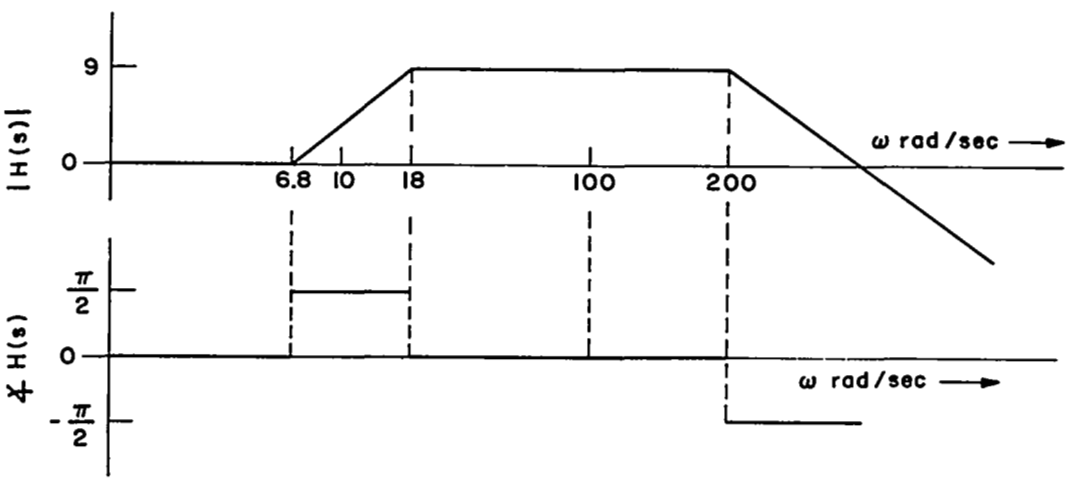

Fig. 12a. Complete block diagram of the spindle receptor model. Inputs are muscle length and length that is due to gamma input and to intrafusal fiber; output is average number of pulses per second.

Fig. 12b. Asymptotic Bode plots of the gain and phase characteristics of H(S), the transfer function of the mechanical part of the spindle receptor model. (Houk and Stark, 1962)

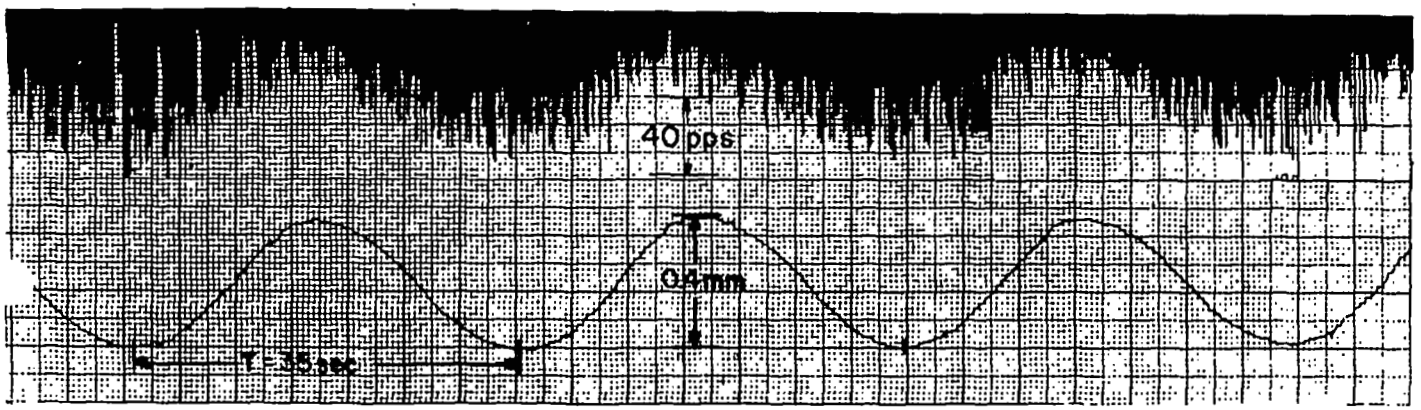

Fig. 13a. Response of spindle receptor to sinusoidal drive. Length of vertical lines in top record is proportional to interval between successive nerve pulses from spindle; peak-to-peak change in instantaneous frequency, ~40 pps. Bottom record shows sinusoidal component of spindle stretch, the input (frequency ≈0.03 cps). (Houk, Sanchez & Wells, 1962)

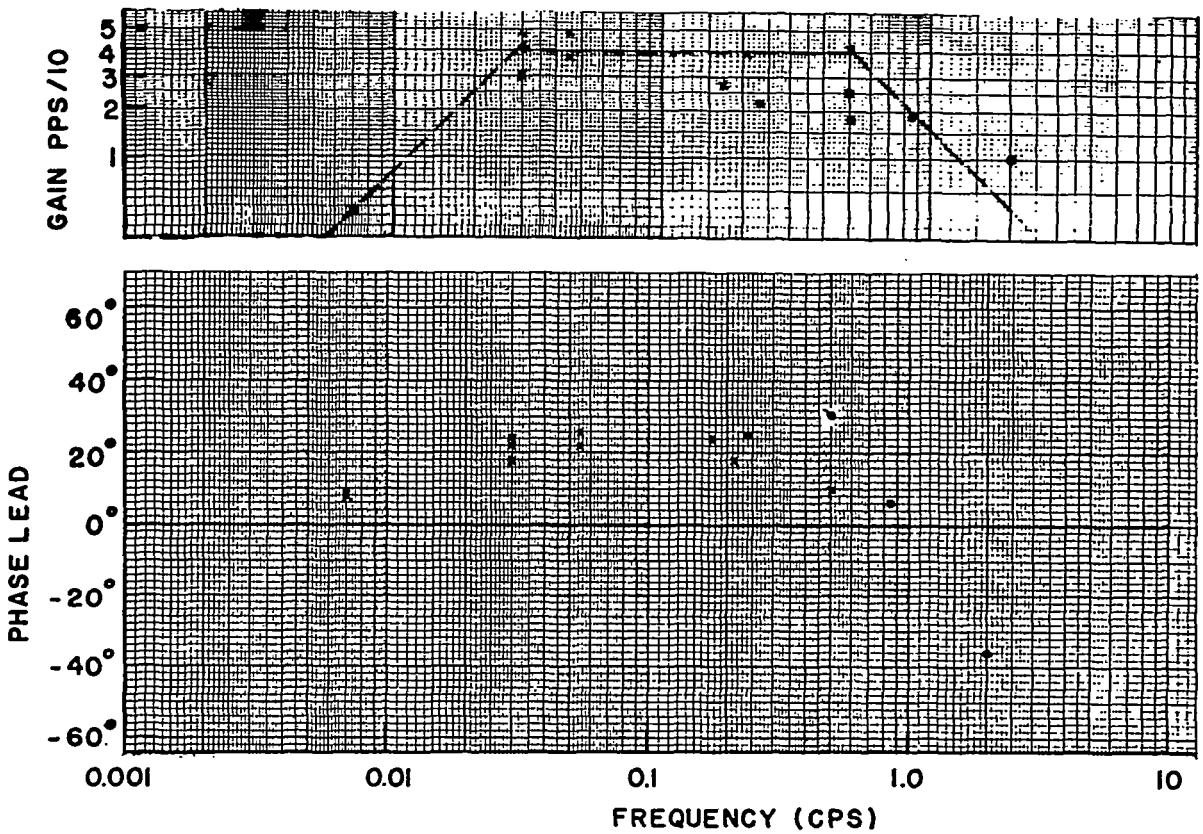

Fig. 13b Frequency response of a frog spindle receptor. Rough asymptotes have been drawn on the gain curve. (Houk, Sanchez & Wells, 1962)

SKETCH SHOWING MECHANICAL PORTION OF APPARATUS

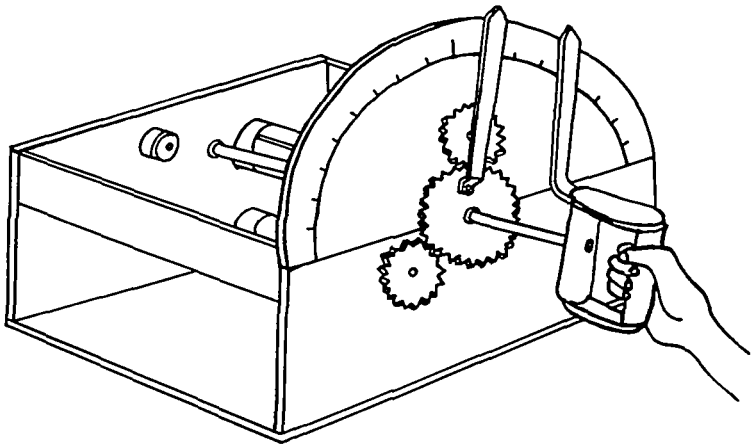

Fig. 14 (Stark, Iida and Willis, 1961)

PREDICTABLE INPUT EXPERIMENT

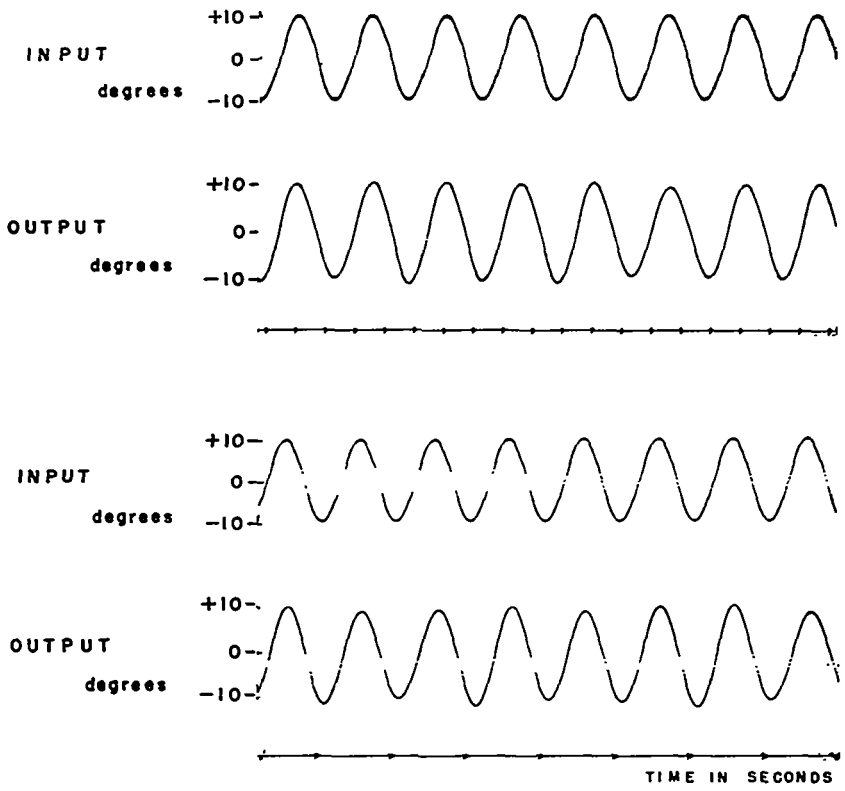

Fig. 15 (Stark, Iida and Willis, 1961)

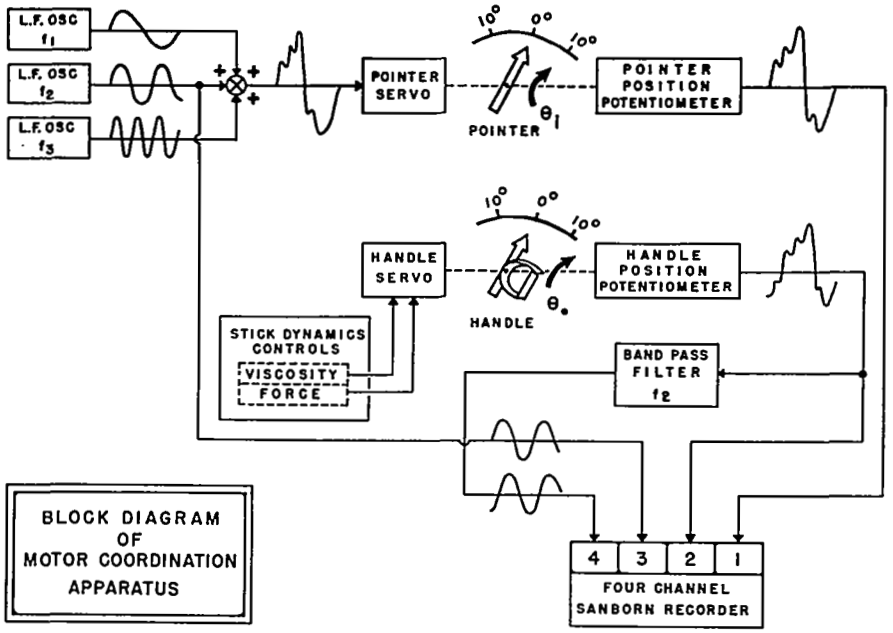

Fig. 16 (Stark, Iida and Willis, 1961)

TRANSIENT EXPERIMENT

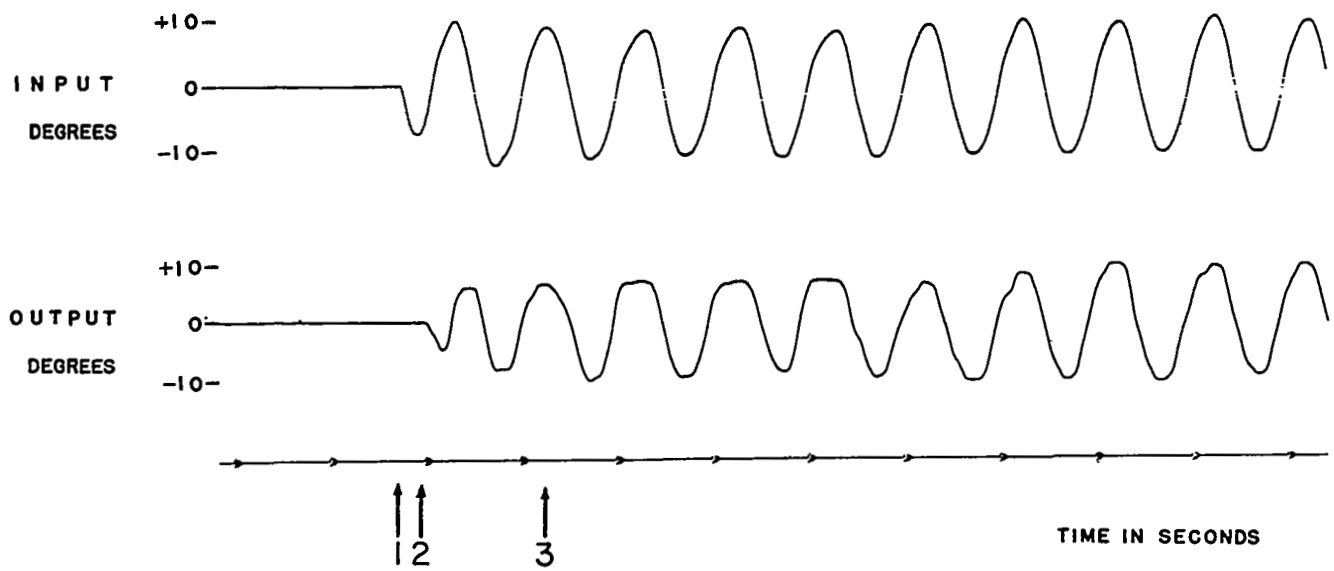

Fig. 17 (Stark, Iida and Willis, 1961)

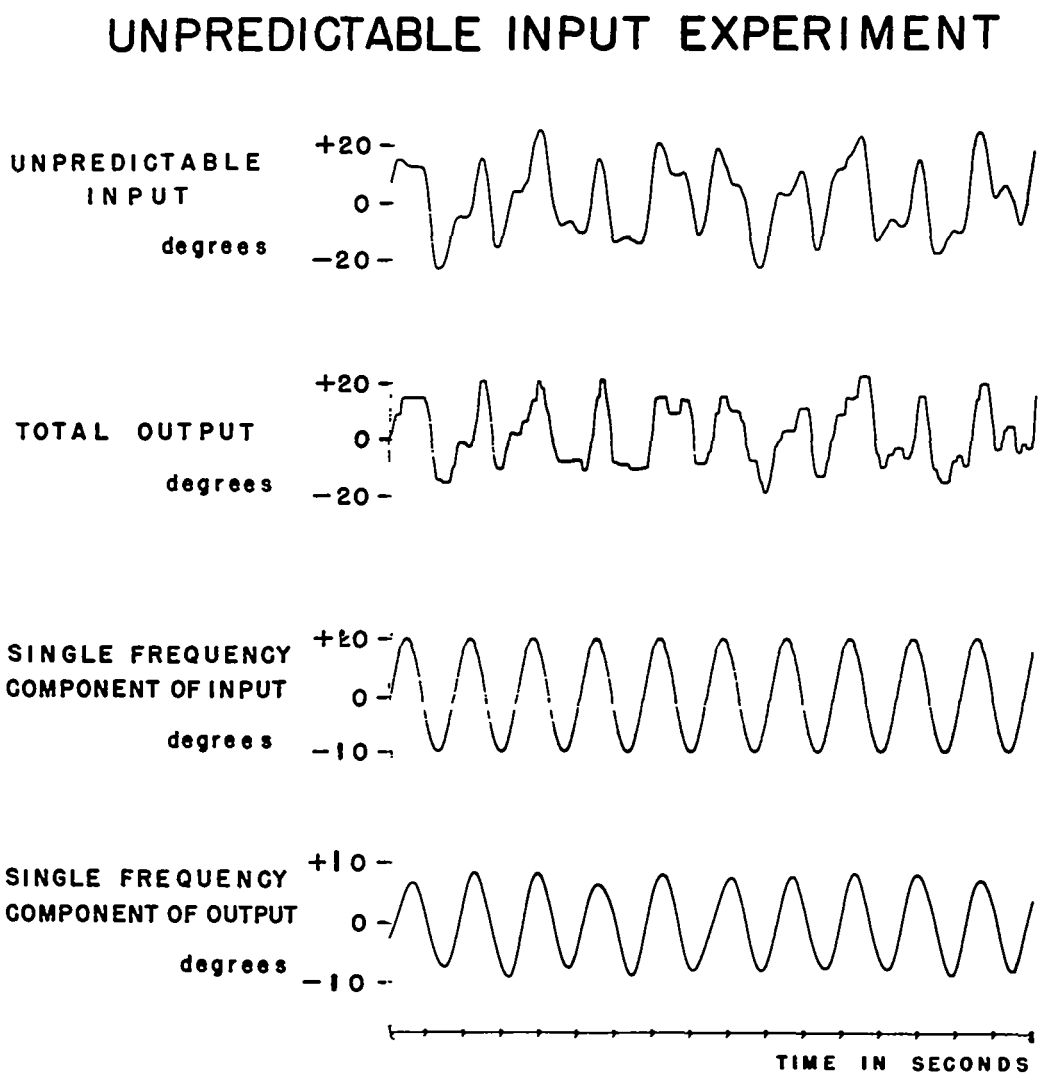

Fig. 18 (Stark, Iida and Willis, 1961)

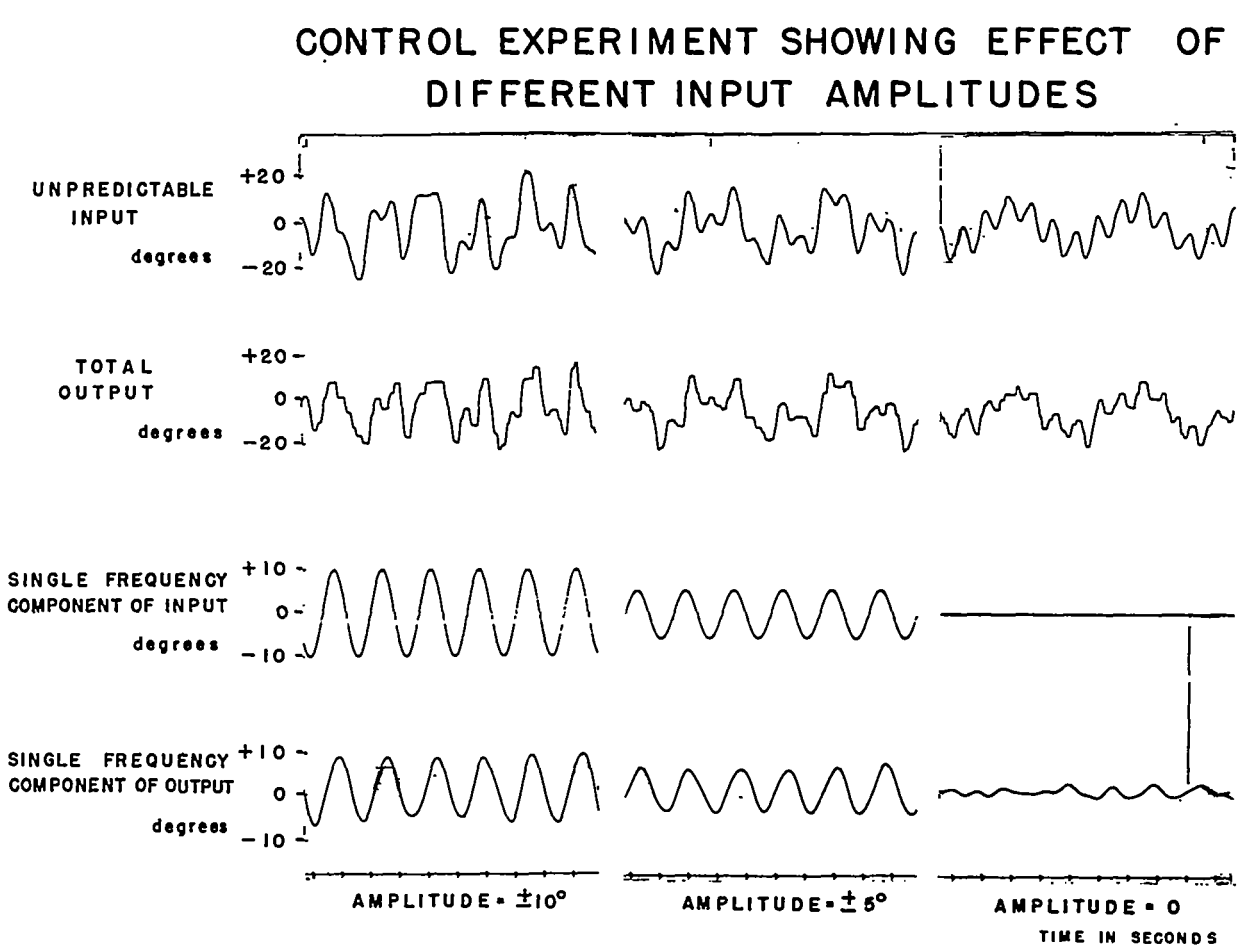

Fig. 19 (Stark, Iida and Willis, 1961)

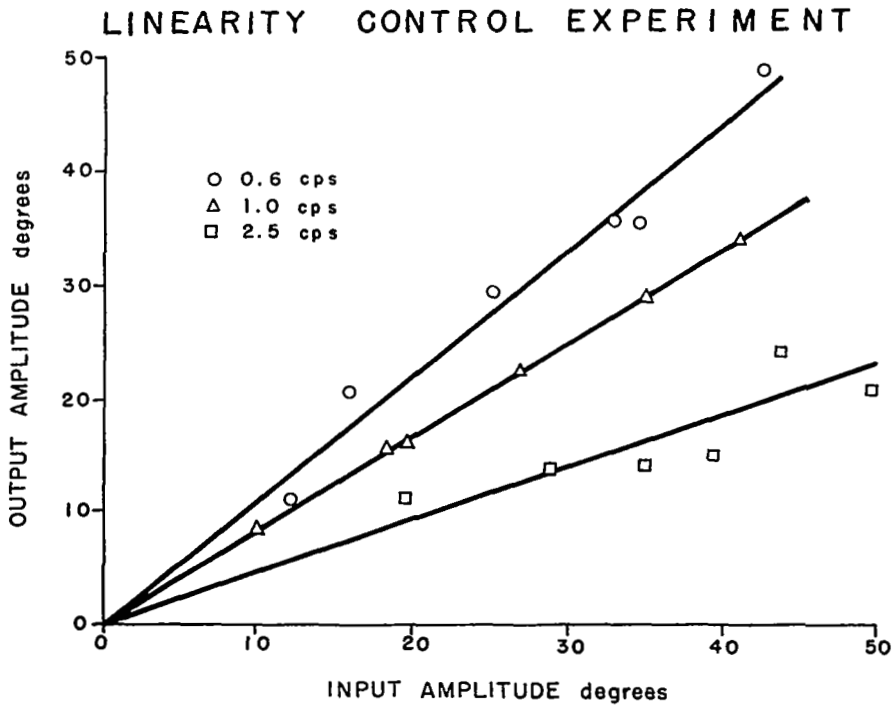

Fig. 20 (Stark, Iida and Willis, 1961)

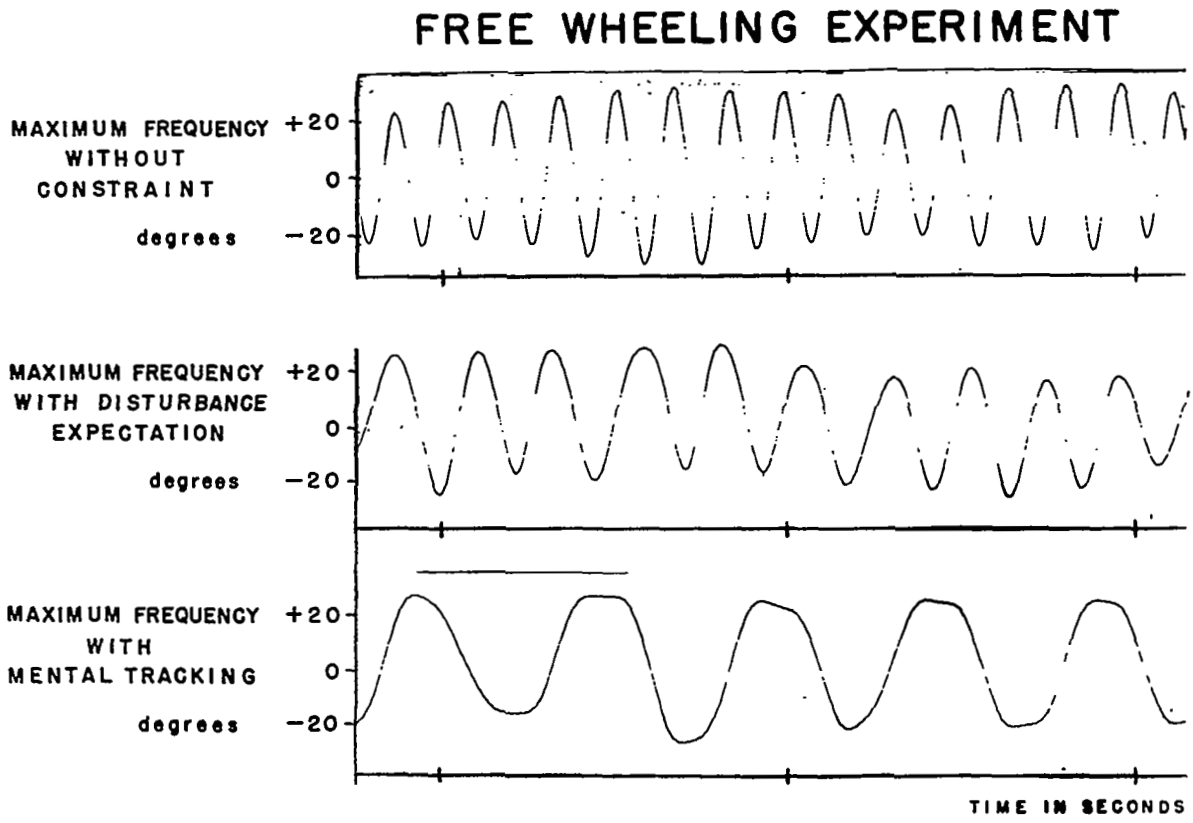

Fig. 21 (Stark, 1961)

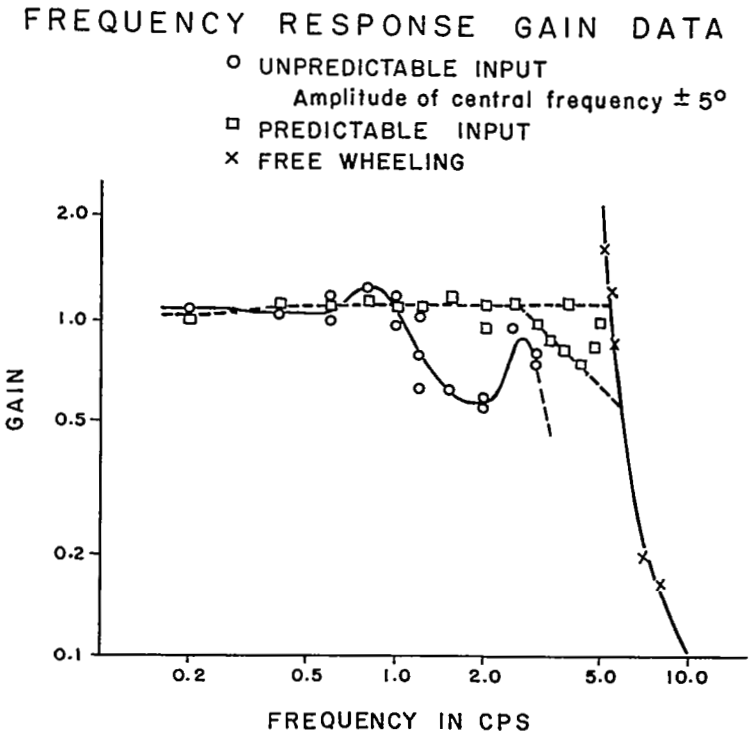

Fig. 22 (Stark, Iida & Willis, 1961)

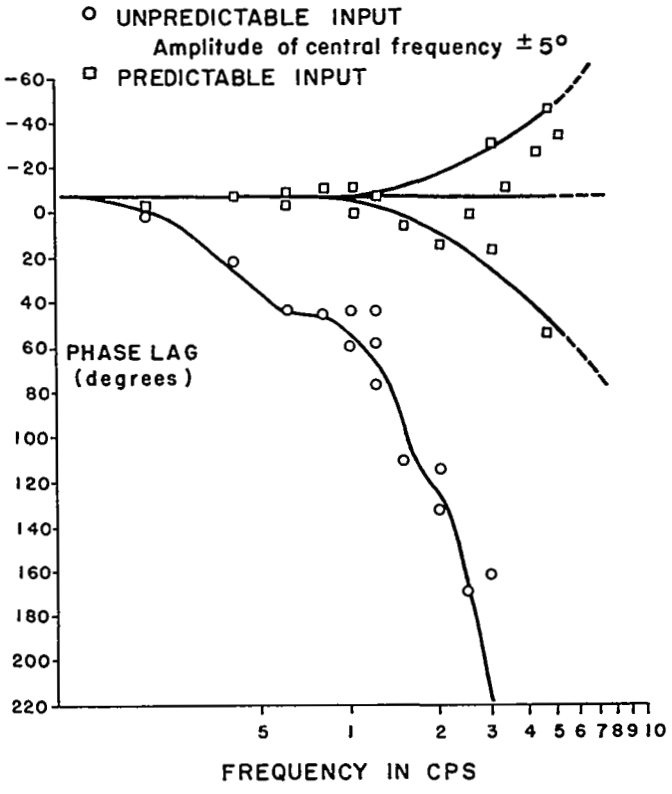

Fig. 23 (Stark, Iida & Willis, 1961)

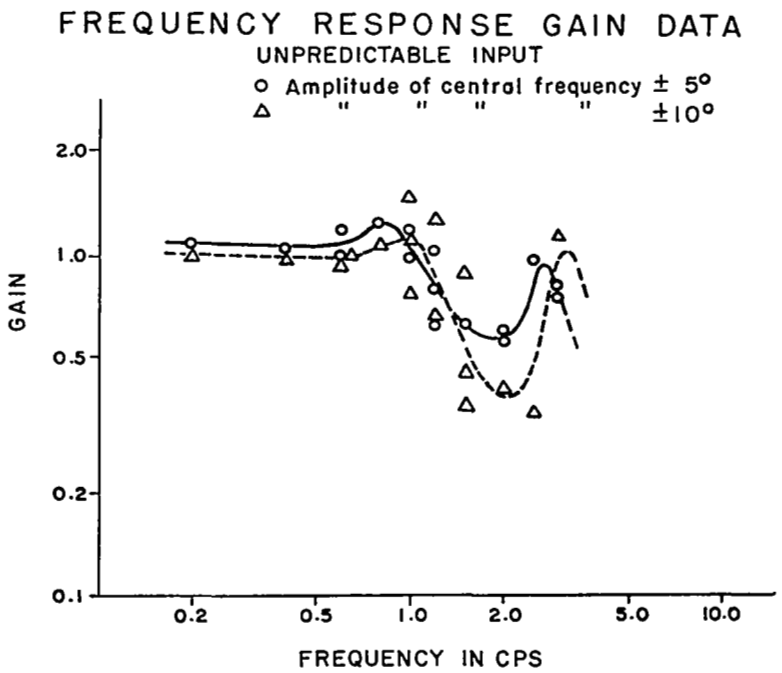

Fig. 24 (Stark, Iida & Willis, 1961)

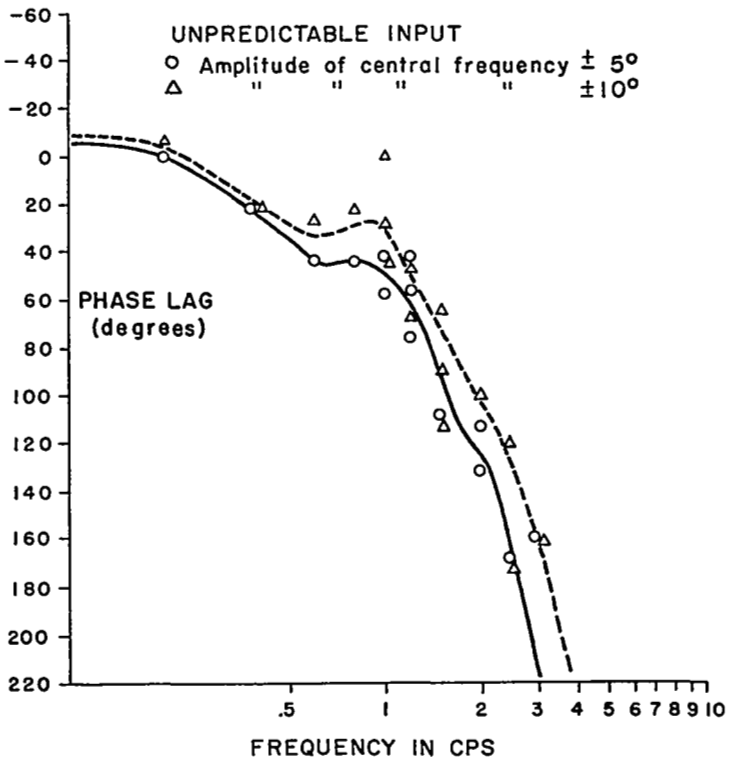

Fig. 25 (Stark, Iida & Willis, 1961)

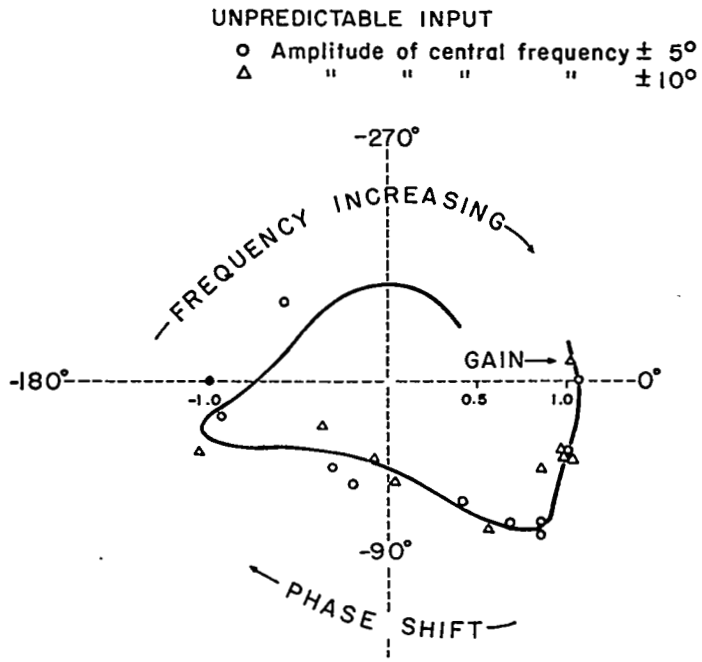

Fig. 26 (Stark, Iida & Willis, 1961)

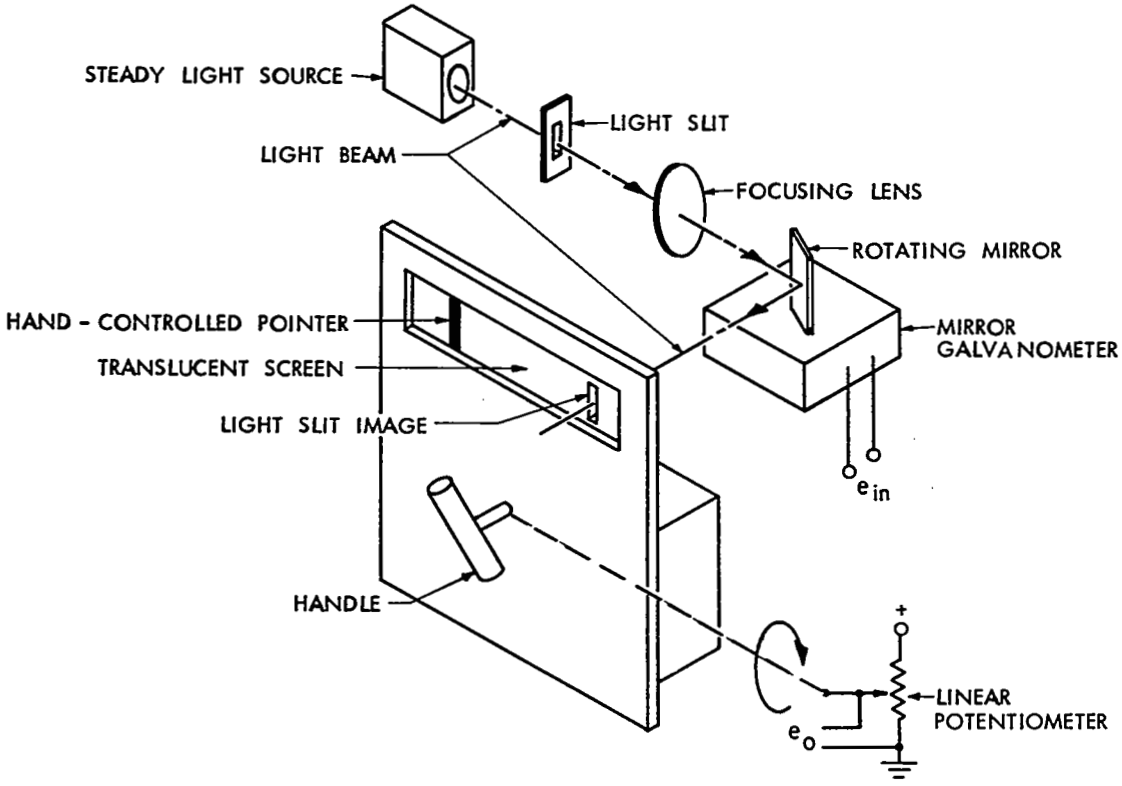

Fig. 27 Sketch of apparatus (Houk et al., 1962)

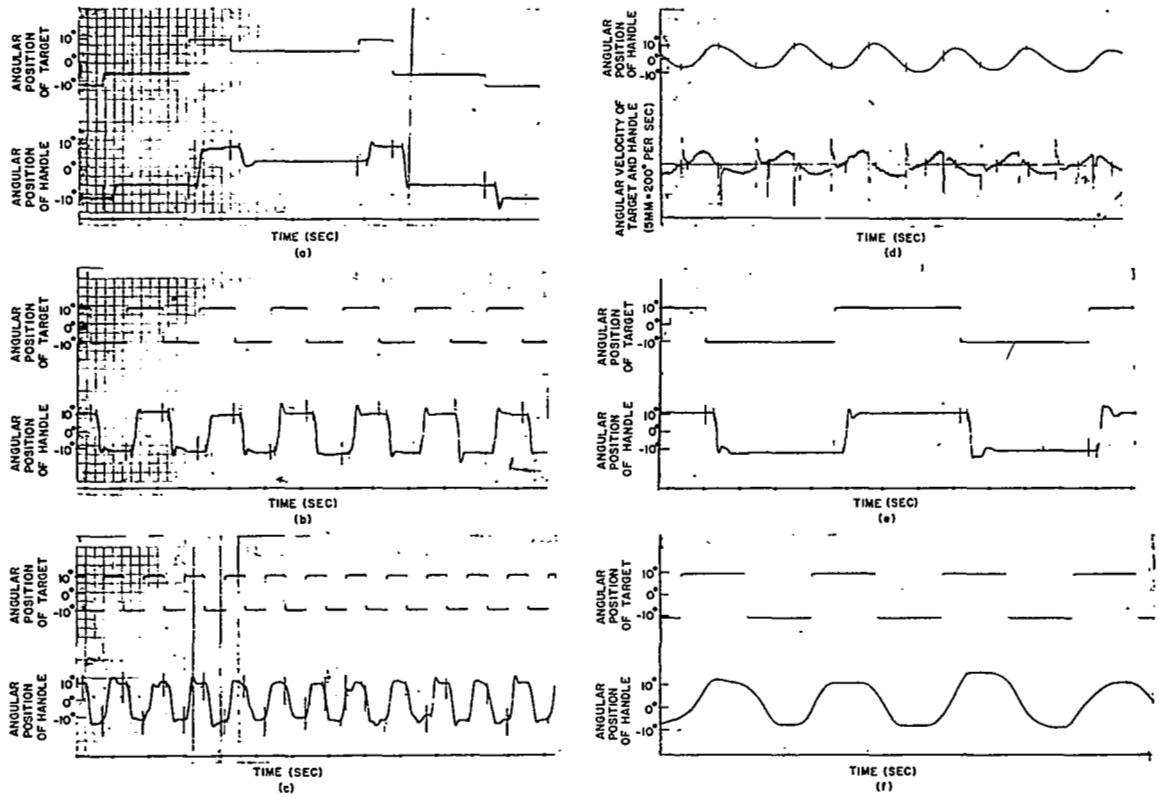

Figure 28. Time function records of angular target position and angular wrist handle position: (a) random steps (b) regular square waves at 0.5 cps (c) regular square waves at 0.9 cps (d) regular square waves at 2.5 cps, here the bottom trace has both target and handle angular velocity superimposed. (Houk et al., 1962)

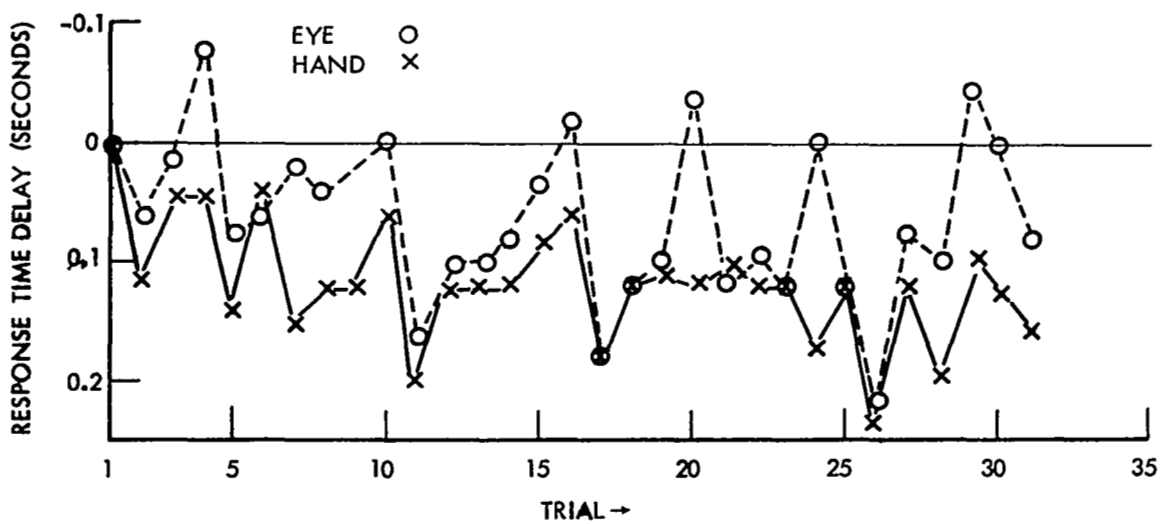

Figure 29. Sequential order of response time delays for both the eye and the hand in simultaneously recorded experiment with input at 0.5 cycles per second. (Okabe et al., 1962b)

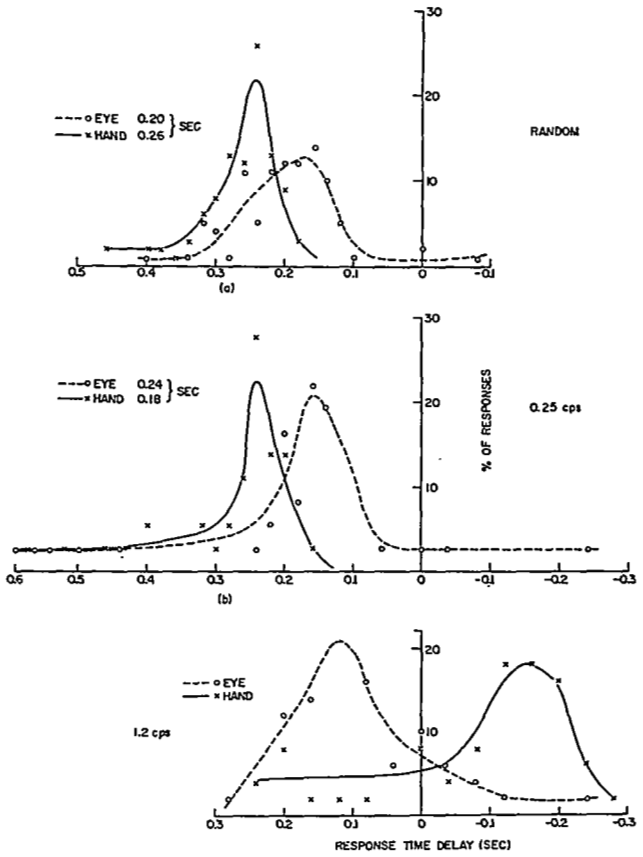

Figure 30. Histograms of response time delays for hand and eye (a) random target (b) regular square waves at 0.5 cps (c) regular square waves at 1.2 cps. (Okabe et al., 1962a)

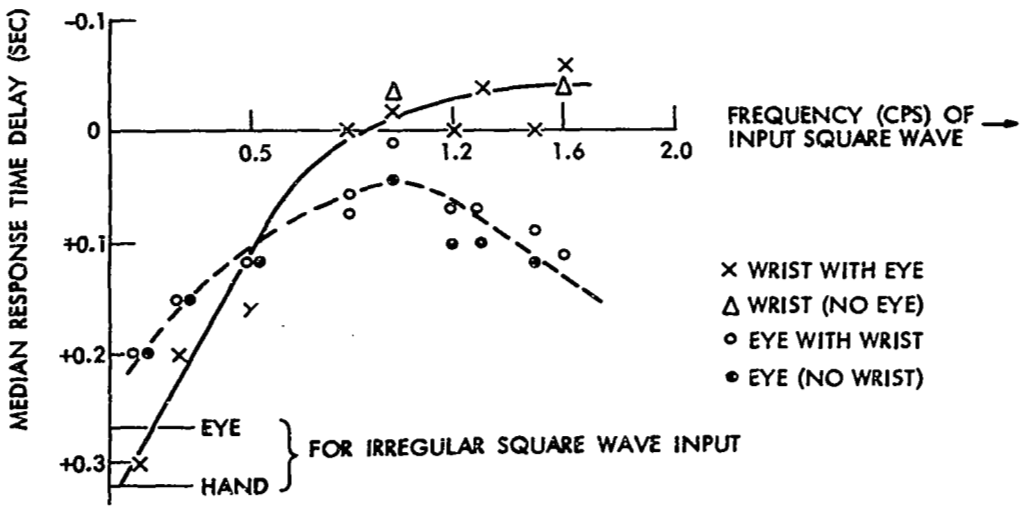

Figure 31. Dependence of median response time delays upon input square wave. Solid line shows wrist tracking; broken line eye tracking. (Okabe et al., 1962a)

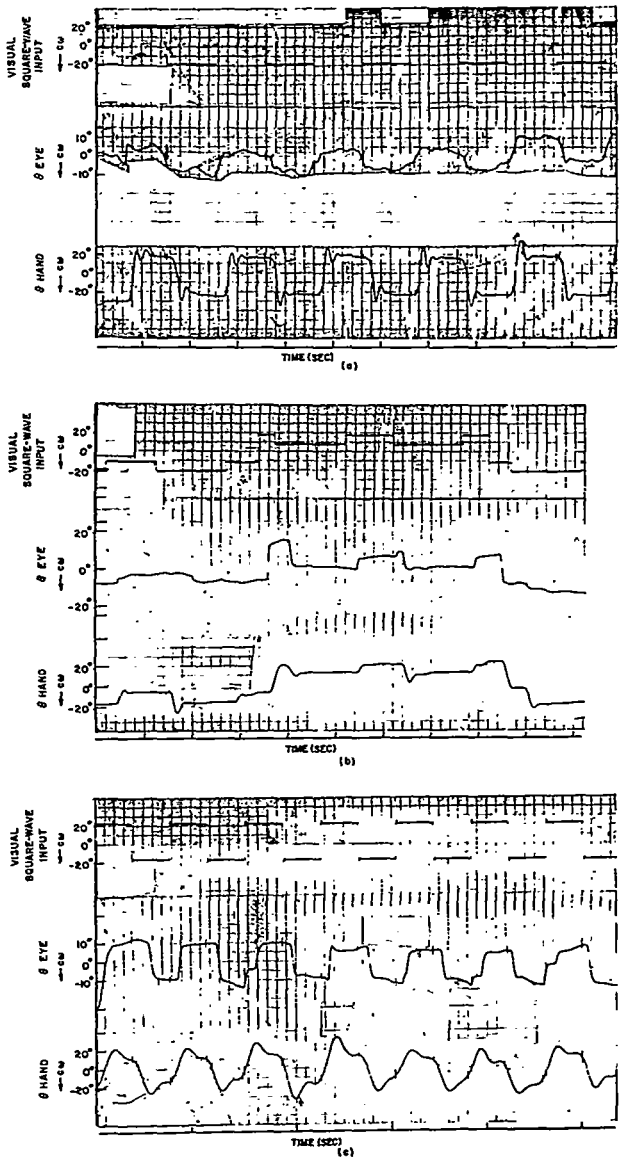

Figure 32. Time function of target, eye and hand, position for two frequencies of input square wave. (a) 0.5 cps (b) for random target position steps (c) 2.5 cps. (Okabe et al., 1962a)

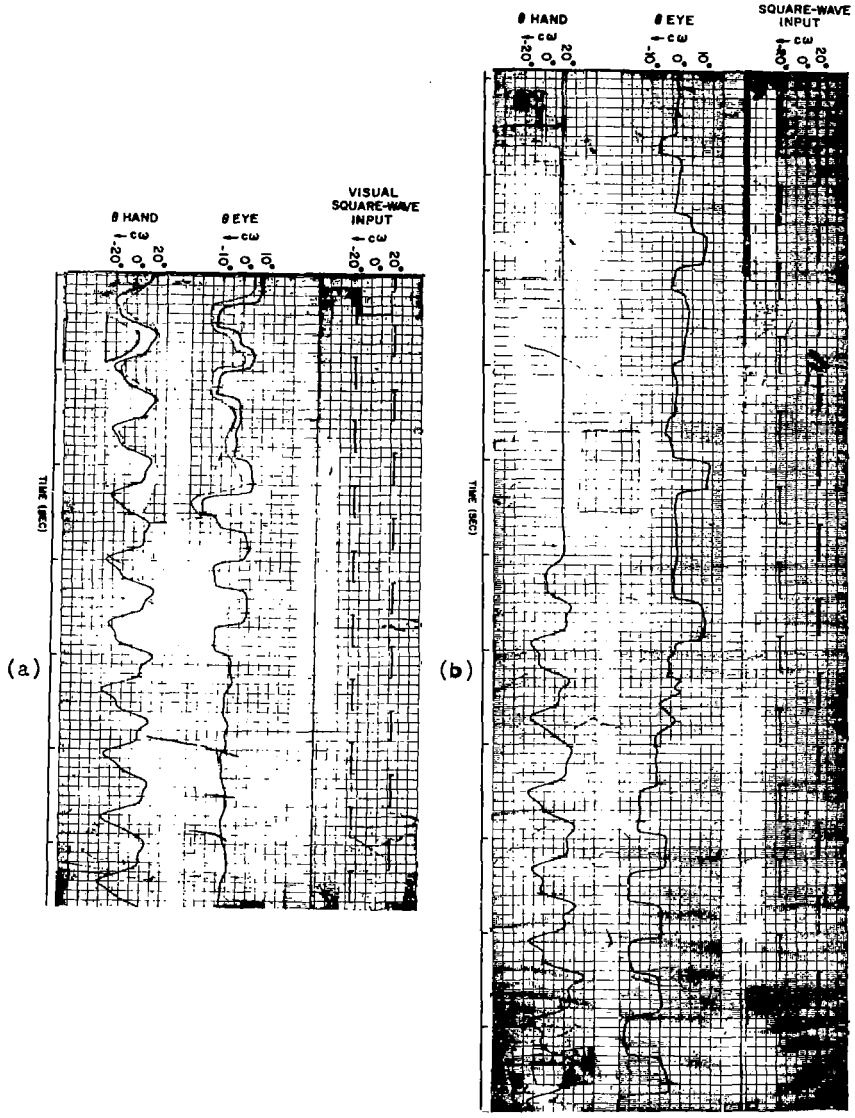

Figure 33. Time function of target, eye and hand position: (a) shows eye tracking movement sequence spontaneously halting with no apparent effect on hand tracking. (b) shows poor to absent eye tracking when hand is still and marked improvement of eye tracking in association with hand tracking. (Okabe et al., 1962a)

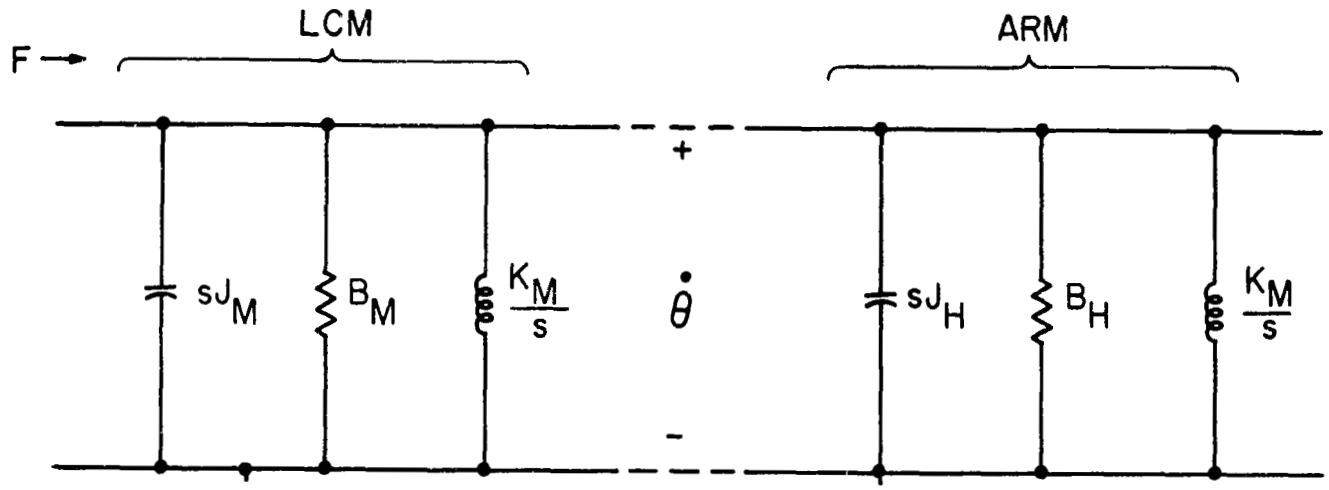

Figure 34. Mobility analog of mechanical parameters of apparatus and hand under experimental conditions. (Okabe et al., 1962b)

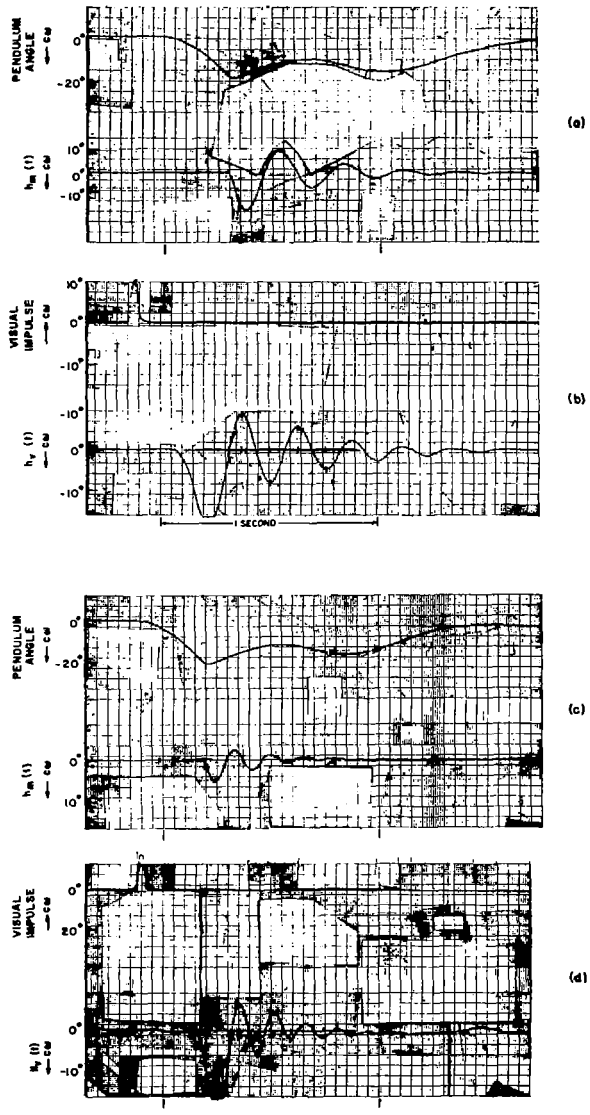

Figure 35. Mechanical, (a) and (c); and visual, (b) and (d), impulse experiments at two levels of tension. (a) and (b) relaxed; (c) and (d) tense. (Okabe et al., 1962b)

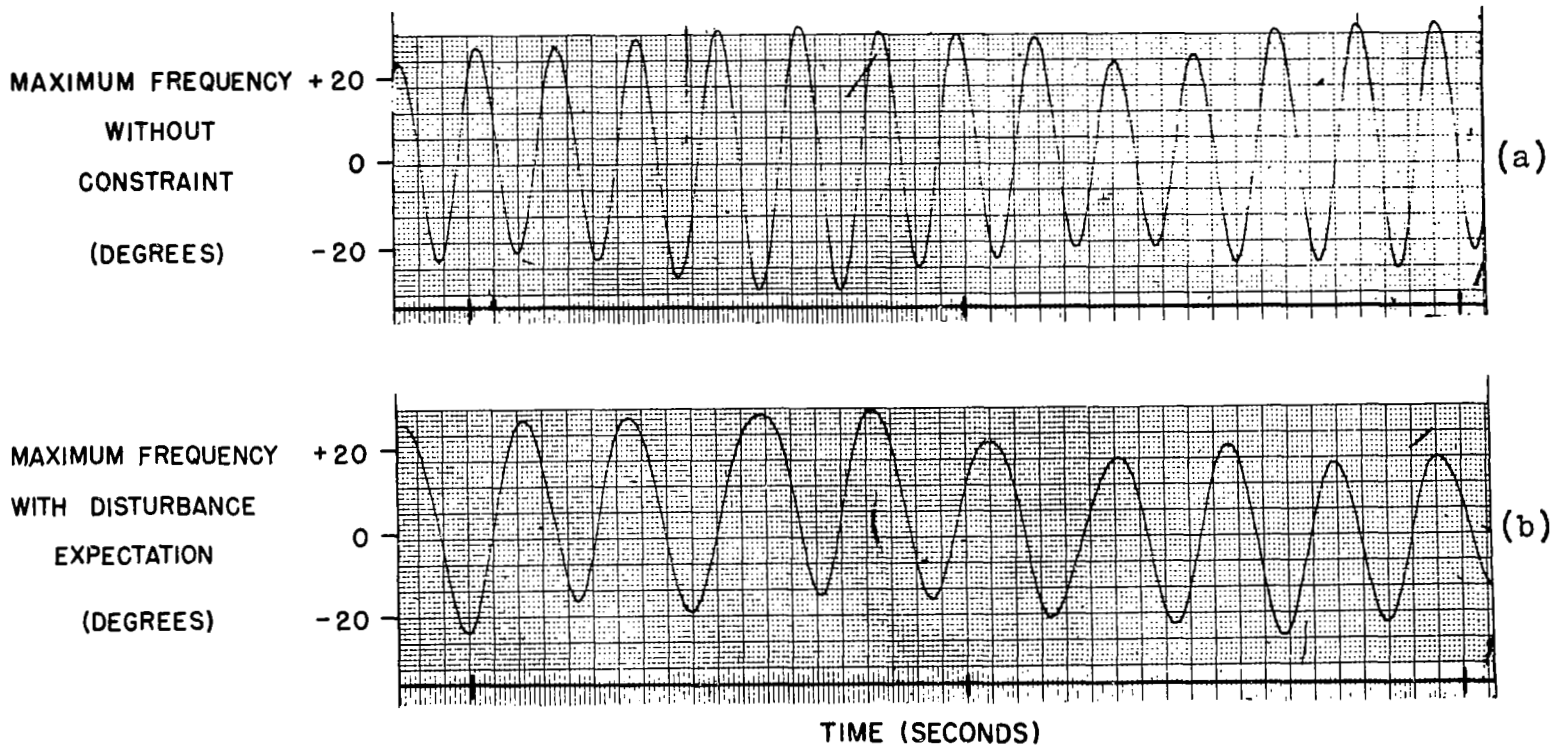

Fig. 36 Freewheeling or succession movement experiment. In (a) subject was instructed to oscillate as fast as possible; antagonist muscle went quite lax. In (b) lower trace, subject was instructed primarily to minimize disturbance error due to possible injected mechanical impulse and secondarily to oscillate at the same amplitude as rapidly as possible; antagonist muscles always maintained considerable tone, thus position control system slowed oscillation. (Stark, Iida & Willis, 1961)

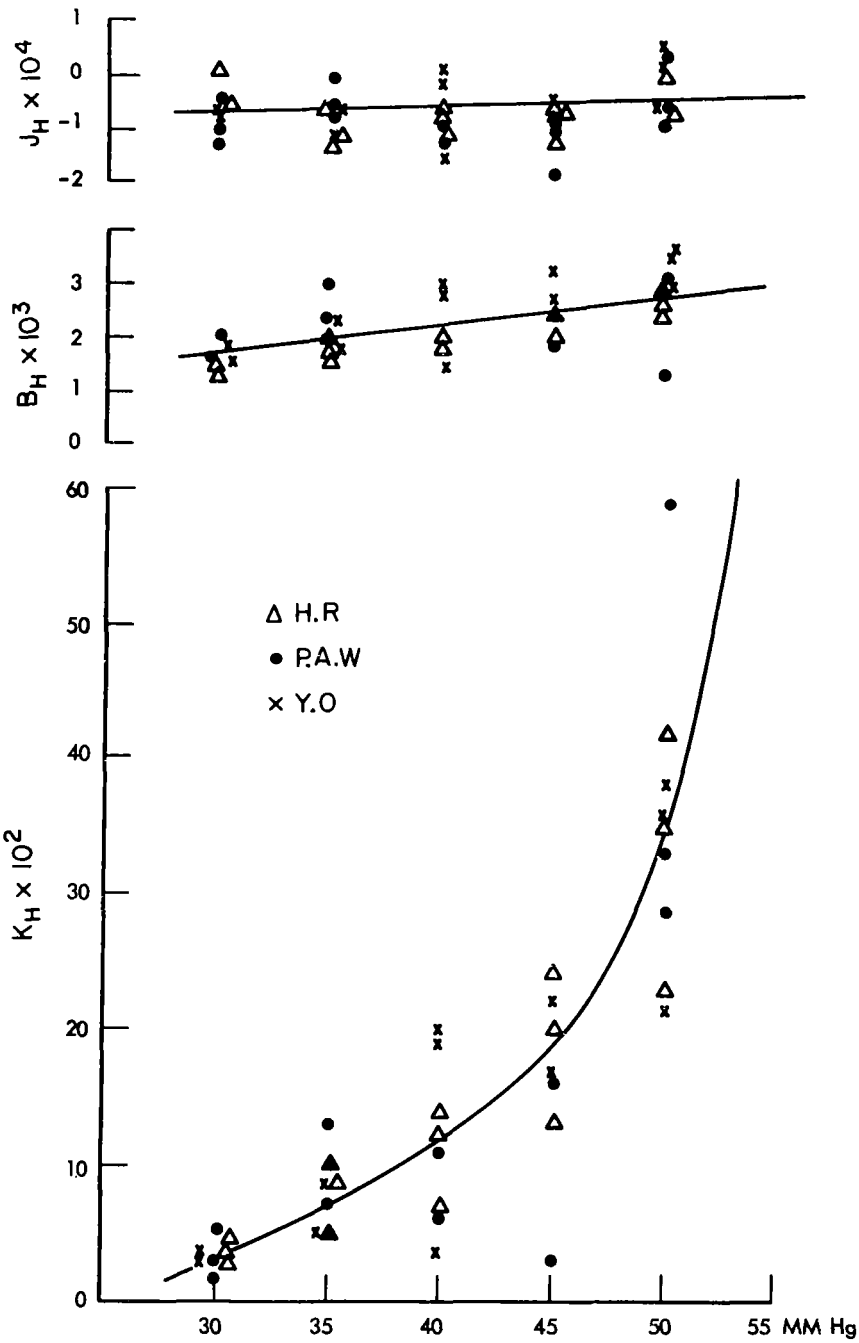

Figure 37. Mechanical parameters of hand as functions of tension. J_H is rotational inertia in newton-meters-second^2-radians^{-1}; B_H is viscosity in newton-meters-second-radian^{-1}; and K_H spring constant in newton-meter-radian^{-1}. (Okabe et al., 1962b)

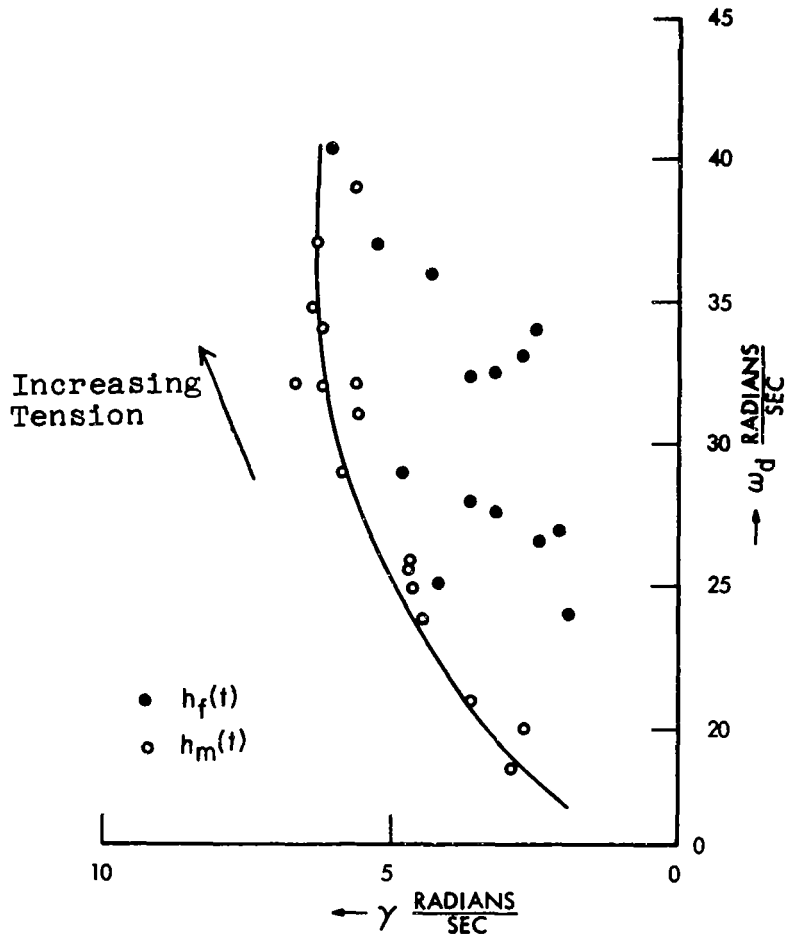

Fig. 38 Root locus of the positive pole of a complex pair fitted to $h_m(t)$ and $h_f(t)$. The scales are imaginary frequency ω_d and real frequency in radian-seconds^{-1}. (Okabe et al., 1962b)

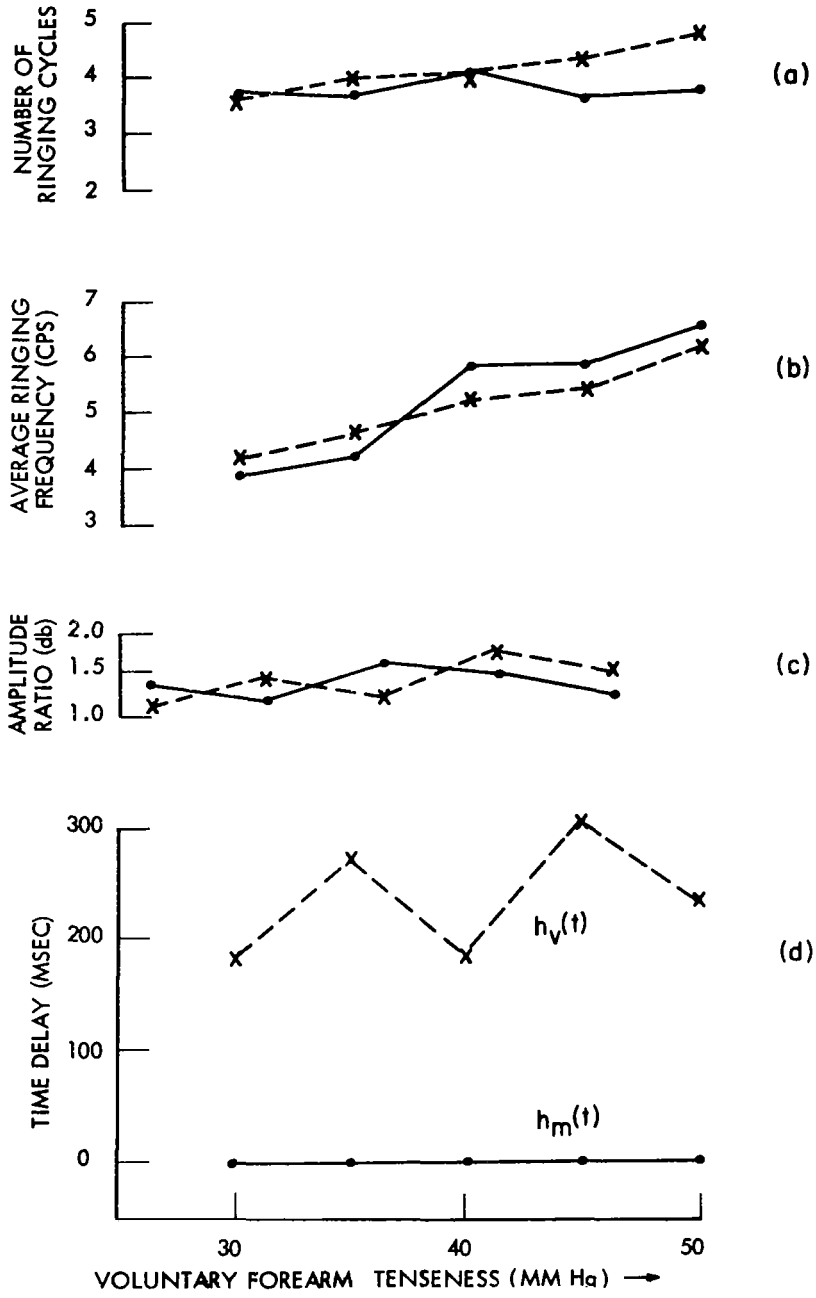

Figure 39. Parameters of visual and mechanical impulses as function of tension. (Okabe et al., 1962b)

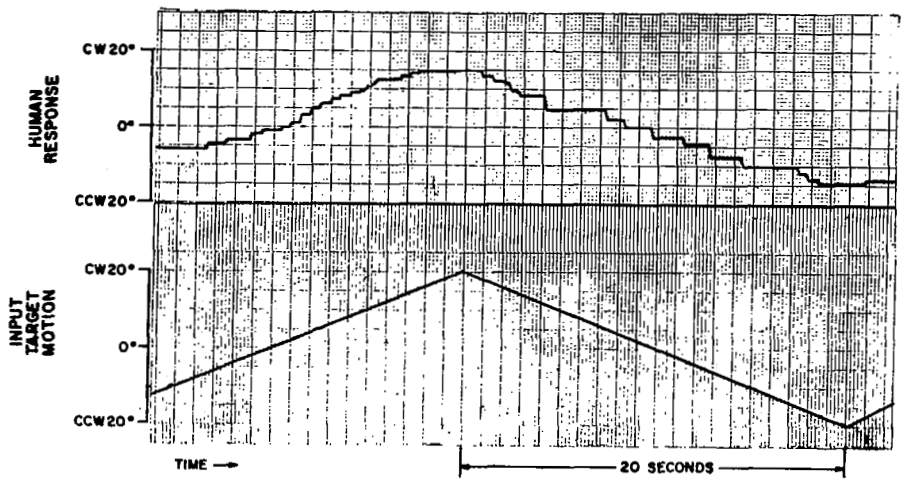

Figure 40. Discontinuous change of hand position to slow target ramps. (Stark, Okabe, & Willis, 1962)

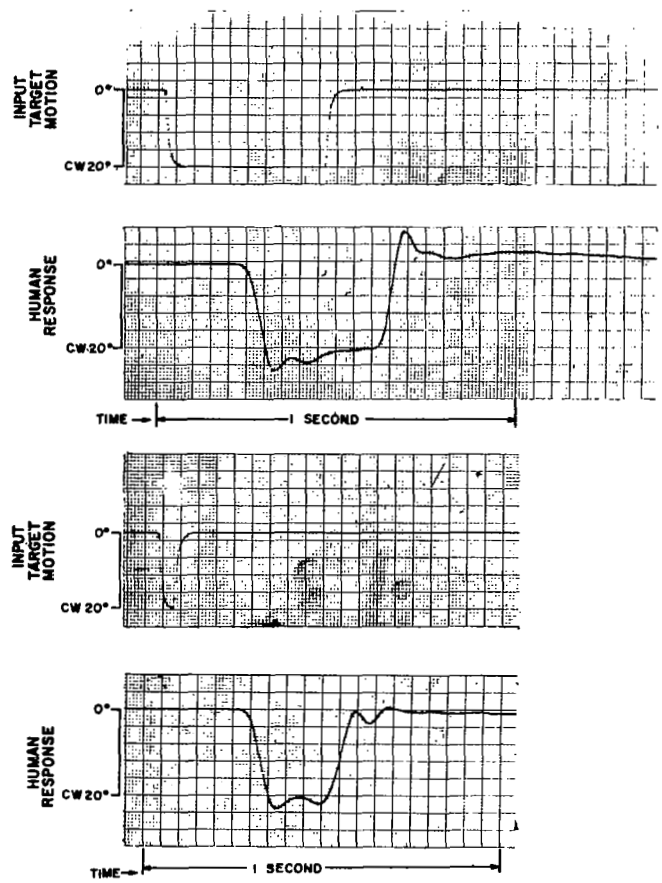

Figure 41. Response to pulses showing time delays and refractory period when pulse widths are unpredictable. (Stark, Okabe & Willis, 1962)

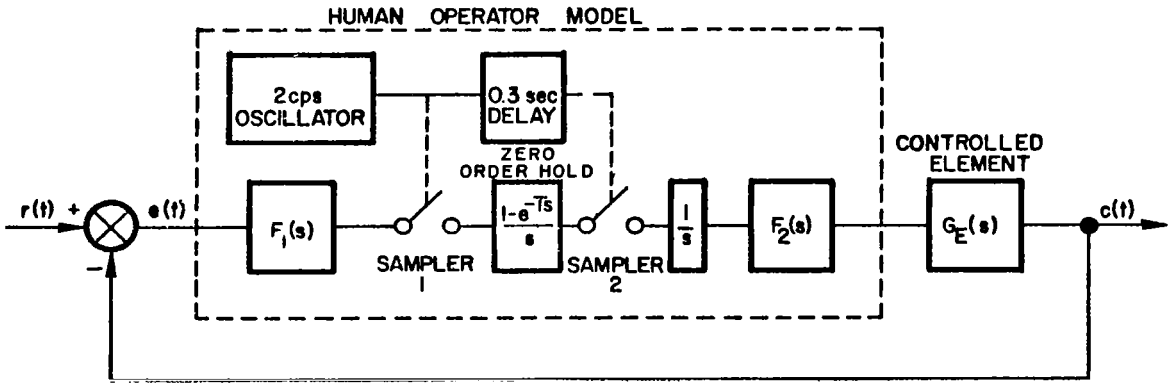

Figure 42. Sampled-Data Model after Ward.(Bekey thesis)

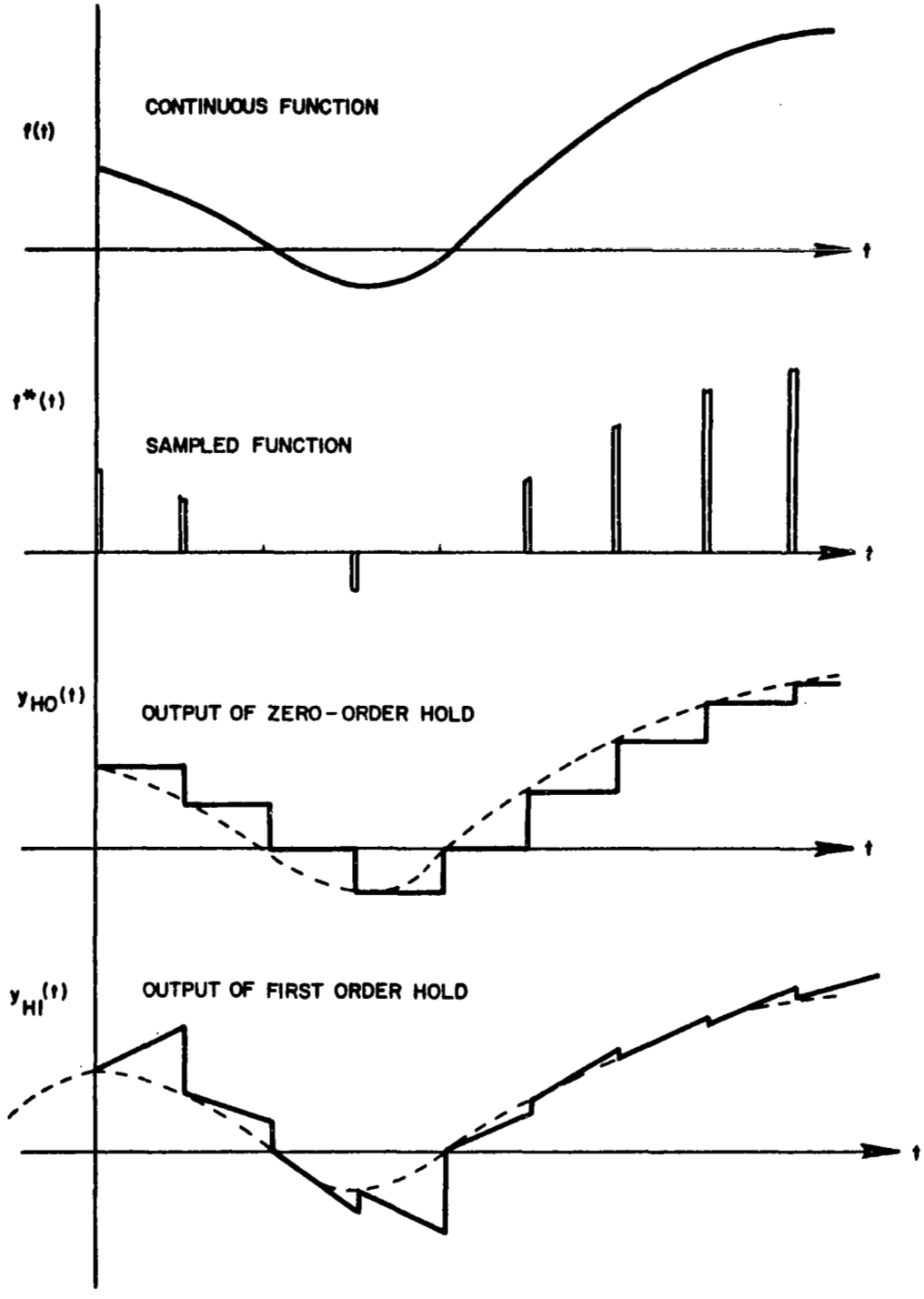

Figure 43. Zero and First Order Hold Circuits. (Bekey thesis)

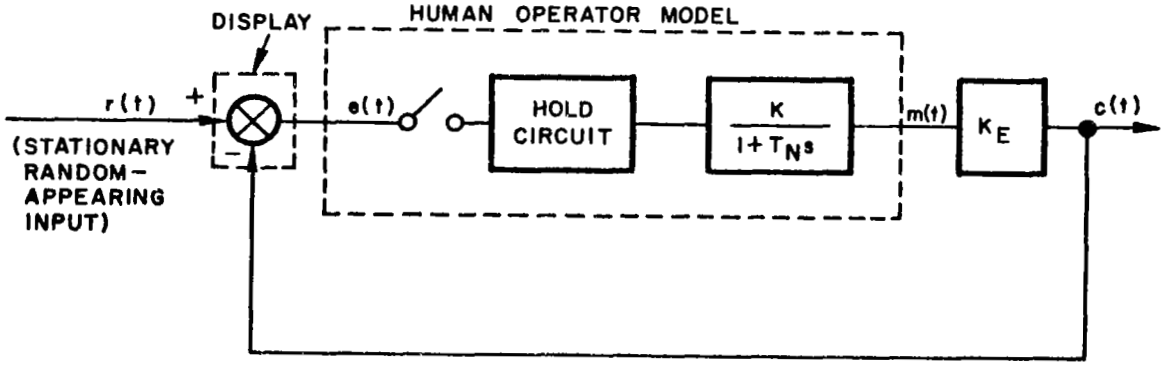

Figure 44. Proposed Sampled-Data Model of the Human Operaton (Bekey thesis)

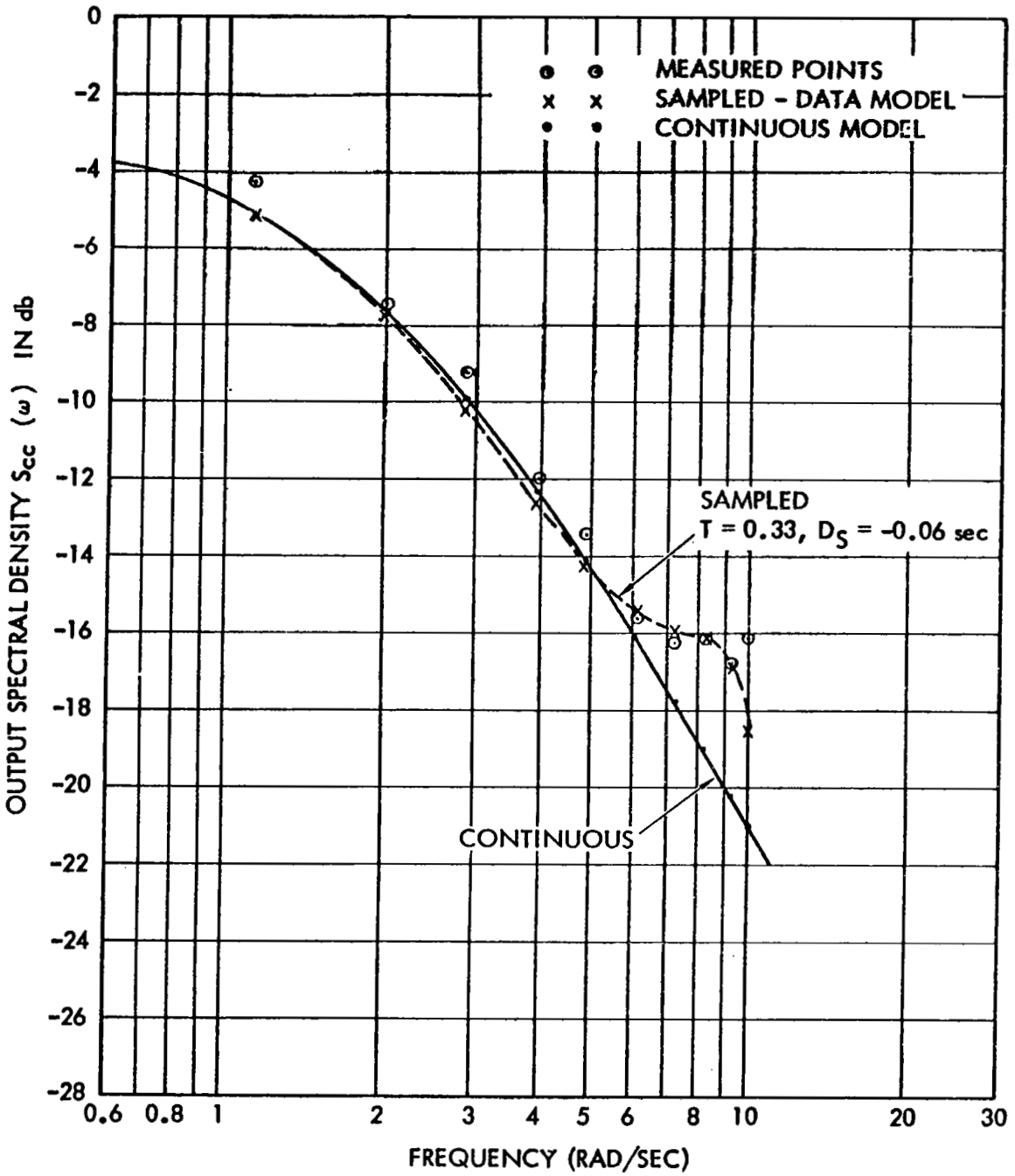

Figure 45. Comparison of Experimental and Analytical Values of Output Power Spectral Density (Bekey, IFAC)

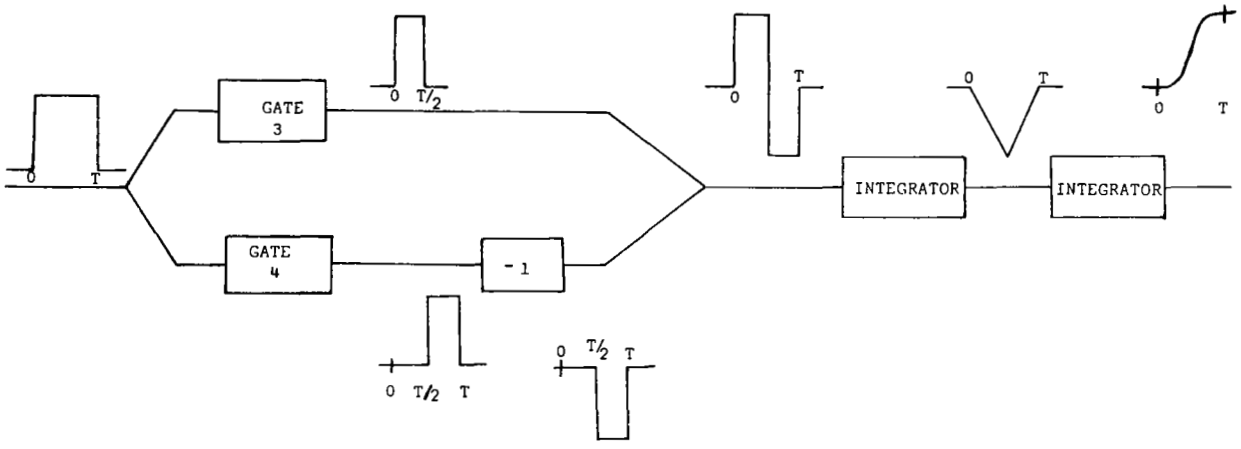

Figure 46. Full acceleration - full deceleration mechanism. (Lemay & Westcott, 1962)

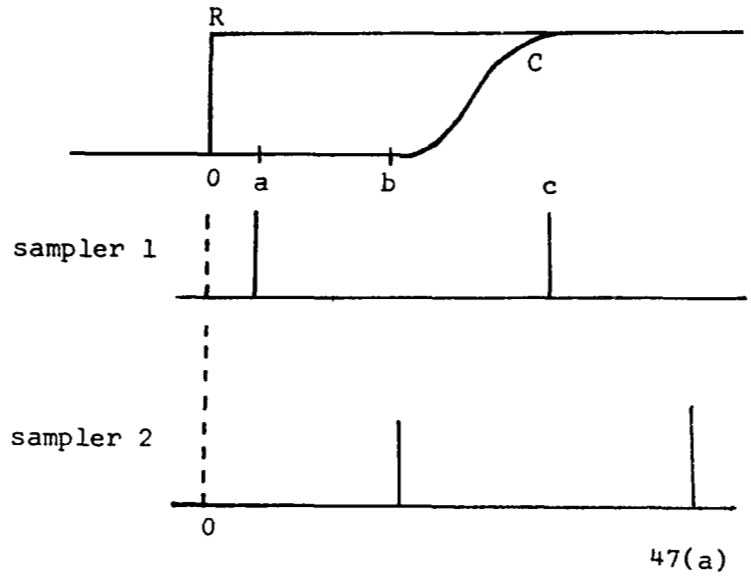

47(a)

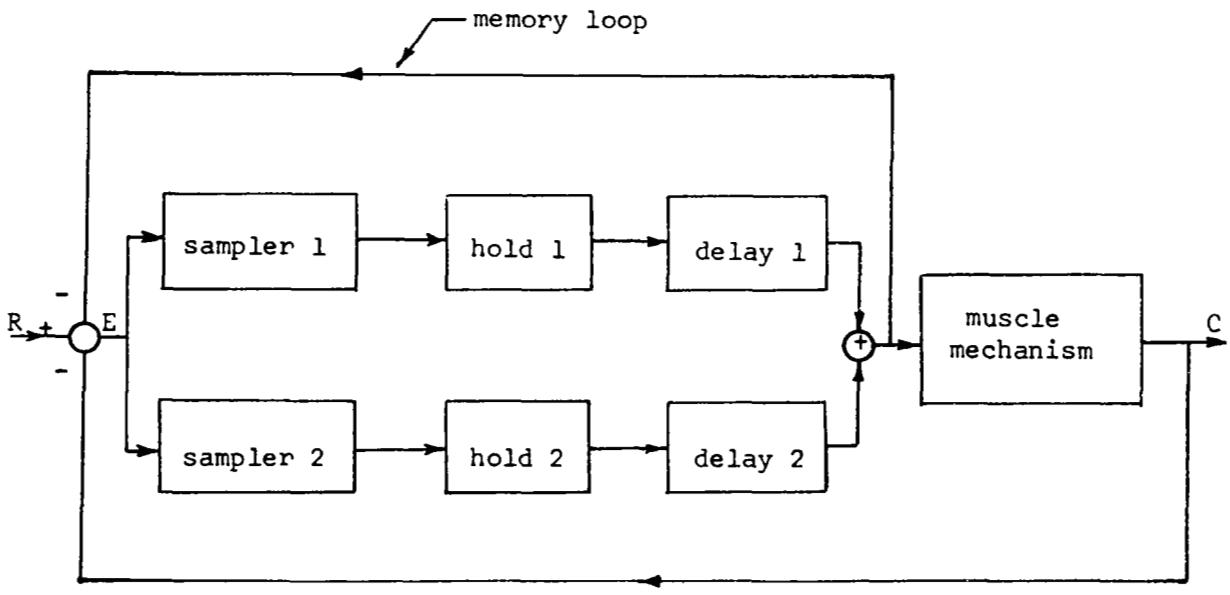

47(b)

Figure 47. The sampled-data model.
(Lemay & Westcott, 1962)

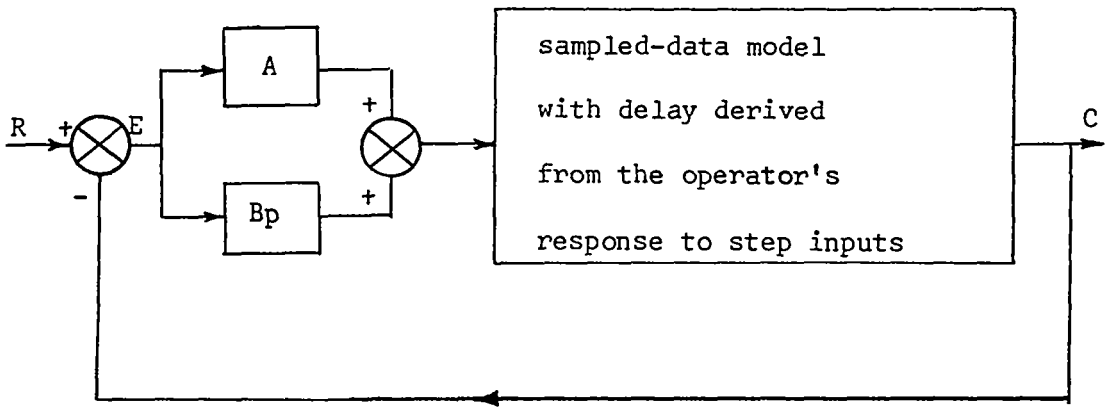

Figure 48. Model with predictor.
(Lemay & Westcott, 1962)

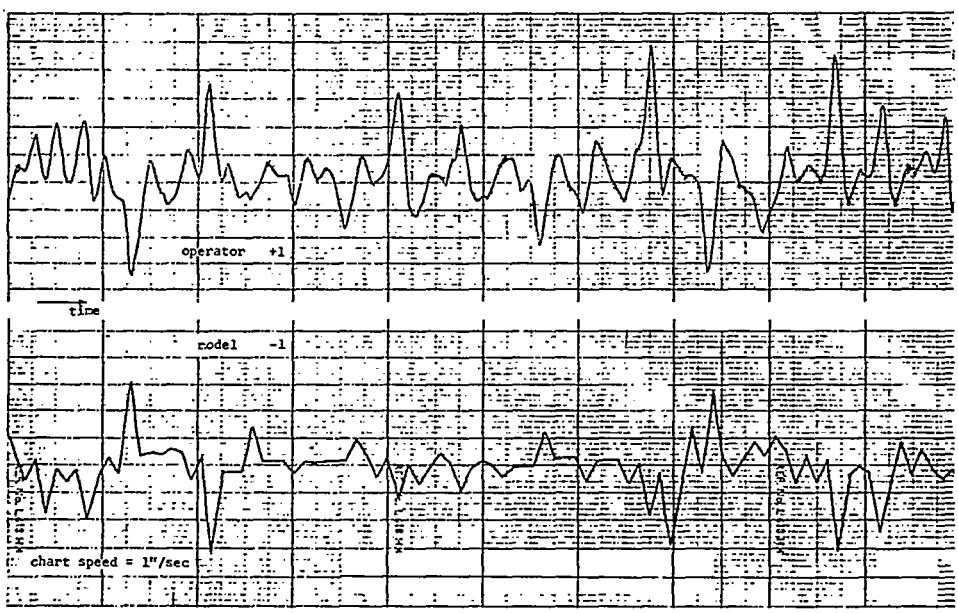

Figure 49. Operator and model velocity outputs.
(Lemay & Westcott, 1962)

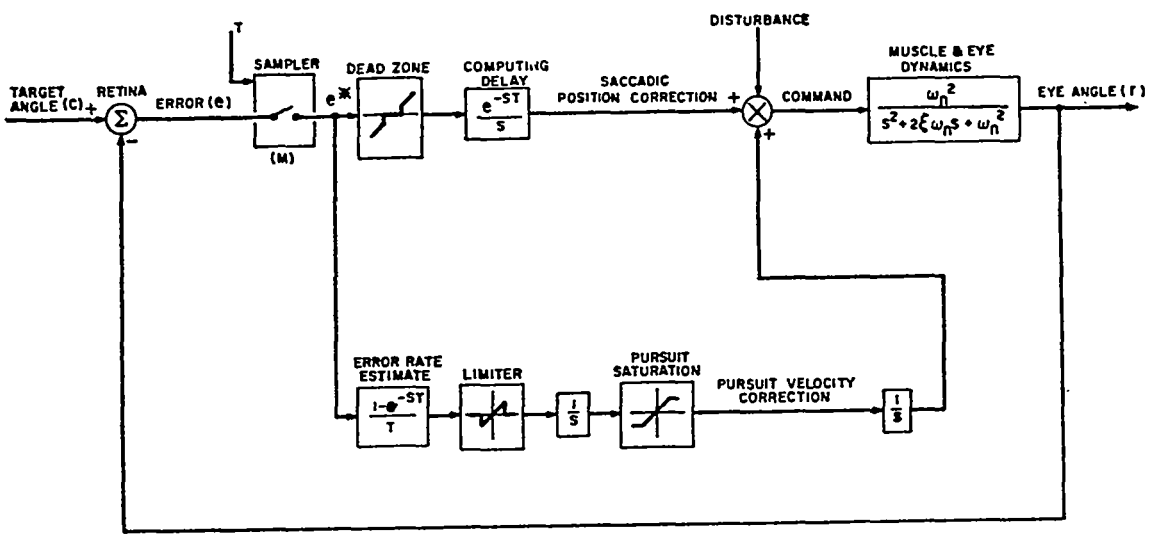

Figure 50. Sampled data model for eye tracking movements (Young & Stark, 1963)

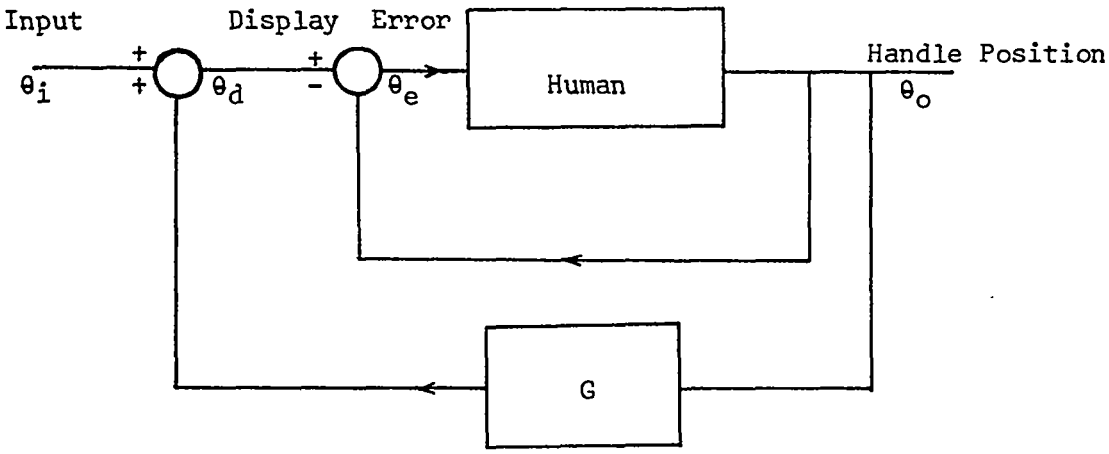

(a)

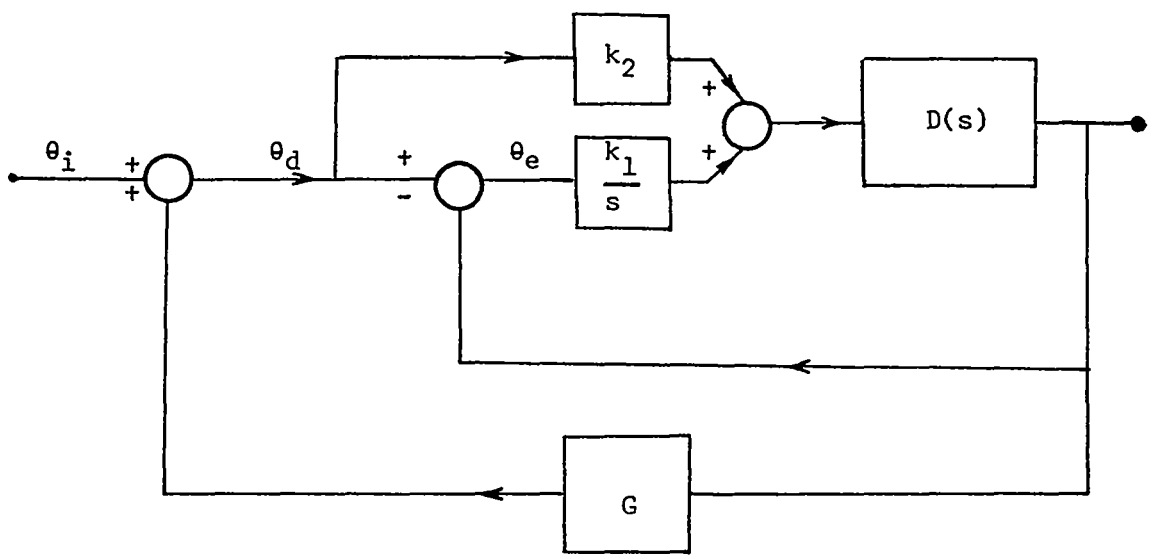

(b)

Figure 51. Open Loop
(a) Simple Model
(b) More general block diagram.
(Navas, 1963)

Figure 52. Open loop responses, handle loaded with friction and inertia. Step responses. Vertical scale 4°/div., horizontal scale 0.5 sec/div. except c and d, 50 msec/div. (Navas, 1963)

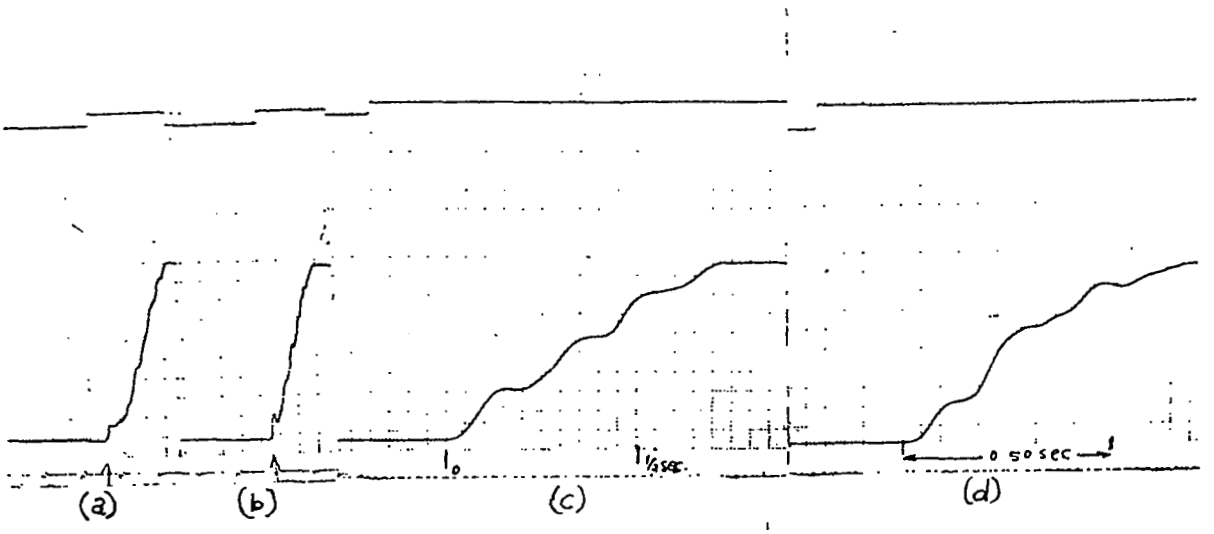

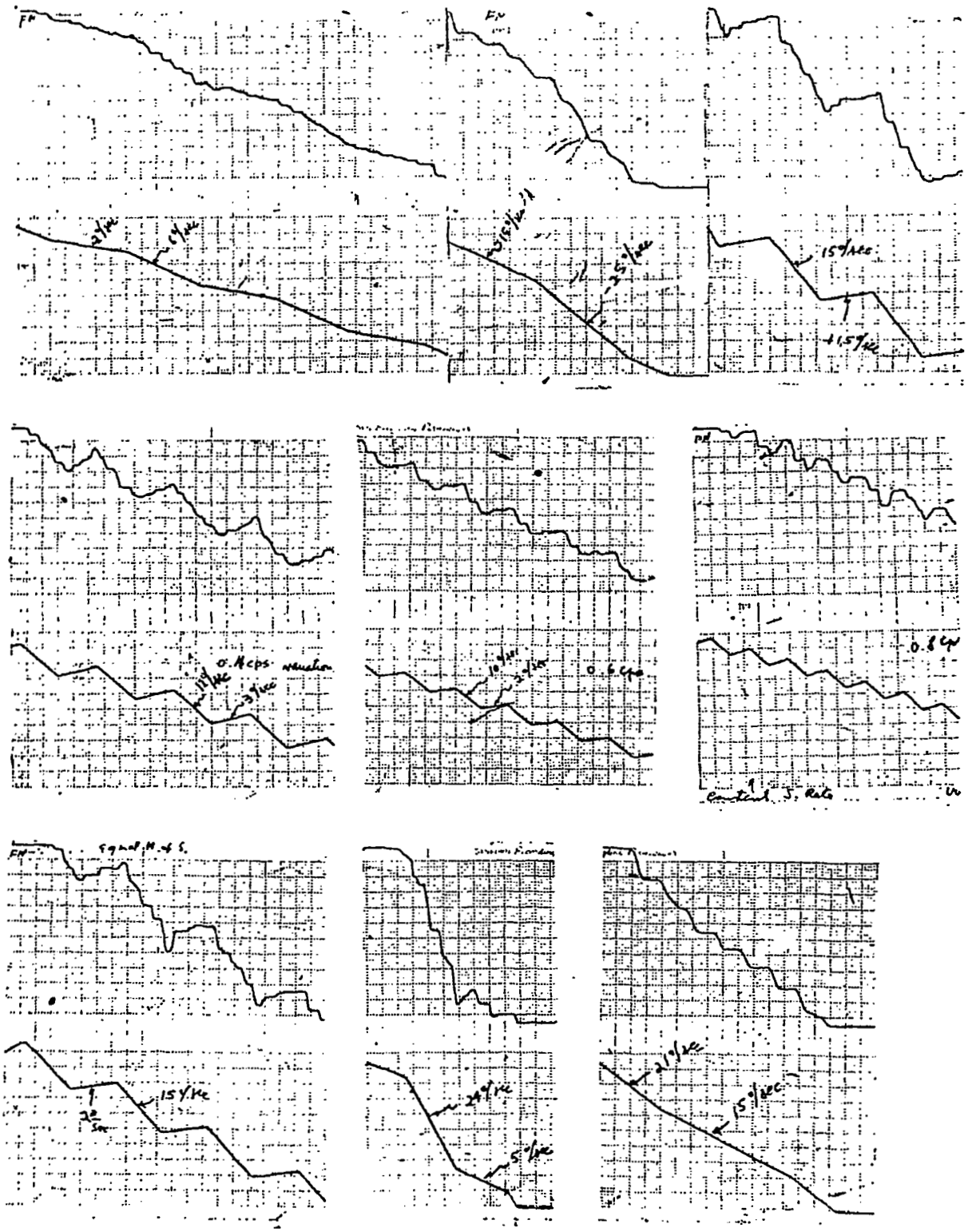

Figure 53. Responses to randomlike combinations of ramps. Inertia and friction added. Input scale 6°/div. Output scale 4°/div. Time in seconds indicated. (Navas, 1963)

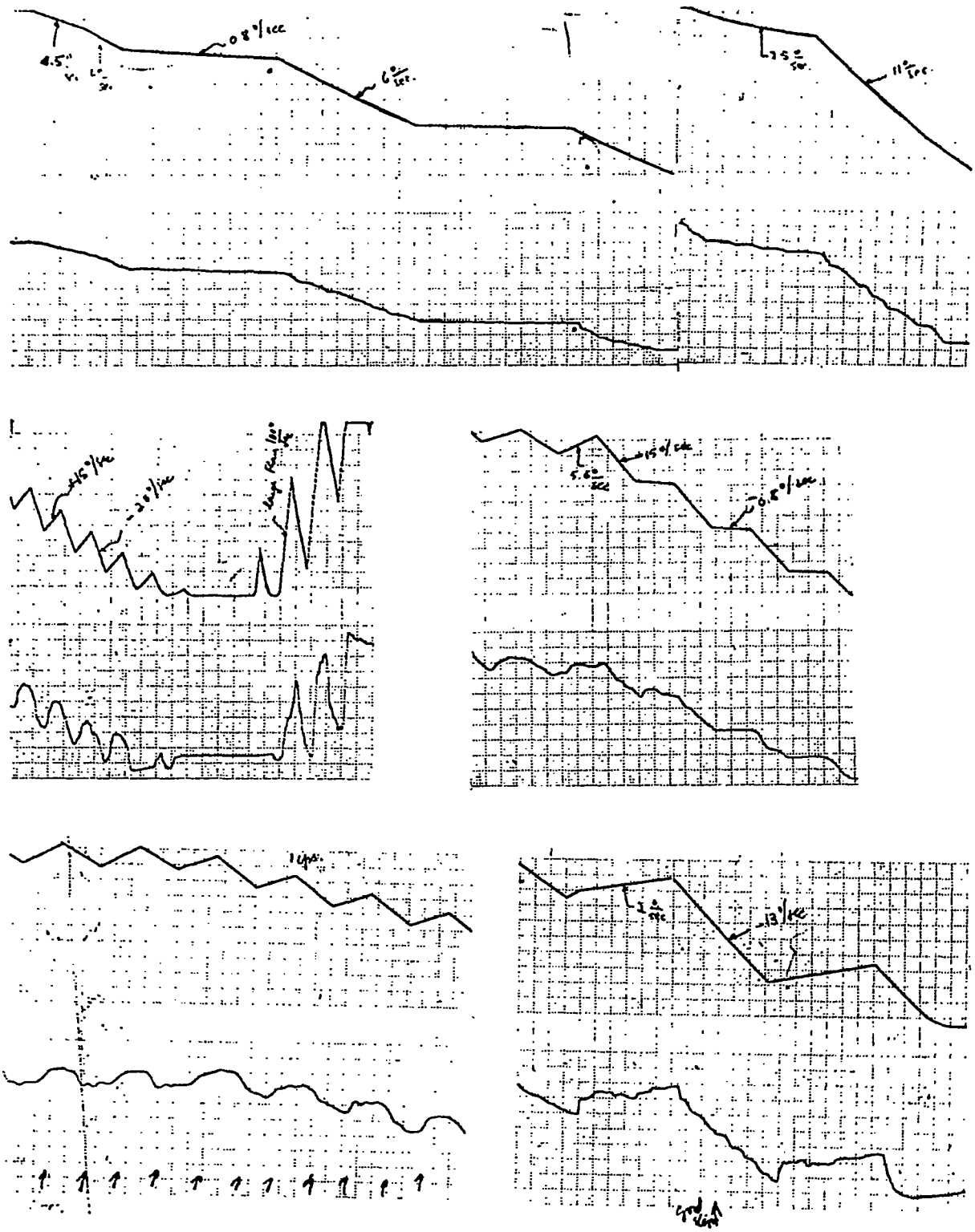

Figure 54. Further responses to randomlike combinations of ramps. Input scale 6°/div. Output scale 10°/div. Time in seconds indicated. (Navas, 1963)

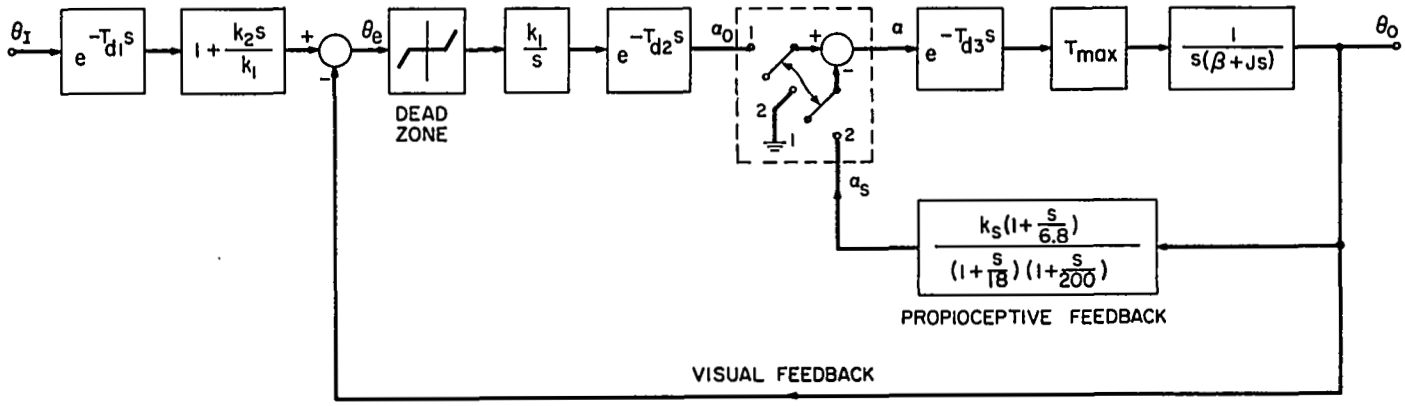

Figure 55. Proposed model for pursuit tracking of unpredictable inputs. (Navas, 1963)

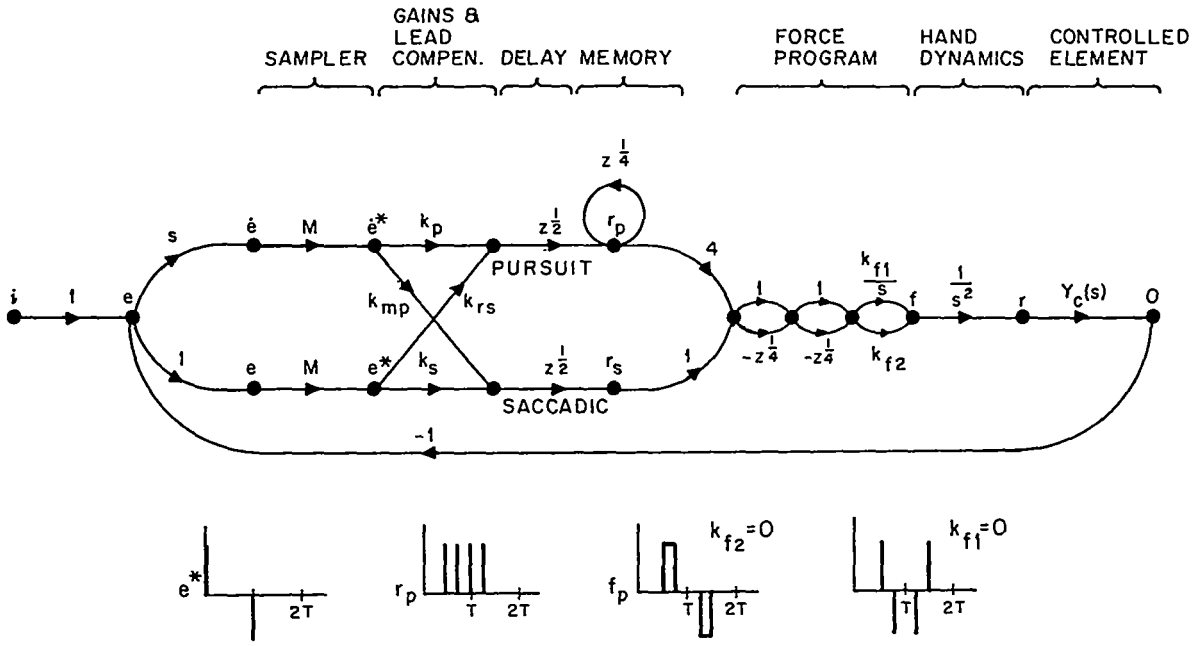

Figure 56. Proposed hand tracking model. (Elkind, Kelly, & Payne, 1964)

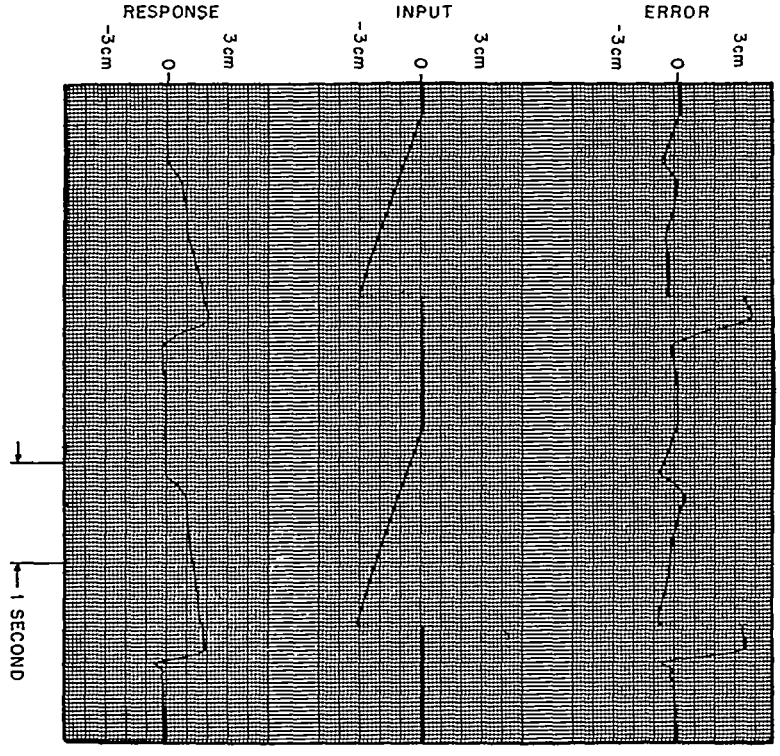

Figure 57. Records of hand tracking of ramps (Elkind, Kelly, & Payne, 1964)

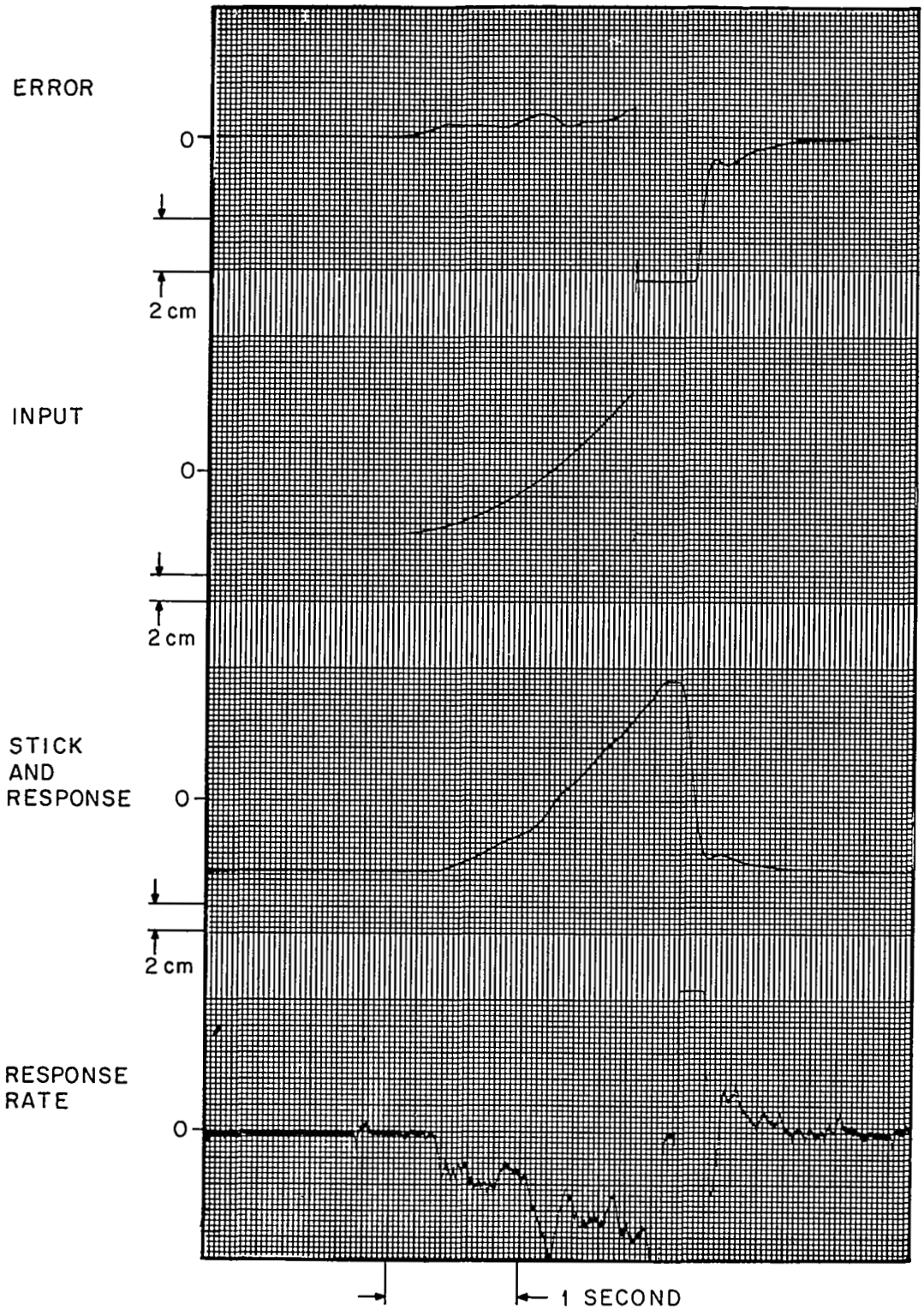

Figure 58. Records of hand tracking of a parabola. (Elkind, Kelly, & Payne, 1964)

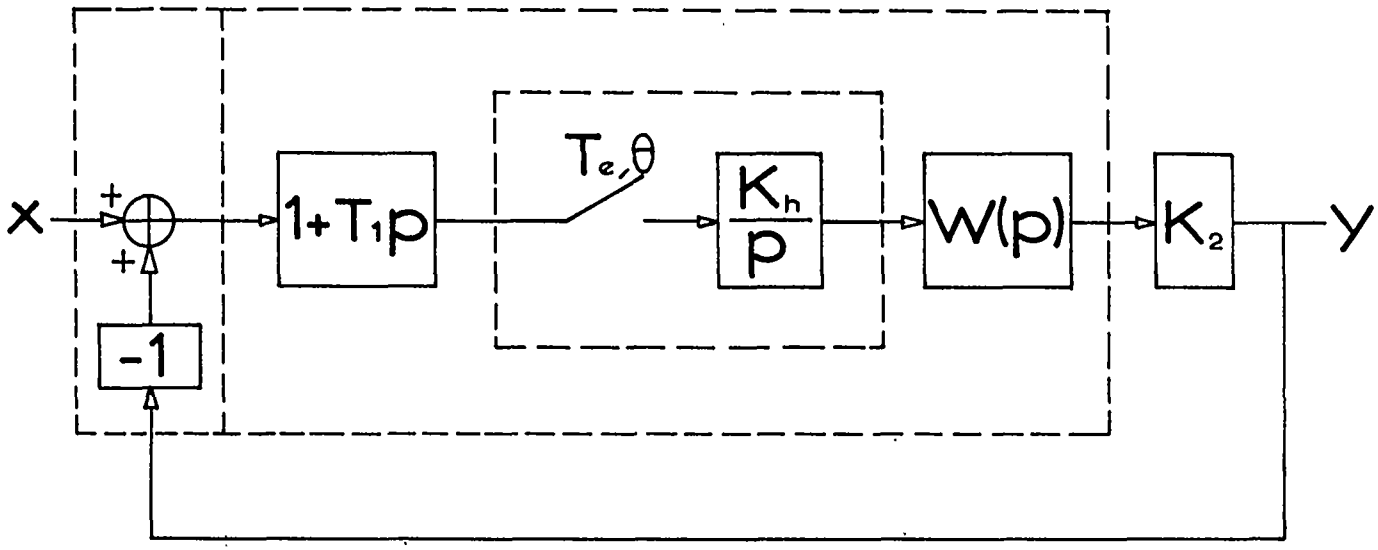

Figure 59. Raoult's sampled data model for manual tracking. (Raoult, 1962)

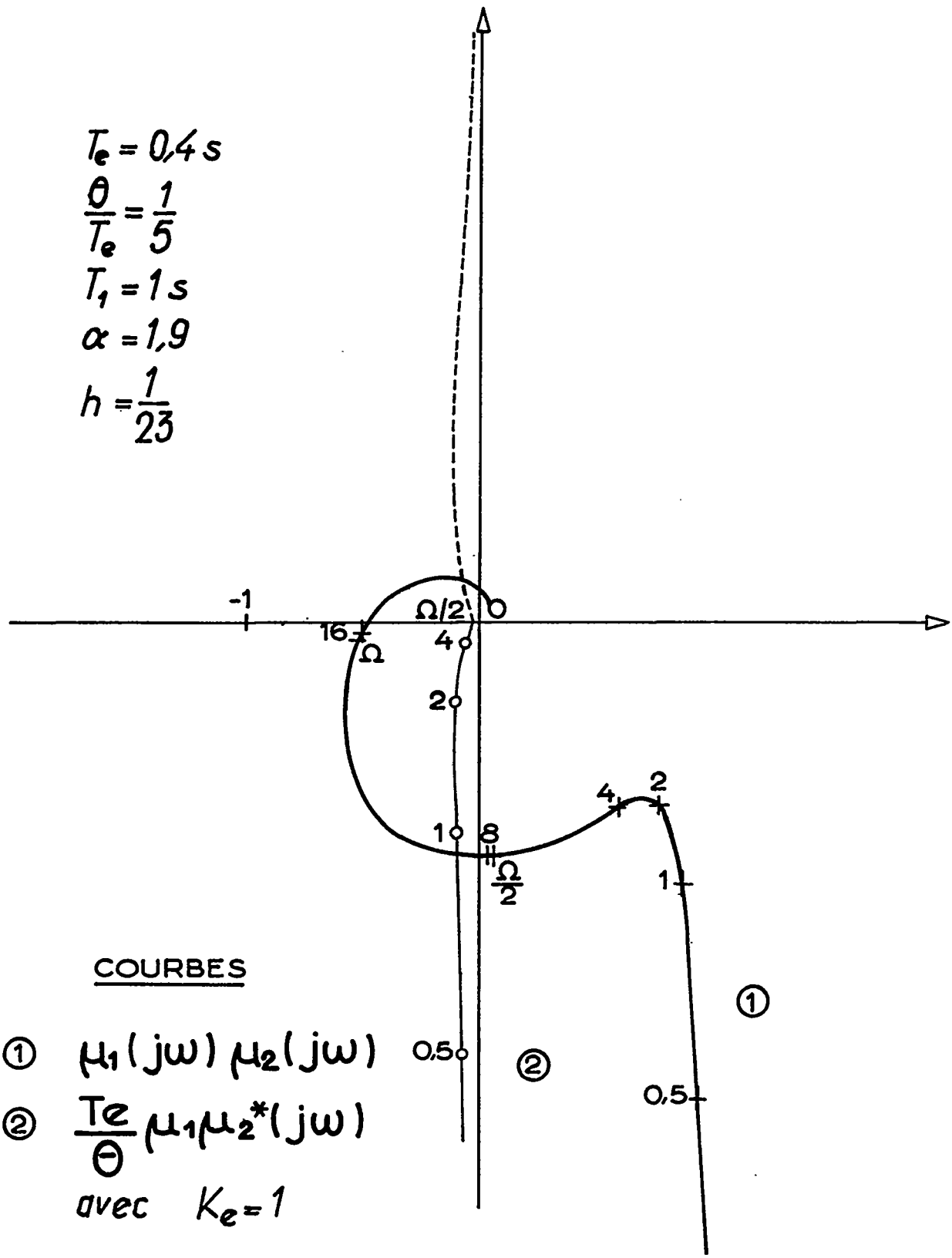

Figure 60. Nyquist diagram for Raoult's model. (Raoult, 1962)

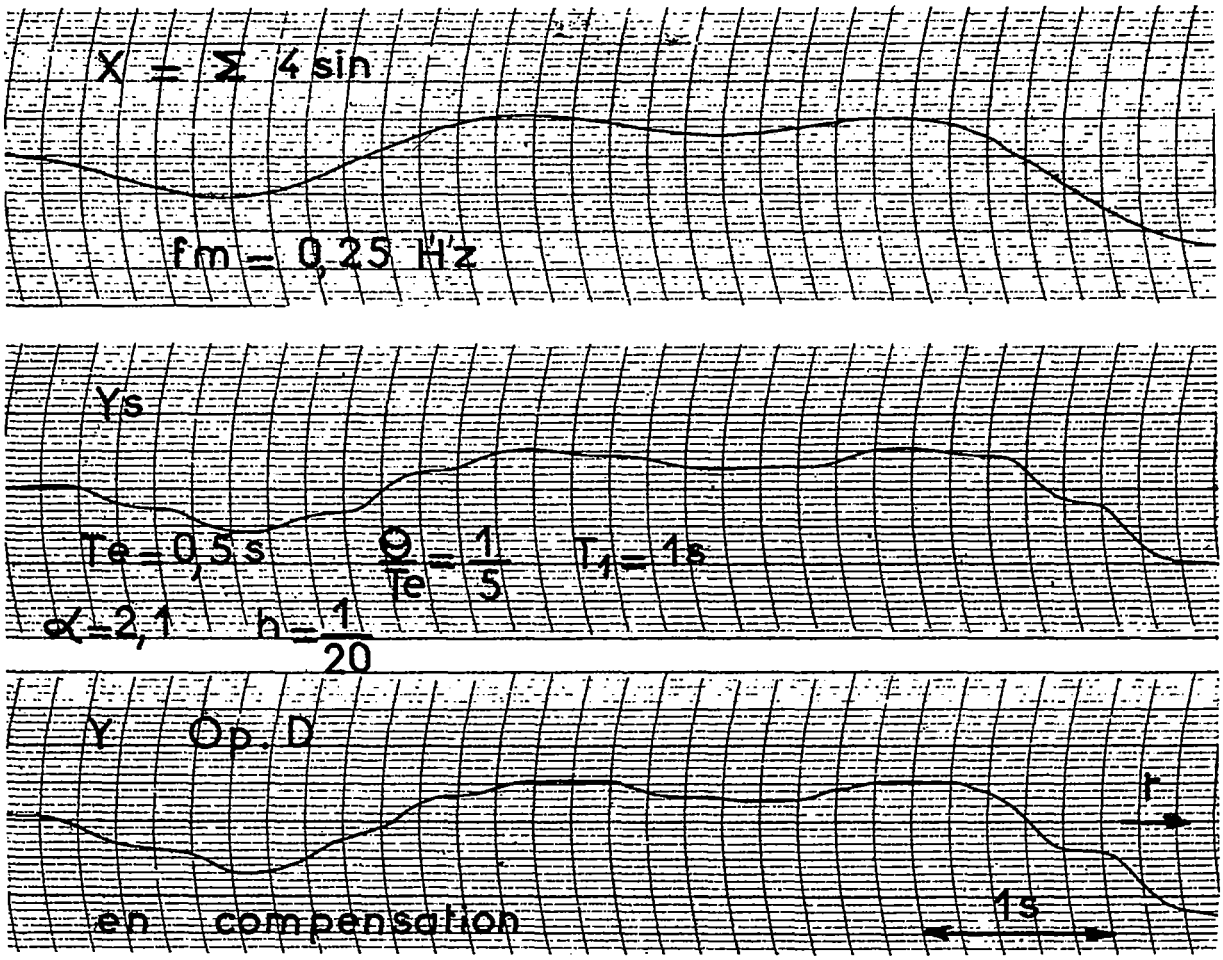

Figure 61. Comparison of Raoult's model output (Y_s) with human response (Y) in tracking pseudo random input (X). (Raoult, 1962)

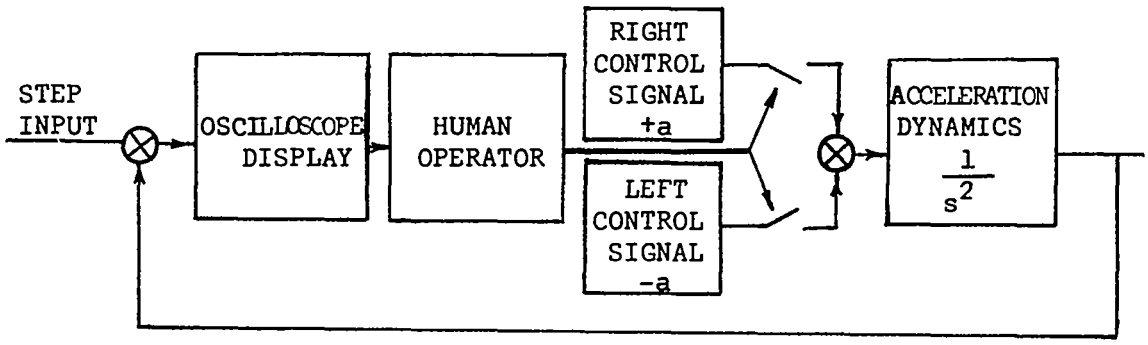

Figure 62. Block diagram of manually operated relay control system. (Pew, 1964)

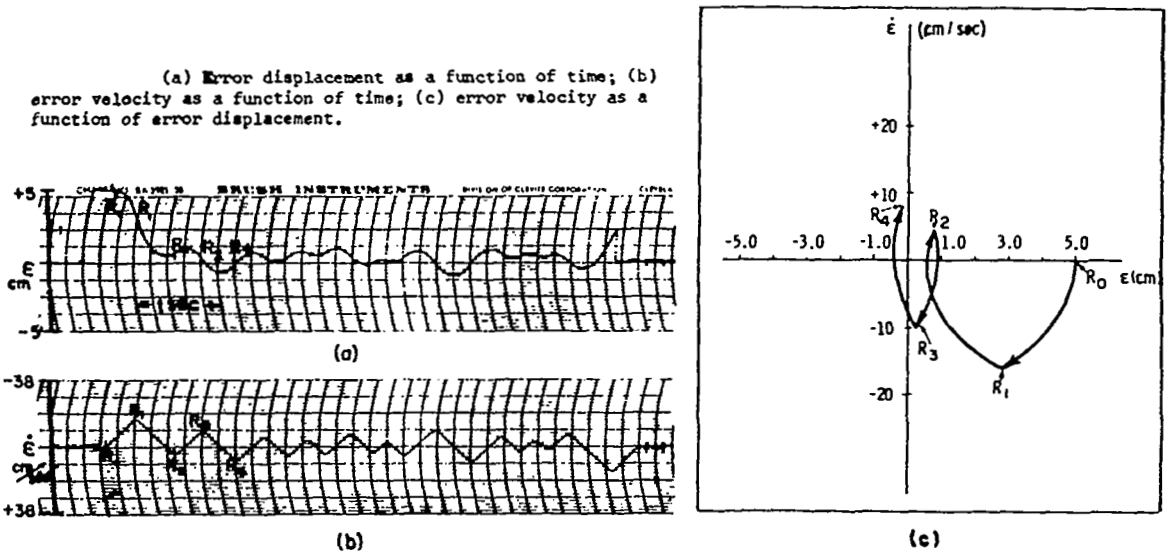

Figure 63. Graphic records of operator performance on a single trial of the experiment. (Pew, 1964)

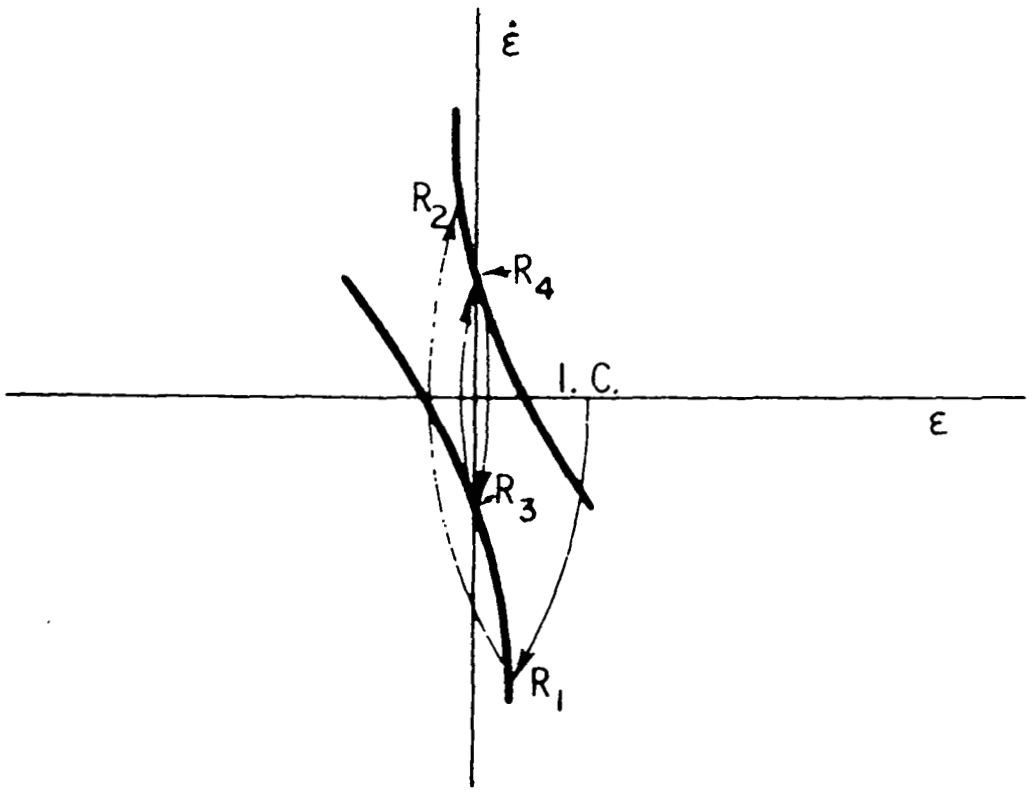

Figure 64. Illustration of a phase-plane switching locus which may be used to predict an operator's switching performance. (Pew, 1964)

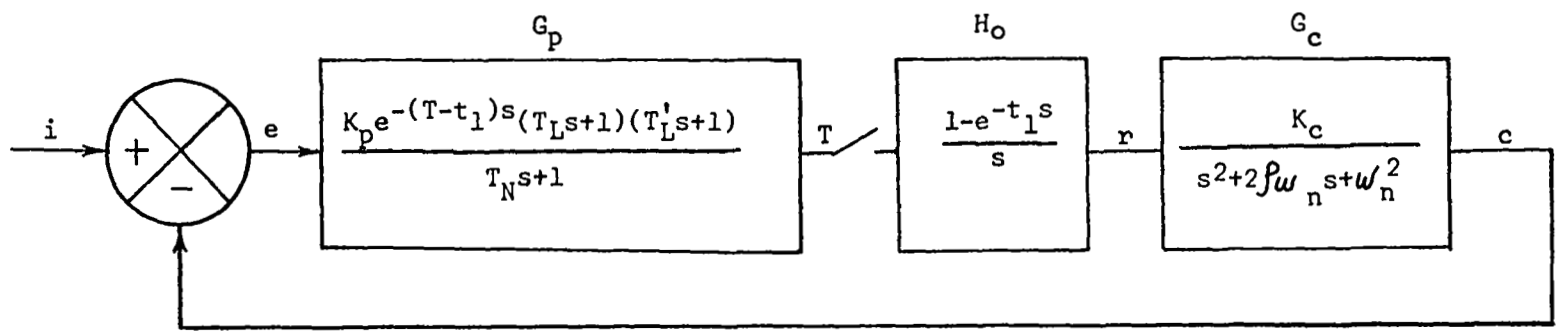

Figure 65. Block diagram of sampled-data model for one channel (Kohlhaas, 1962)

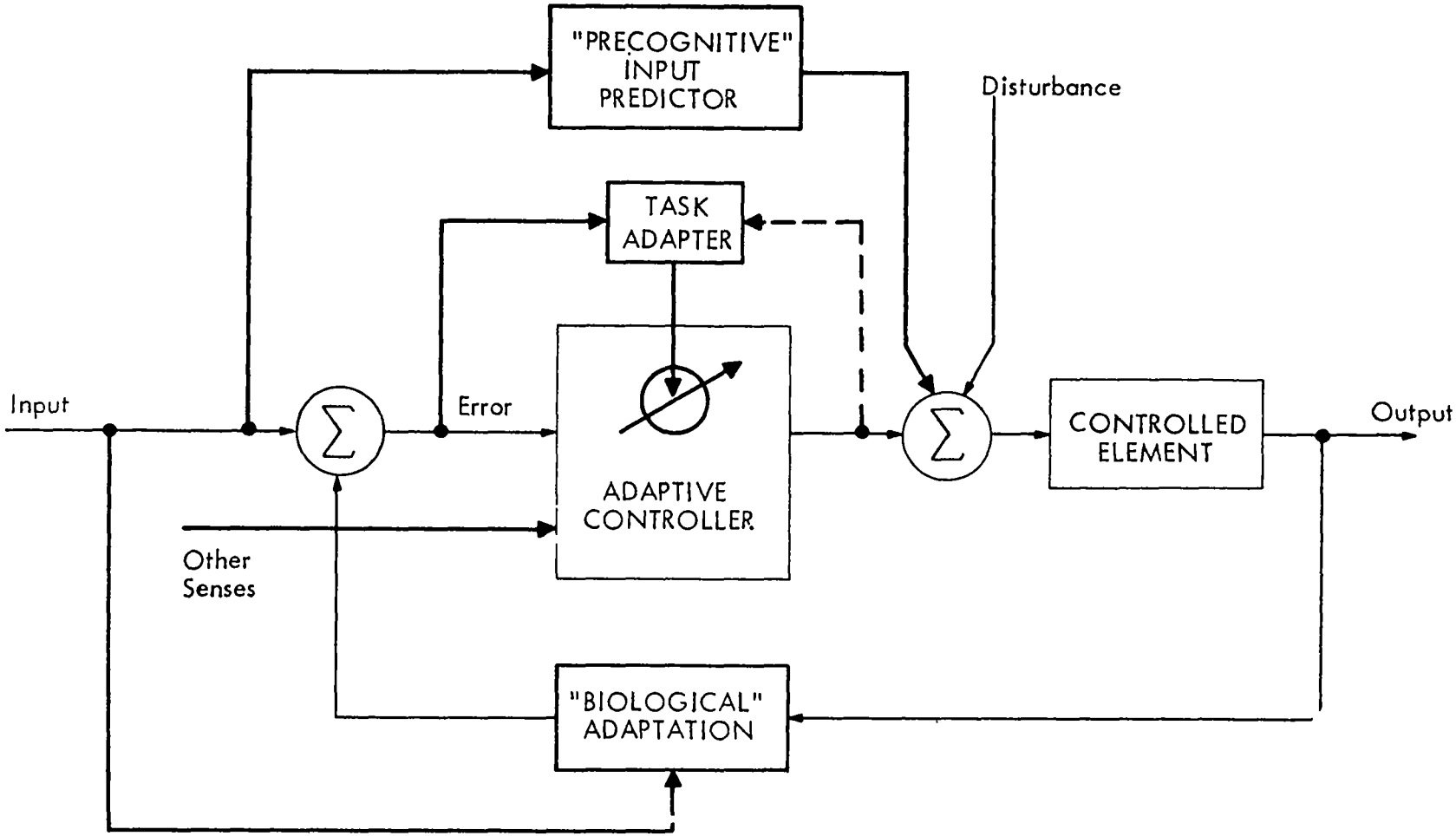

Figure 66. Various classes of adaptation of importance in biological servomechanisms. (Stark & Young, 1963)

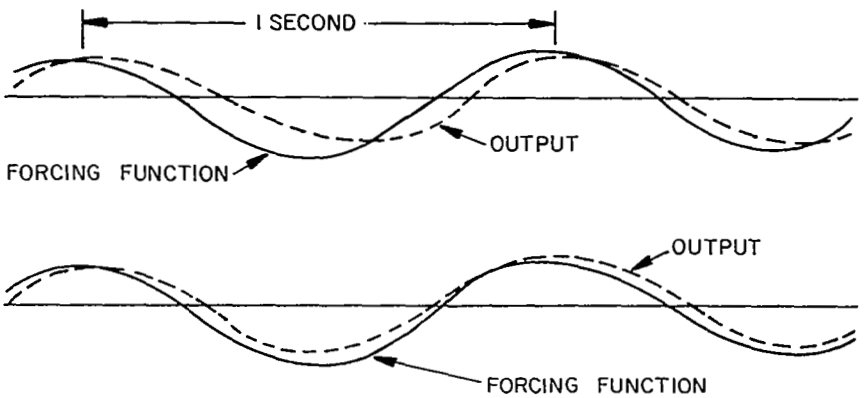

Figure 67. Typical parts of a closed loop response (at top) and a synchronous response to a simple sinusoid. (Krendel & McRuer 1960)

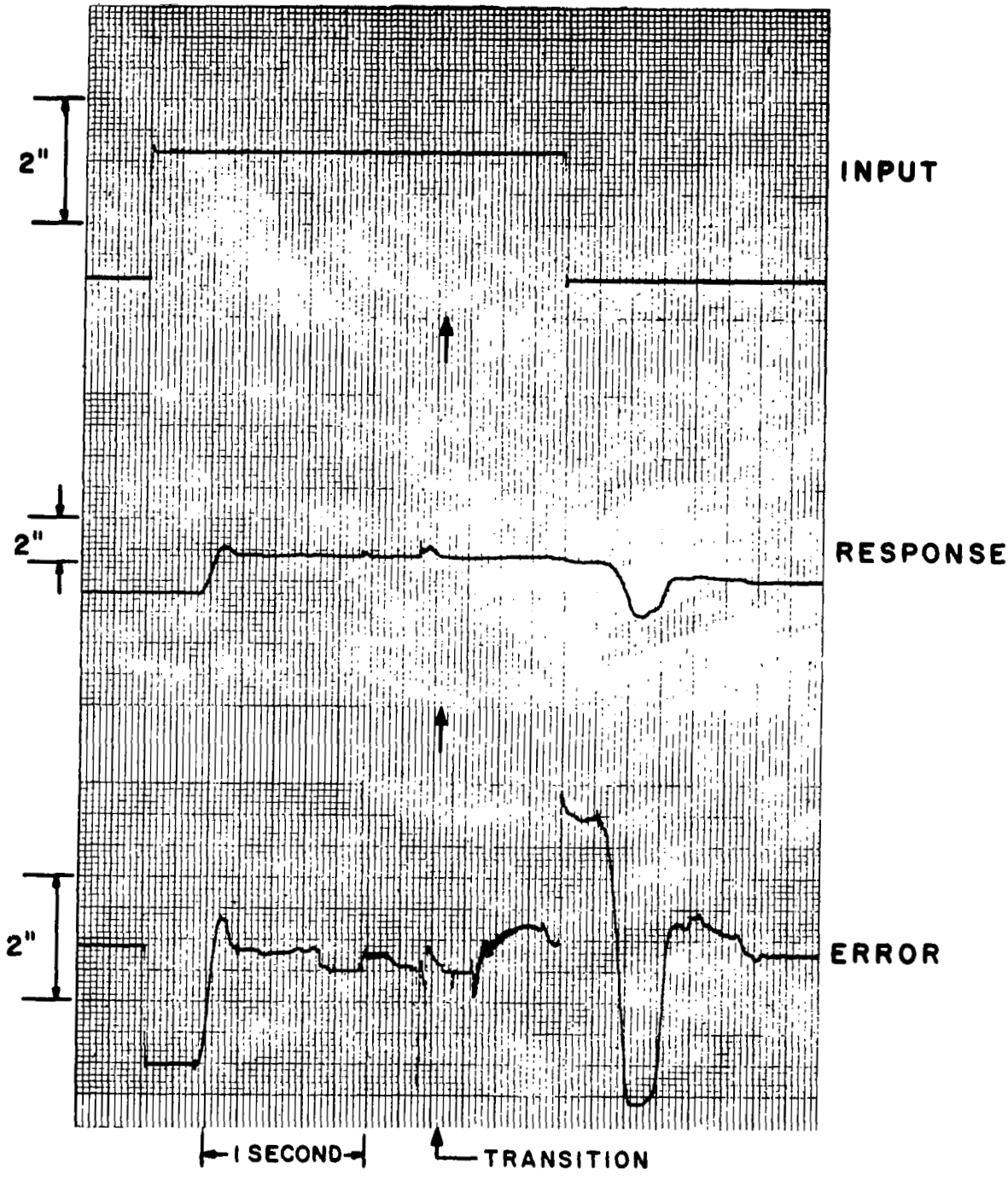

Figure 68. Step response before and after a gain increase. (Young, Green, Elkind & Kelly, 1964)

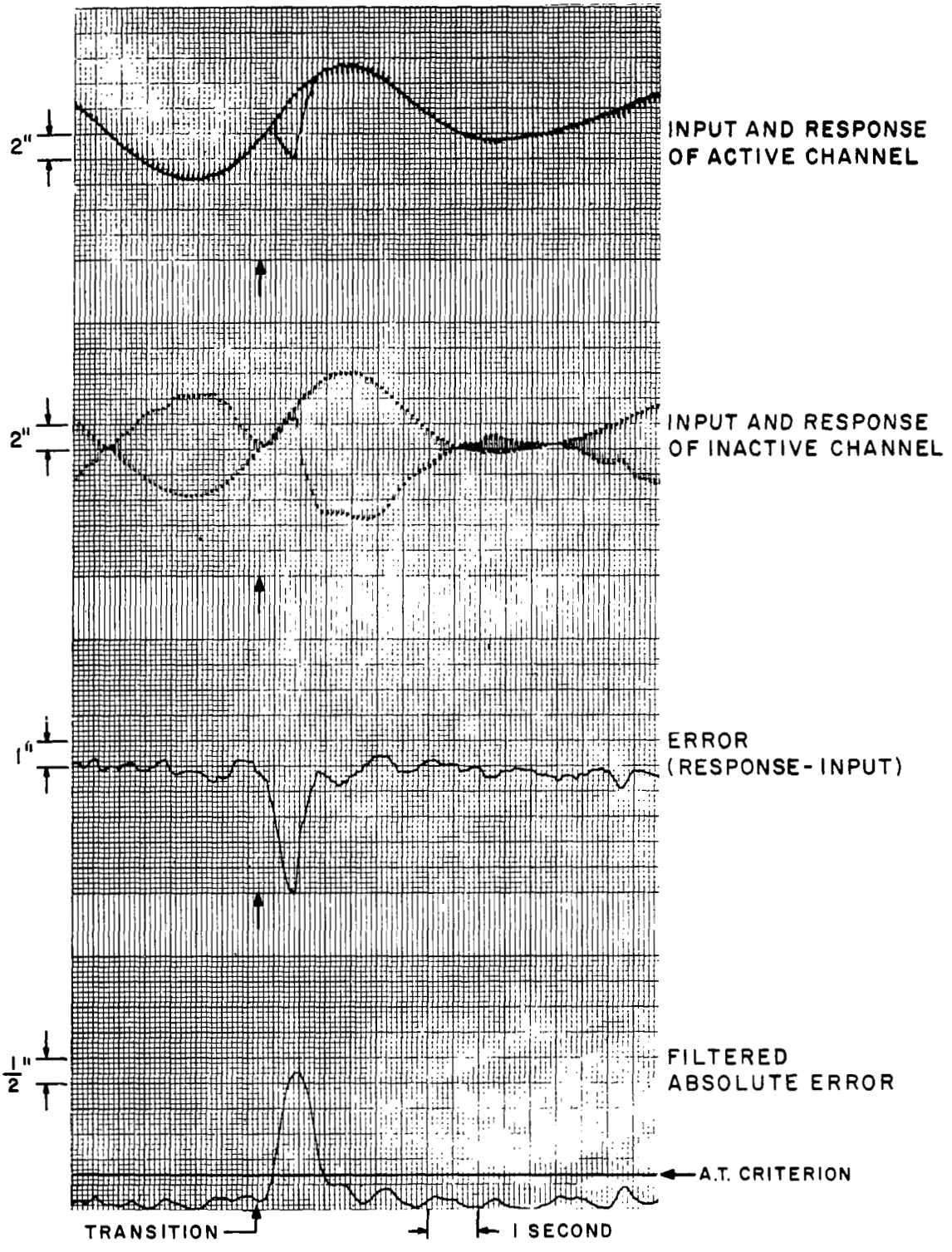

Figure 69. Time tracing with polarity reversal. (Young, Green, Elkind & Kelly, 1964)

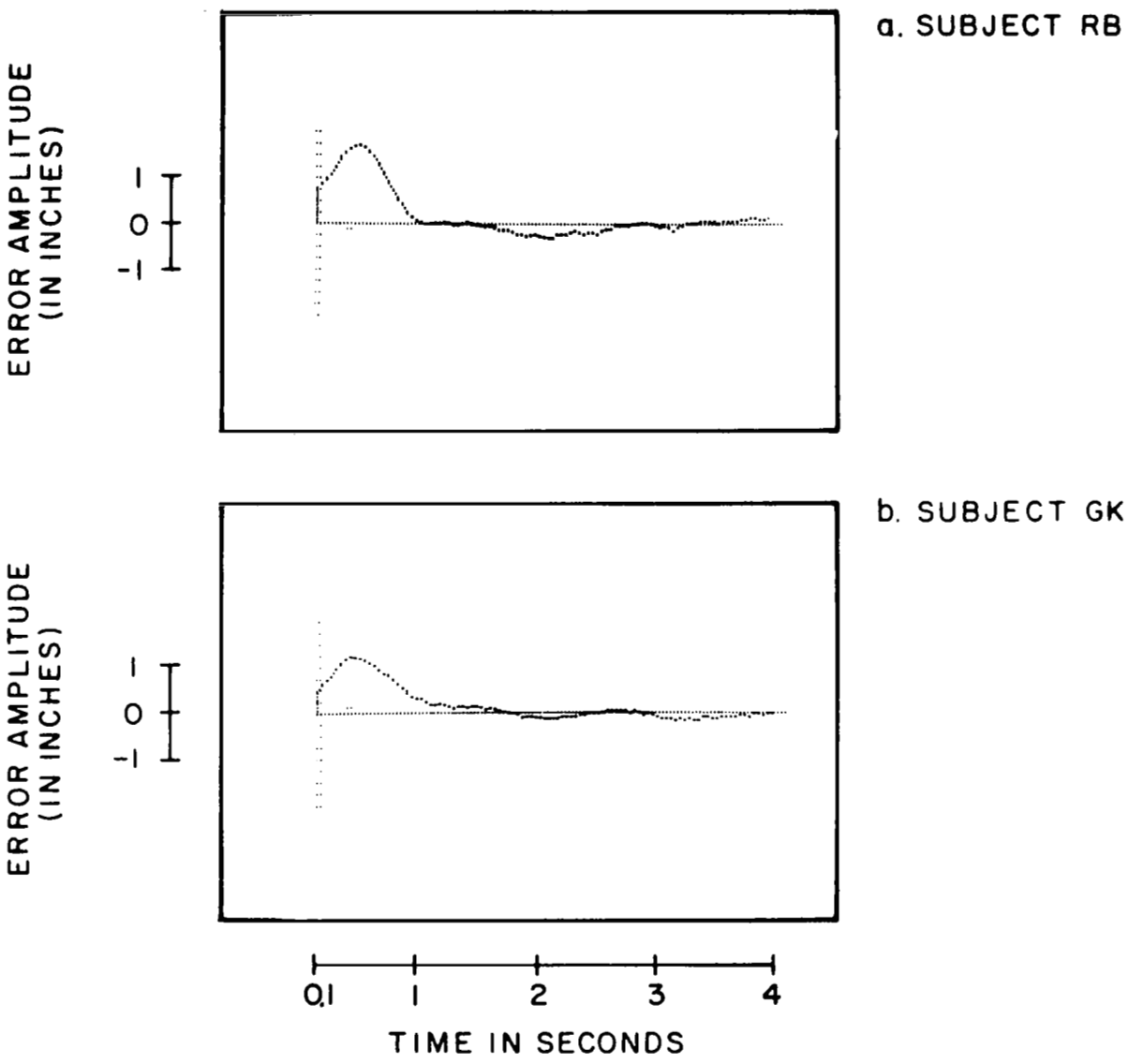

Figure 70. Average error waveform with polarity reversal. (Young, Green, Elkind & Kelly, 1964)

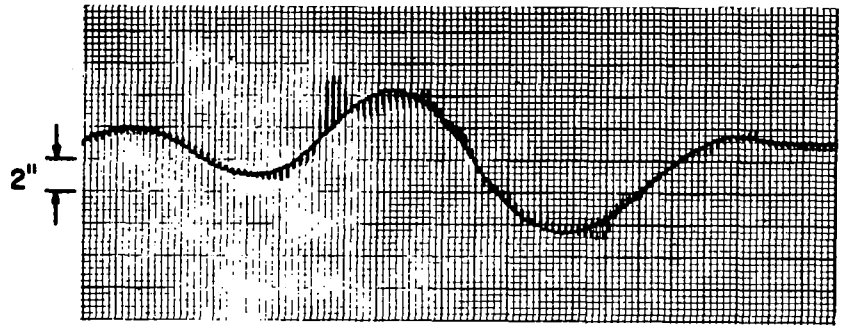

(a)

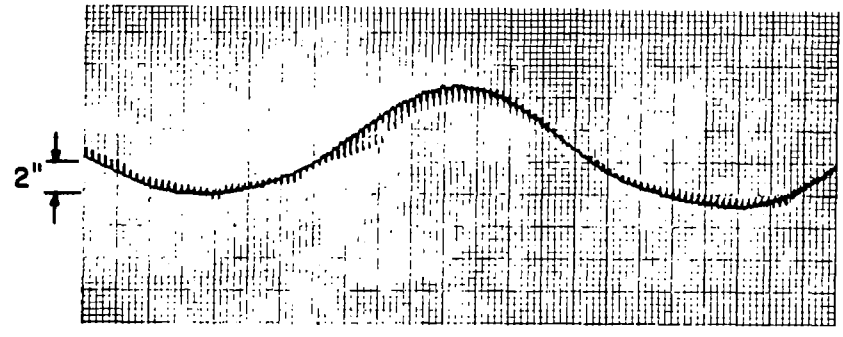

(b)

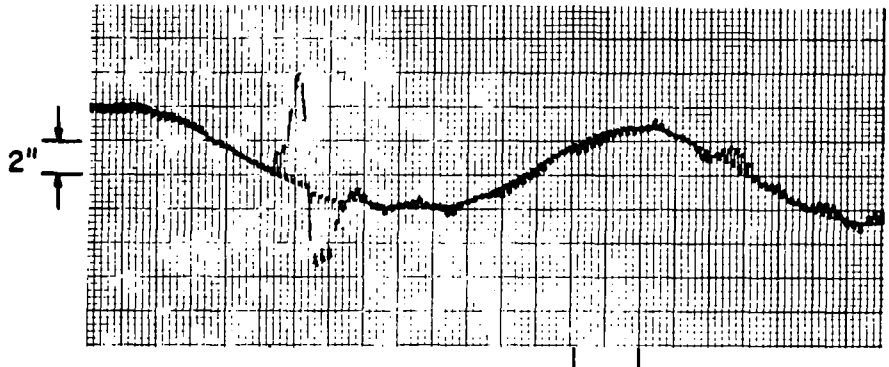

(c)

Figure 71 a,b,c Typical time records for sudden gain increase, gain decrease and polarity reversal with gain increase. (Young , Green, Elkind, & Kelly 1964)

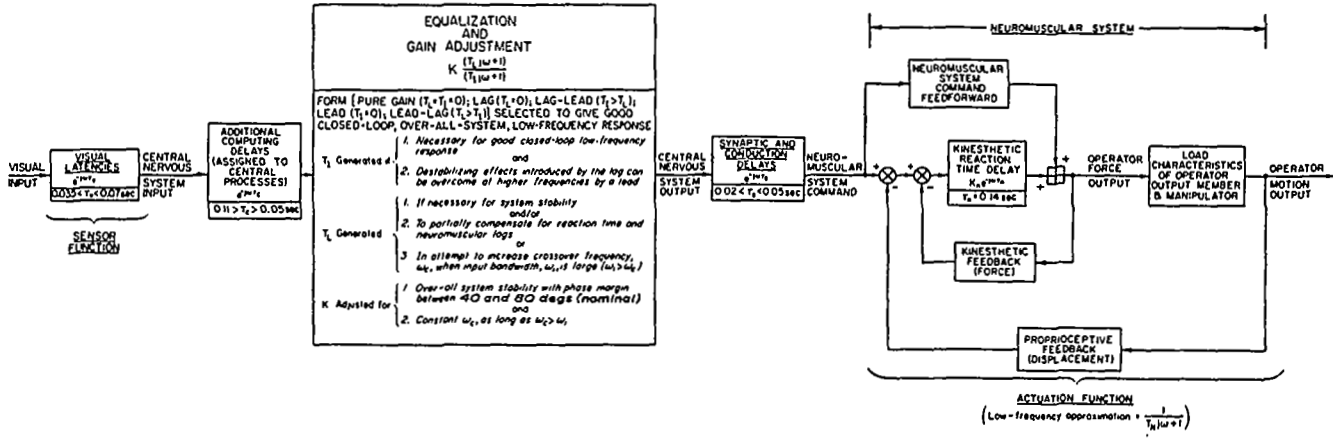

Figure 72. McRuer & Krendel Model of Human Operator. (McRuer & Krendel 1962)

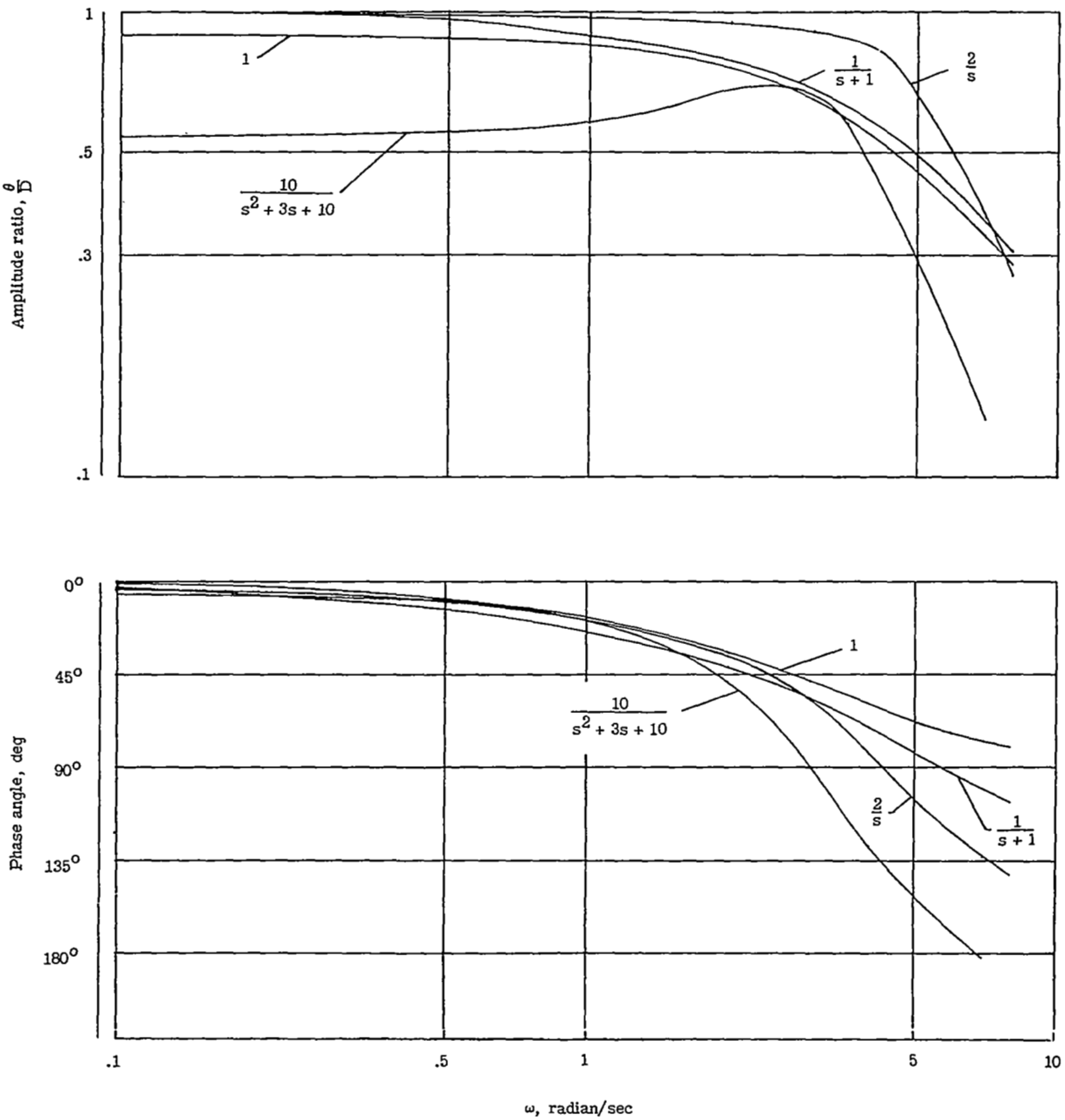

Figure 73. Closed-loop frequency response with pilot E. The curves are identified by the dynamics of the simulated closed-loop equations. (Adams & Bergeron, 1963)

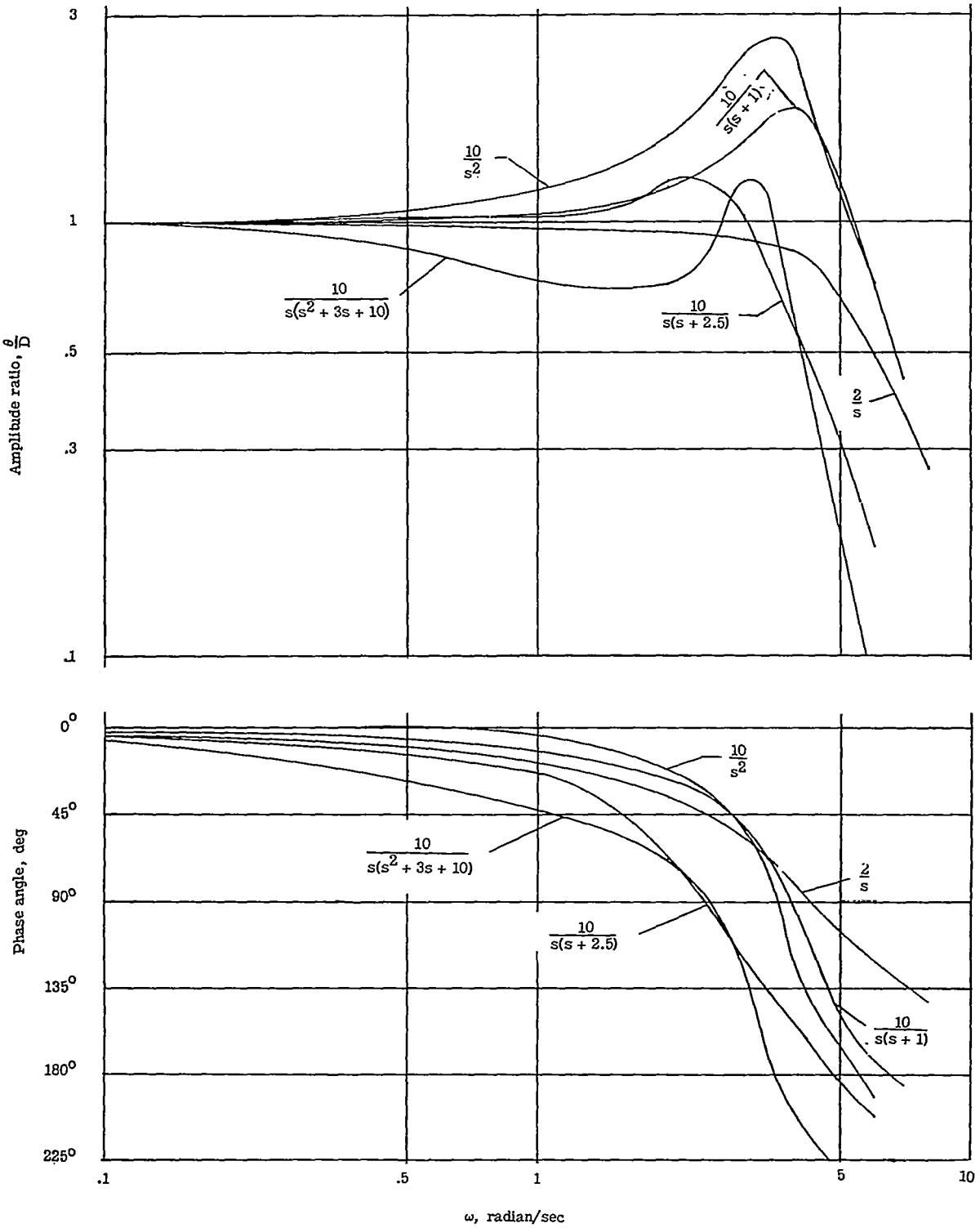

Figure 74. Closed-loop frequency response with pilot E. The curves are identified by the dynamics of the simulated closed loop equations. (Adams & Bergeron, 1963)

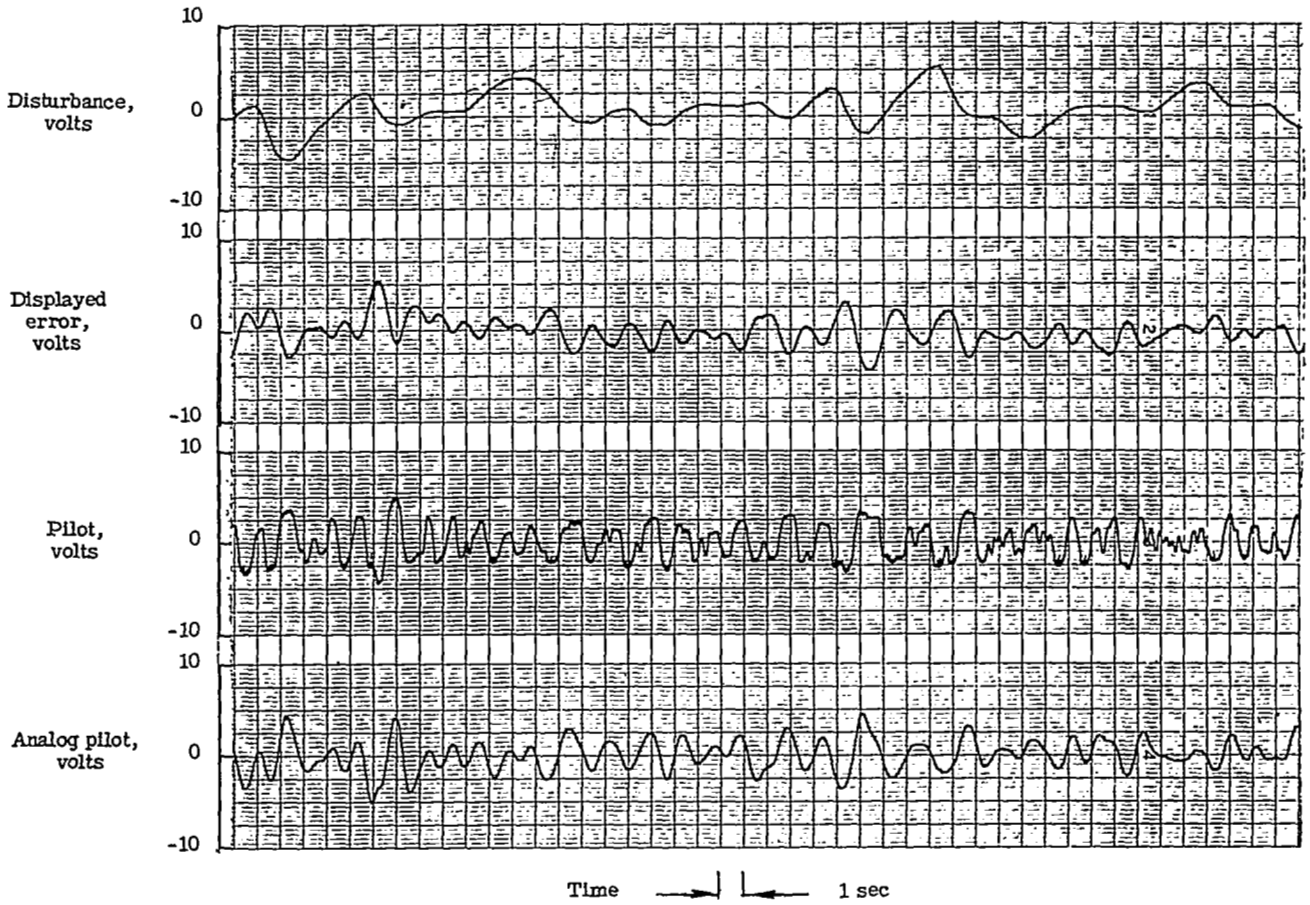

Figure 75. A tracking record with pure acceleration control. Dynamics $10/s^2$ (Adams & Bergeron, 1963)

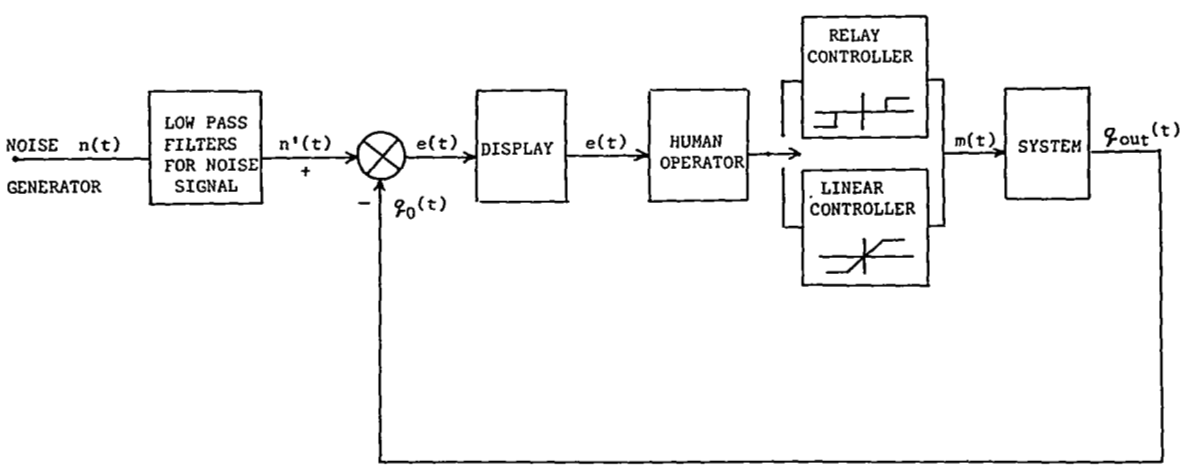

Figure 76. Block Diagram of the control loop. (Kilpatrick, 1964)

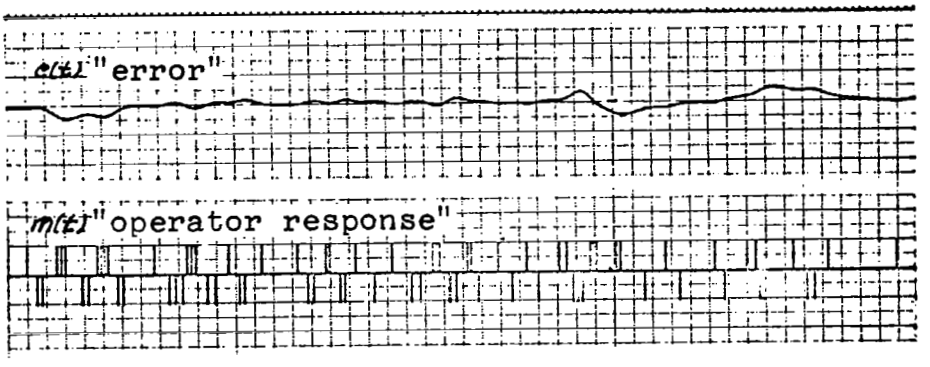

(a)

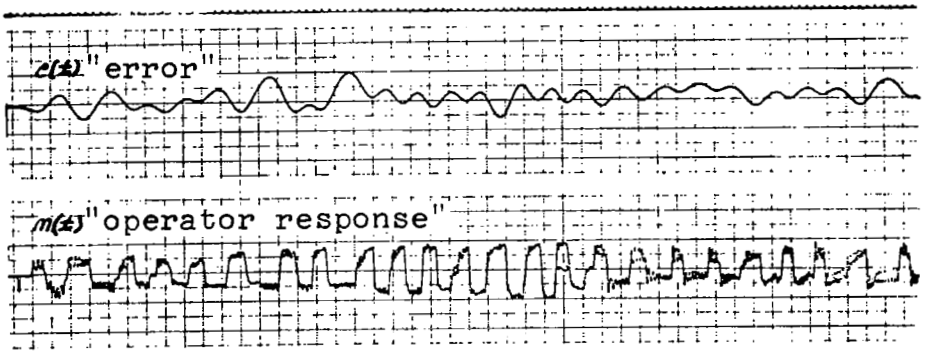

(b)

Figure 77a & b. Operator error and response

$$-\frac{10}{s^2(s+1)}$$

a) Bang-bang control.
b) Continuous control.

(Kilpatrick, 1964)

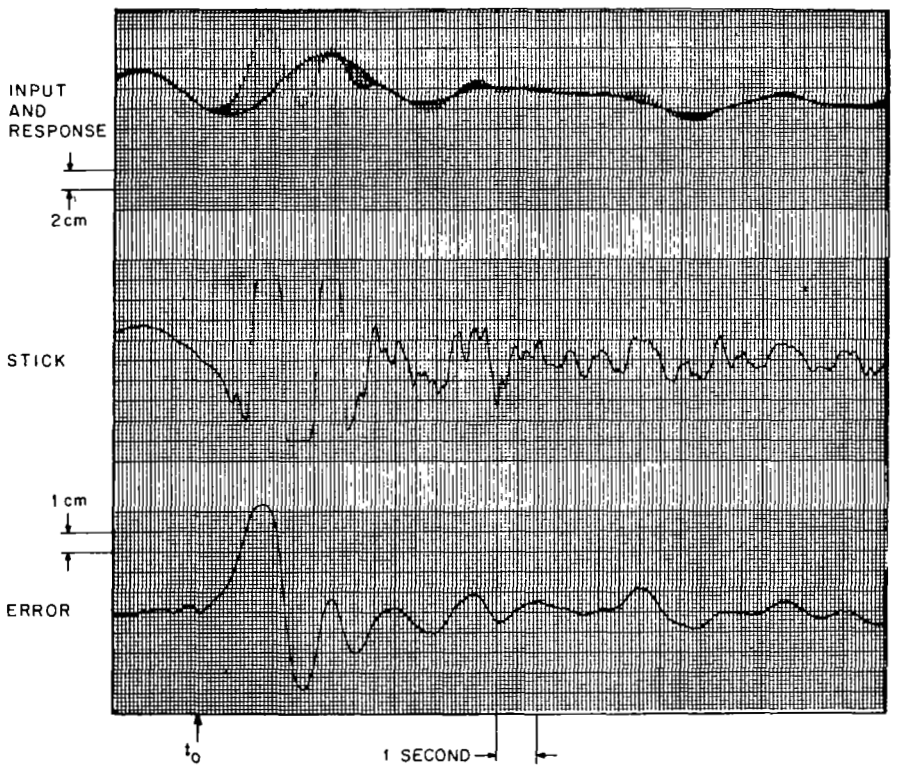

Figure 78. Tracking record for $Y_c(s) = K/s^2$ showing saccadic movements. At t_o $Y_c(s)$ changed from +2 to $-8/s^2$

(Elkind, Kelly and Payne, 1964)

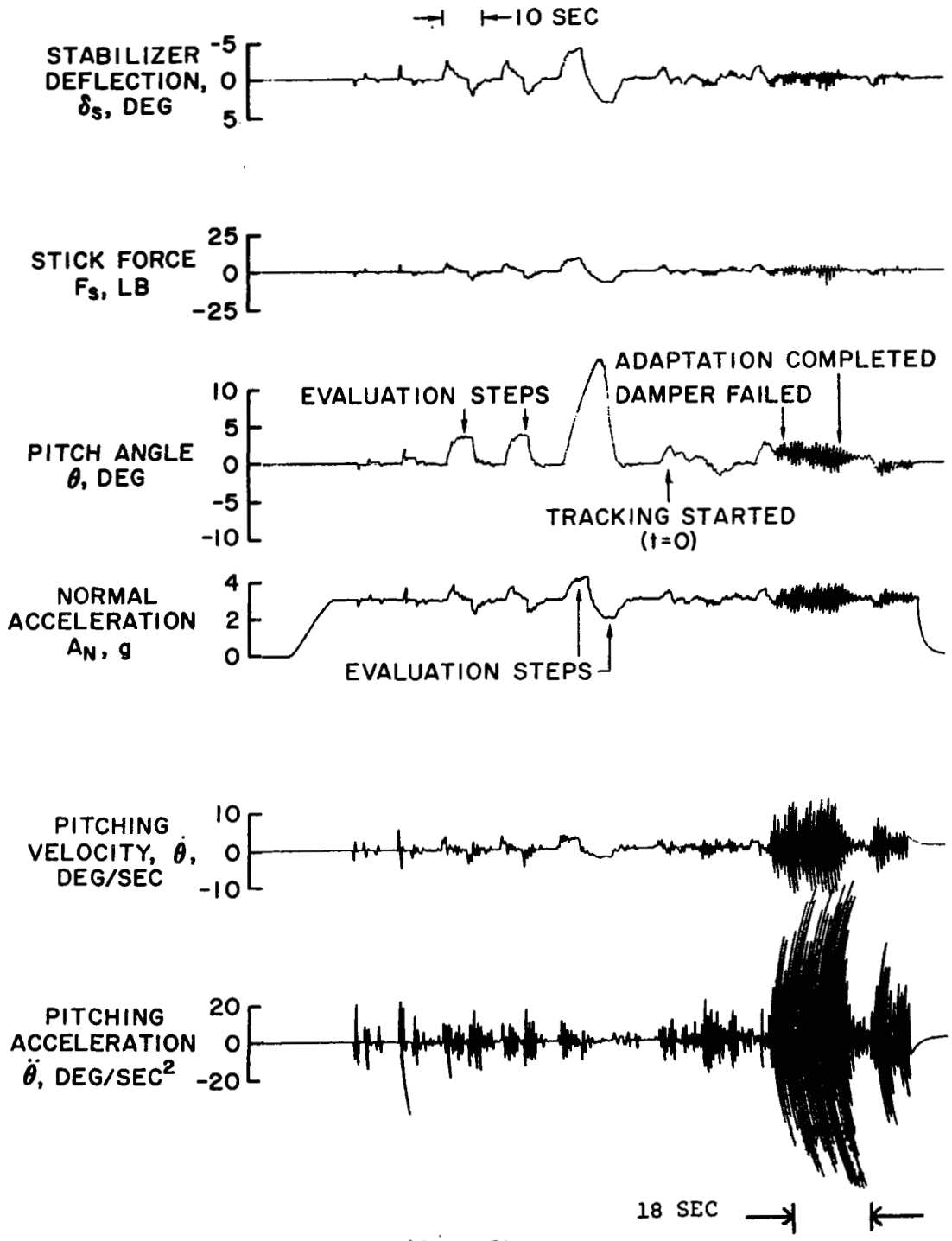

Figure 79. Time histories of typical pitch-damper failure. (Sadoff, 1962)

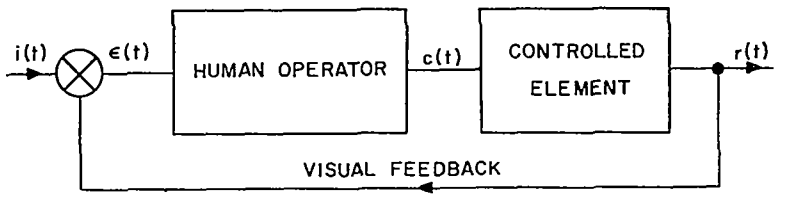

a. Compensatory situation representing the initial phase of the progression sequence.

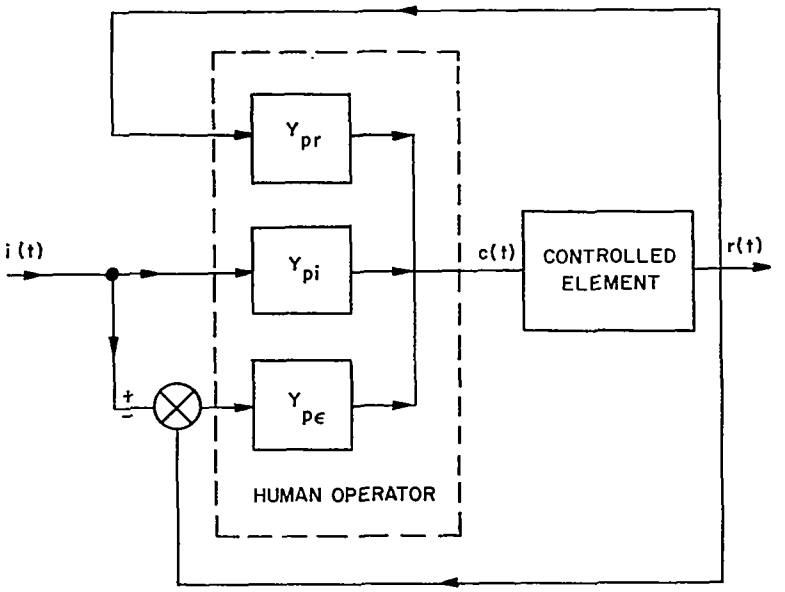

b. Pursuit situation representing the second phase of the progression sequence.

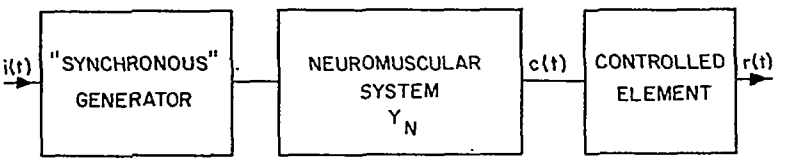

c. Open outer loop representing the synchronous phase of the progression sequence.

Figure 81a,b,c. Three representations for the human operator corresponding to three different display conditions. (Krendel & McRuer, 1960)

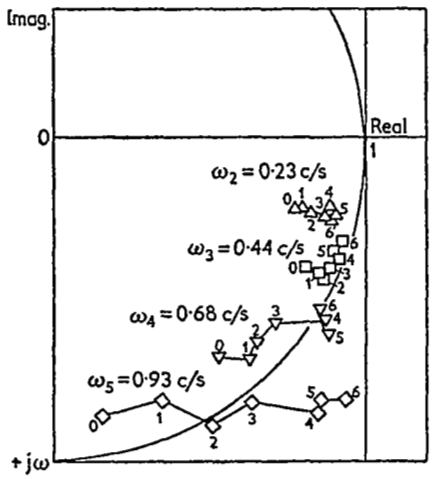

Figure 82. Sample median characteristics of human operator systems following change in display from compensatory to pursuit (0,1,2,3,4,5 are at 0,7·5,15, 30,45,60 sec after change; 6 is average for next minute (Sheridan, 1962)

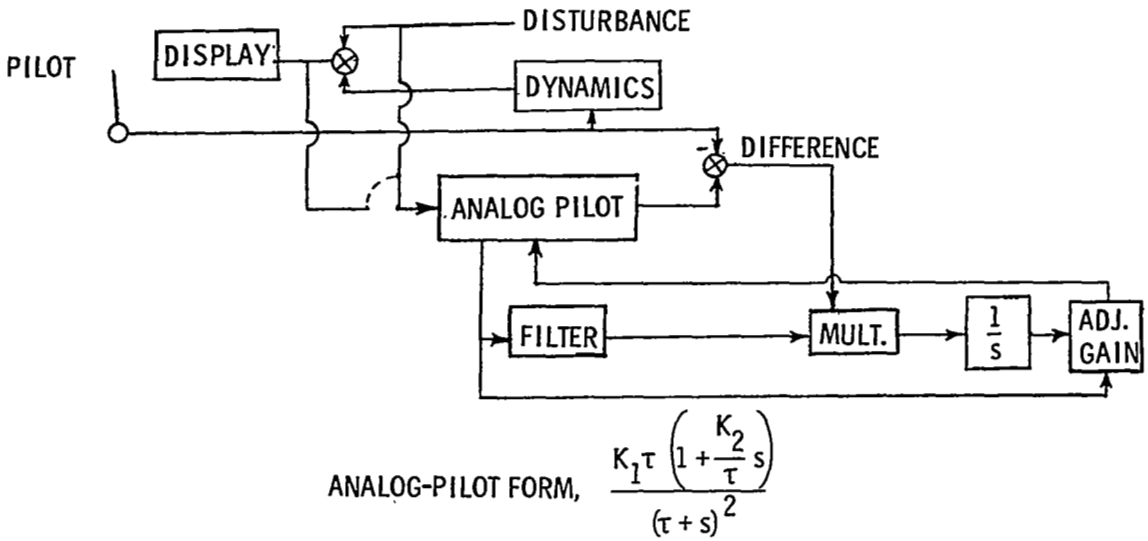

Figure 83. Block diagram of test equipment. (Adams & Bergeron, 1963)

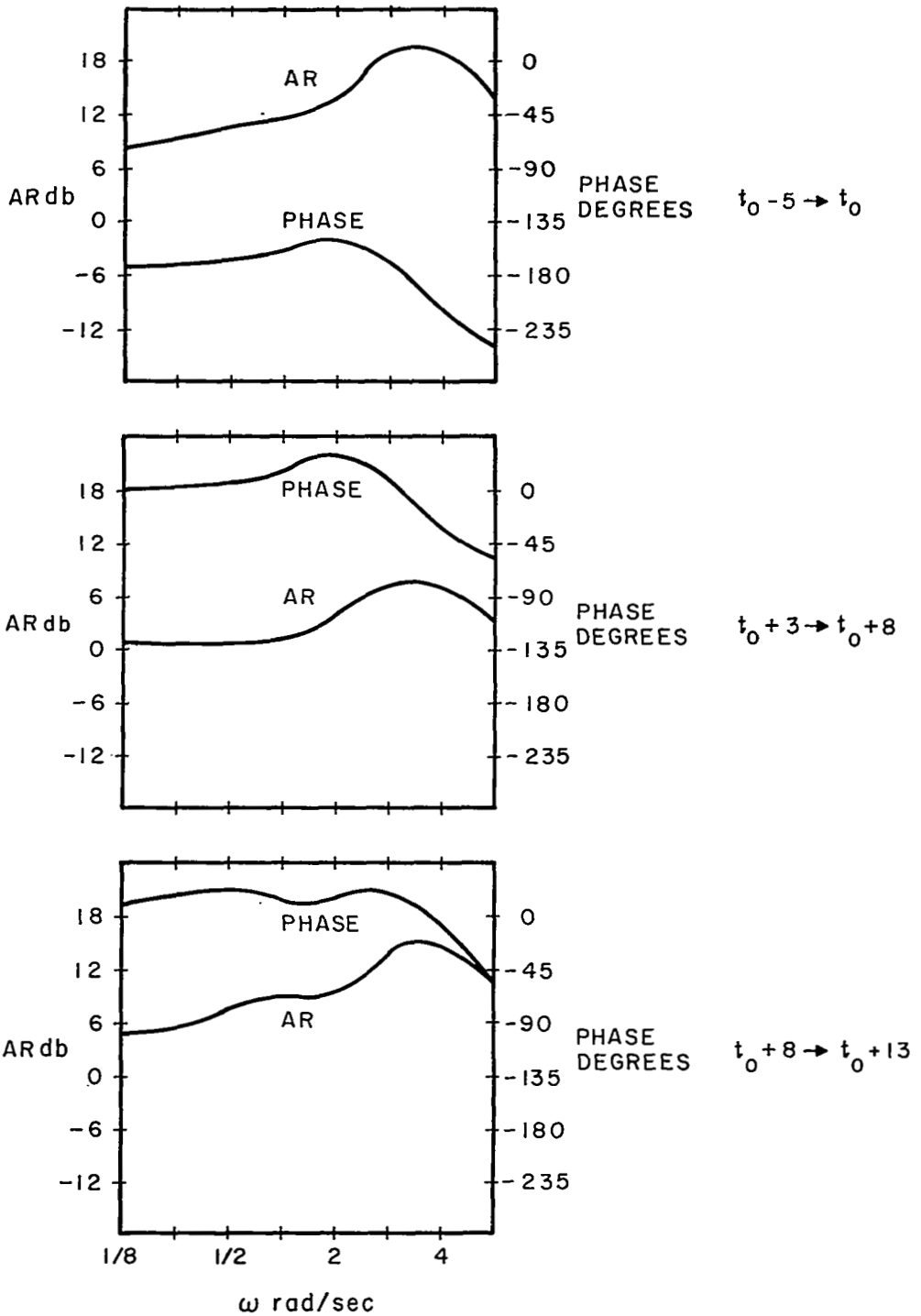

Figure 84. Bode plots of human controller describing functions obtained from successive five second samples of error and stick signals before and after a change in $Y_c(s)$ from $-4/s^2$ to $+8/s^2$. (Elkind, Kelly & Payne, 1964)

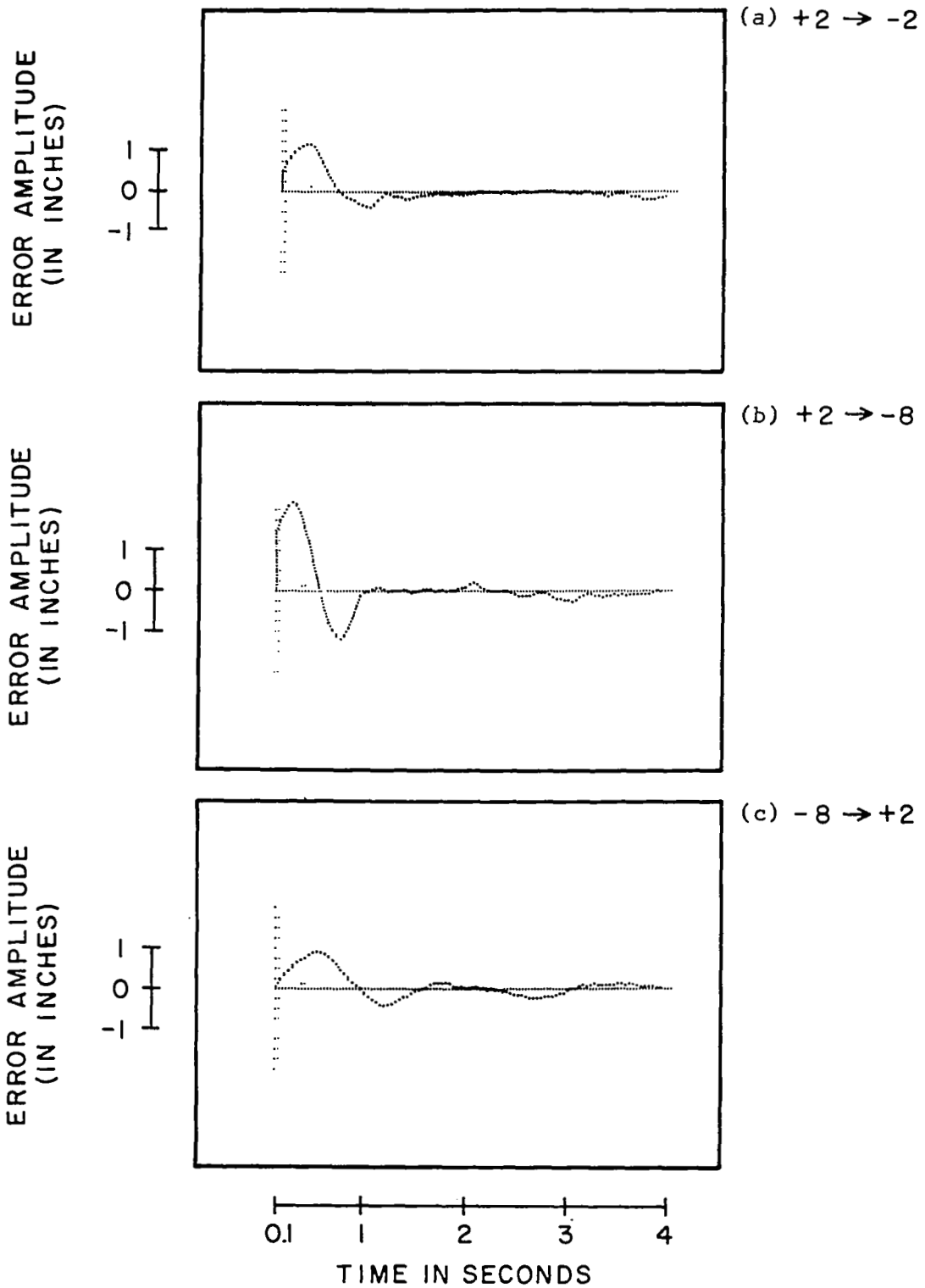

Figure 85a,b,c. Average error waveforms with different types of transition. (Young, Green, Elkind & Kelly, 1964)

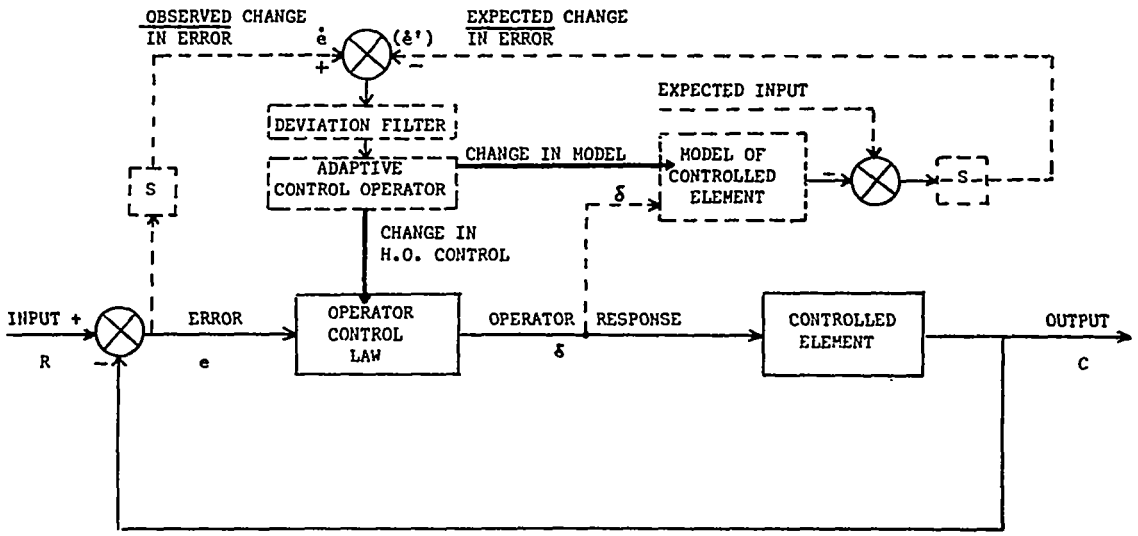

Figure 86. "Model Reference" model for human adaptive tracking.

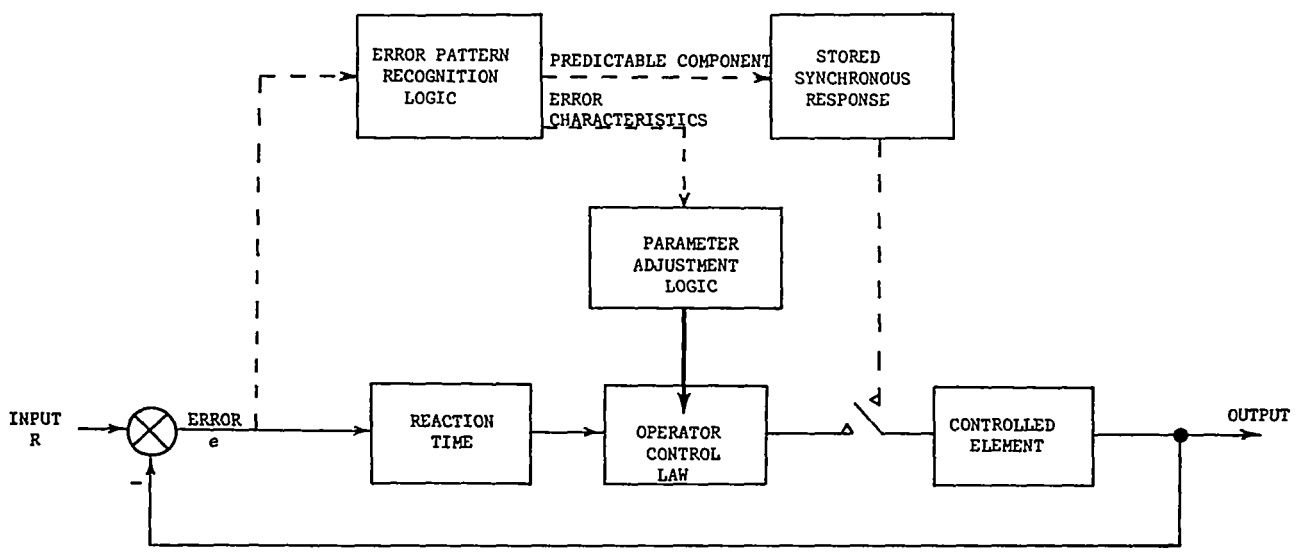

Figure 87. Error pattern recognition model for human adaptive tracking.

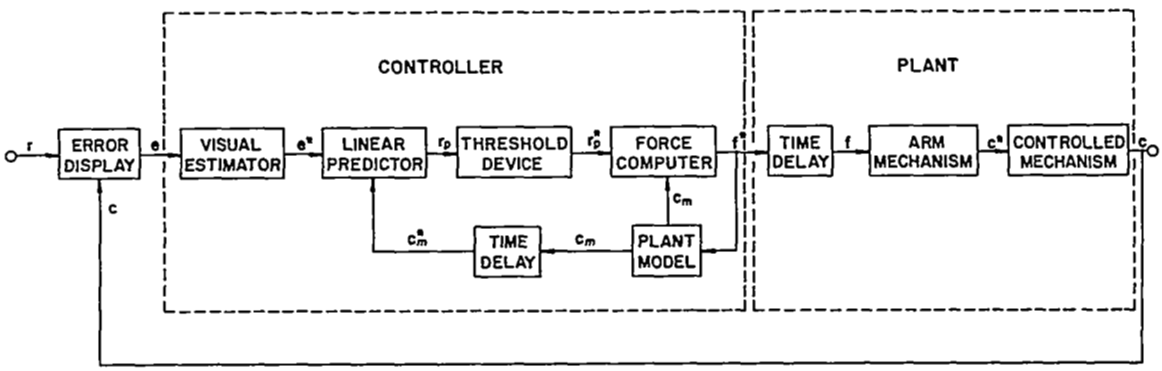

Figure 88. Proposed block diagram of the human operator. (Knoop & Fu, 1964)

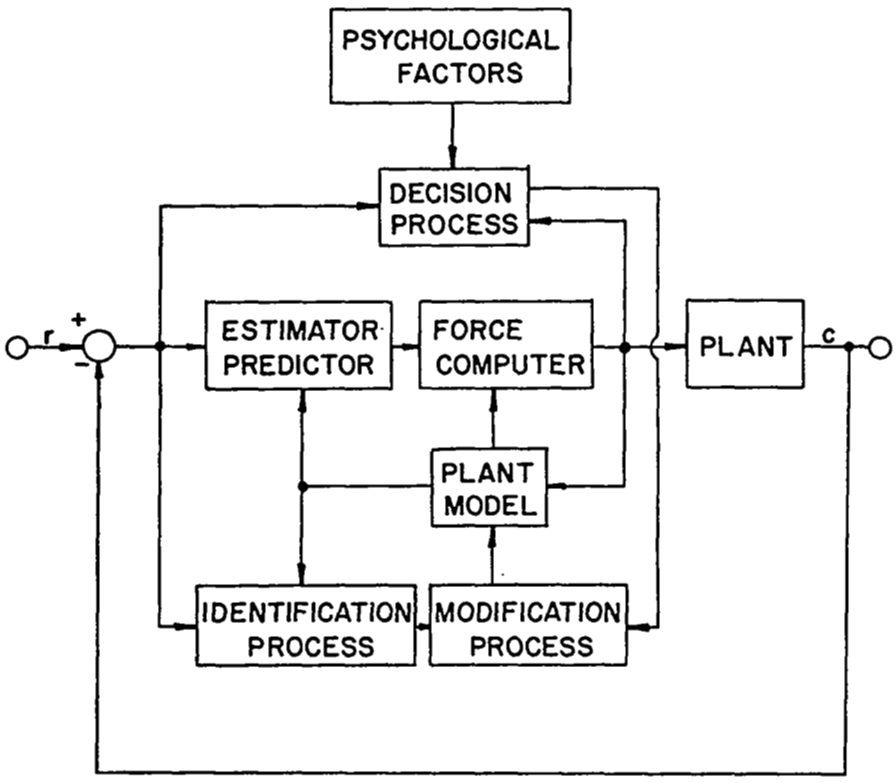

Figure 89. Block diagram of proposed system including adaptive mechanism. (Knoop & Fu, 1964)

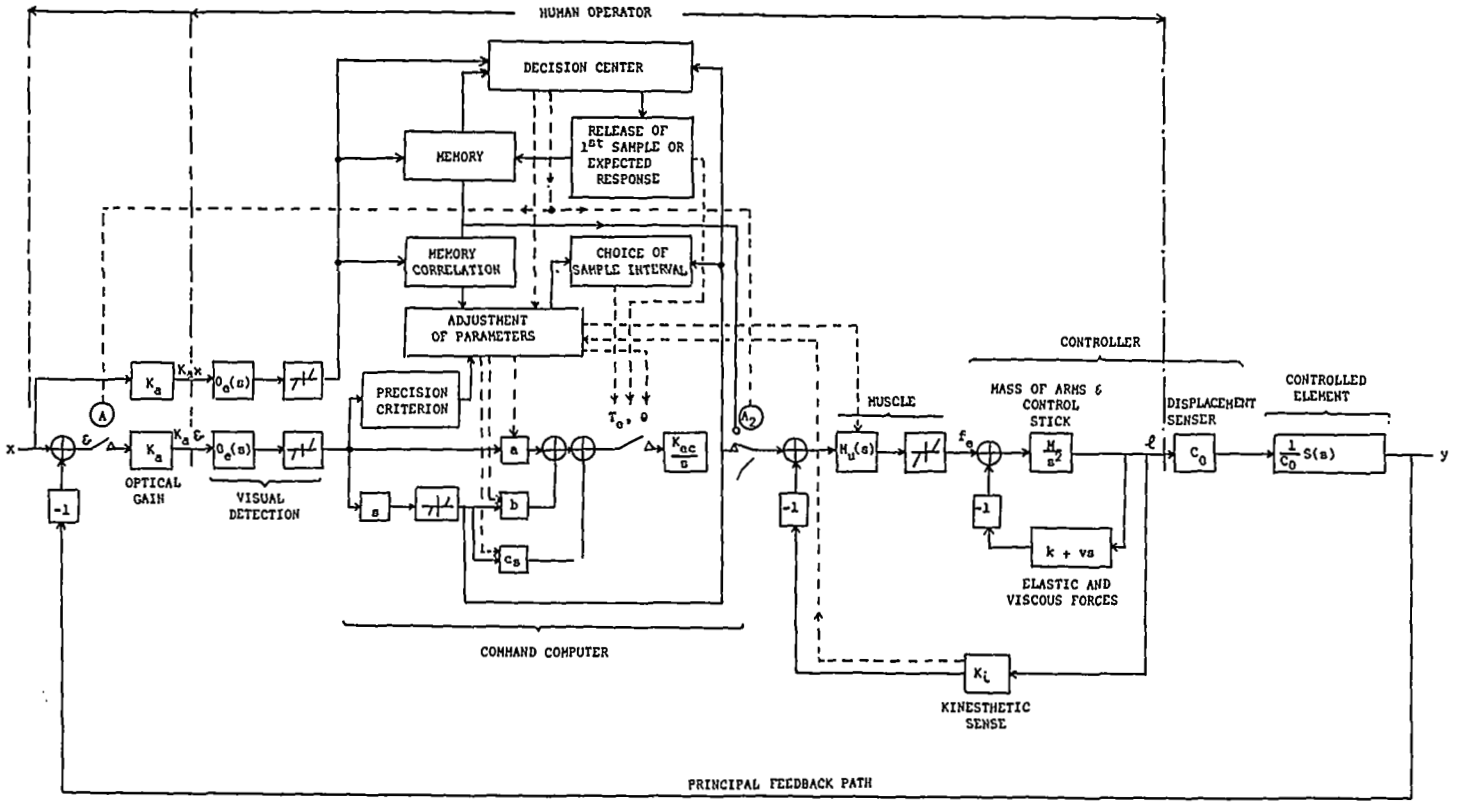

Figure 90. Raoult's schematic model for human adaptive tracking. (Raoult, 1962)